Beta2 Glycoprotein I derived peptides and their mechanism of tumor control

by

Haley Elizabeth Smalley

B.S., Kansas State University, 2019

A THESIS

submitted in partial fulfillment of the requirements for the degree

MASTER OF SCIENCE

Division of Biology
College of Arts and Sciences

KANSAS STATE UNIVERSITY
Manhattan, Kansas

2020

Approved by:

Major Professor
Sherry D. Fleming

Copyright

Abstract

Melanoma is one of the deadliest forms of skin cancer in the United States. The rate of melanoma diagnoses has been increasing steadily over the past few decades. The growth and survival of melanoma tumors is affected by many factors, including angiogenesis and the immune response. Angiogenesis, the growth of new blood vessels, is usually held in check by pro-angiogenic molecules such as vascular endothelial growth factor, and anti-angiogenic molecules such as soluble Flt-1 (sFlt-1). In addition, the serum protein Beta2 Glycoprotein I (β2-GPI) both increases and decreases angiogenesis depending on concentration and conformation. Angiogenesis can alter and be influenced by cells and cytokines produced by the immune response in the tumor. The immune response including tumor-associated macrophages (TAMs), can increase angiogenesis, while angiogenesis can control the phenotype of TAMS in the tissue. We hypothesized that peptides derived from the binding domain of β2-GPI could reduce melanoma growth by controlling angiogenesis and thus altering TAM phenotypes. We used a mouse melanoma model and cell culture to determine whether the β2-GPI-derived peptides regulate angiogenesis to control tumor growth. We found that the peptides reduced tumor growth by increasing the secretion of sFlt-1 in the tumors. As sFlt-1 is also secreted by macrophages and can affect macrophage polarization, we investigated whether the β2-GPI-derived peptides could alter macrophage phenotype. We examined this change in macrophage phenotype by examining RNA from tumors and bone marrow-derived macrophages (BMDMs) treated with β2-GPI-derived peptides. We found that treatment with β2-GPI decreased anti-inflammatory cytokines in BMDMs and altered inflammatory cytokines in the tumors as well. These data indicate that treatment with β2-GPI-derived peptides reduces melanoma growth through regulation of angiogenesis and changes in inflammatory response.

Table of Contents

List of Figures vii
List of Supplementary Tables ix
Acknowledgements x
Chapter 1 - Review of the Literature 1
Melanoma 1
Angiogenesis 4
Abnormal vasculature 6
Markers and cytokines involved in angiogenesis 7
Beta2 Glycoprotein I 11
Structure and function 11
Peptides 14
Macrophages 16
Macrophage phenotypes 16
M1 macrophages 17
M2 macrophages 19
Macrophages and melanoma 21
Function of macrophages in melanoma 23
Conclusion 24
Chapter 2 - Beta2 Glycoprotein I Derived Therapeutic Peptides Induce sFlt-1 Secretion to Reduce Melanoma Vascularity and Growth 26
1. Introduction 26
2. Materials and Methods 28
2.1 Cells 28
2.2 β2-GPI peptides 29
2.3 Cell co-culture 29
2.4 MTT assay 30
2.5 Transepithelial electrical resistance 30
2.6 Migration assay 30
2.7 *In vivo* tumors 31

2.8 Immunohistochemistry (IHC) 32
2.9 Reverse transcriptase PCR 33
2.10 Statistics 33
3. Results 33
3.1 Peptides increase sFlt-1 secretion and hypoxia-induced vascular permeability but not endothelial cell growth. 33
3.2 Peptide decreases MS-1 endothelial cell migration in a Flt-1 dependent response 38
3.3 Peptides result in a dose-dependent, clinically-relevant reduction of mouse melanoma growth. 40
3.4 *In vivo* peptides reduce tumor vessel markers and upregulate sFlt-1 secretion 43
3.5 Blockade of sFlt-1 increases mouse melanoma growth 46
Discussion 48
Chapter 3 - Beta2 Glycoprotein I Derived Peptides Alter Tumor Associated Macrophages 51
Introduction 51
Methods 53
Cell culture 53
β2-GPI peptides 54
Bone marrow derived macrophage collection and culture 54
In vivo tumors 55
TAM isolation 56
NO assay 57
RNA isolation 57
Reverse-Transcriptase PCR 58
Immunocytochemistry 58
Statistics 59
Results 59
Polarization tests for J774A.1 Cells 59
Treatment with peptides alters inflammatory markers in BMDMs. 63
Peptide treatment reduces tumor growth and alters inflammatory response 70
Tumor associated macrophage isolation 72
Discussion 74

Chapter 4 - Concluding Remarks 79
Future Directions 80
Bibliography 82
Appendix A - Supplementary Figures and Tables 113
Appendix B - Copyright Permissions and Outside Software 115

List of Figures

Figure 1.1 Melanoma stages are determined by thickness. 3
Figure 1.2 Hypoxia and stimulation of angiogenesis in melanoma. 5
Figure 1.3 Tumor angiogenesis includes multiple VEGF pathways and surface markers. 9
Figure 1.4 Beta2 glycoprotein I circulates in a globular conformation (A), ... 12
Figure 1.5 Peptides derived from domain V of β2-GPI. 15
Figure 1.6 Macrophages are categorized into multiple in vitro categories. 18
Figure 1.7 TAMs can support melanoma growth through several mechanisms 22
Figure 2.1 The presence of peptides does not alter cell growth or transendothelial resistance. ... 35
Figure 2.2 Peptides do not affect RNA of angiogenic markers in endothelial cells. 37
Figure 2.3 Peptides reduce sFlt-1 secretion from endothelial cells. 38
Figure 2.4 Peptides, p296c-s and RD-p9, reduce endothelial cell migration through Flt-1. 40
Figure 2.5 Peptide treatments reduce tumor growth. 41
Figure 2.6 Peptide treatments increase VEGF-A, endosialin and endoglin transcription. 44
Figure 2.7 p296c-s and RD-p9 reduced deposition of CD31 and Pan-endothelium in tumor tissues. 45
Figure 2.8 Peptide treatments increase VEGF-A, endosialin, endoglin and sFlt-1 protein secretions. 46
Figure 2.9 Peptide reduction of tumor growth is sFlt-1 dependent. 47
Figure 3.1 Extraction of tumor associated macrophages 56
Figure 3.2 M1-like and M2-like phenotypes polarized in J774A.1 cells 61
Figure 3.3 Peptide treatment increases CD68 expression in J774A.1 cells. 63
Figure 3.4 Treatment with RD-p9 reduces anti-inflammatory and TAM-like mRNA expression in unpolarized bone marrow derived macrophages. 64
Figure 3.5 Treatment with peptides alters the anti-inflammatory markers in IL-4 treated bone marrow-derived macrophages. 65
Figure 3.6 Treatment with p296c-s and RD-p9 alter pro-inflammatory markers in bone marrow derived macrophages 67

Figure 3.7 Treatment with p296c-s and RD-p9 alter pro-inflammatory markers of macrophages treated with IFNγ and LPS. 68
Figure 3.8 Peptide treatment alters secretion of pro- and anti- inflammatory cytokines in BMDMs. 70
Figure 3.9 Peptide treatment reduces tumor growth and increases NO production in tumors. 71
Figure 3.10 Treatment with p296c-s and RD-p9 alters inflammatory response in tumors..... 72
Figure 3.11 Macrophages isolated from mouse tumors. 73

List of Supplementary Tables

Supplementary Table 4.1 The melting temperatures and sequences for primers used in RT-PCR. 113
Supplementary Table 4.2 The melting temperatures and sequences for primers used in RT-PCR. 114

Acknowledgements

I would like to acknowledge and thank the people who have contributed to my work at Kansas State University. First, I would like to thank my mentor and advisor, Dr. Sherry Fleming, for her endless patience and support for me. Dr. Fleming introduced me to research and has been encouraging and guiding my path in it for the past five years. It has truly been a privilege to work with her.

I would also like to thank my committee, Dr. Stephen K. Chapes and Dr. Anna Zolkiewska for their help. I particularly appreciate their help in the recommendations and ideas they had for my thesis, which helped shape my projects. I also want to thank the Kansas-IDeA Network for Biomedical Excellence program for both financial support, invaluable experience, and the chance to meet incredible peers. I also would like to thank the Johnson Cancer Research Center for their funding in this project, as well as the H.L Snyder Medical Foundation. Funding for this project comes from the K-INBRE (NIH P20 GM103418) and the Defense Medical Research and Development Program, (Award No. W81XWH-18-1-0716). Opinions, interpretations, conclusions, and recommendations are those of the author and are not necessarily endorsed by the Department of Defense or the National Institutes of Health).

I would also like to thank my lab mates, past and present, particularly the incredible Jen Rowe. My friends, as well, for their constant support of me through graduate school. I would also like to thank my family for their love and support. Mom, Dad, and Michael, I couldn't have done this without you, thank you very much.

Chapter 1 - Review of the Literature

Diagnoses of melanoma, one of the deadliest forms of skin cancer, have been increasing over the past few decades. Attributed to an increase in tanning beds and decrease of skin protection, educational campaigns have been used to improve public awareness of melanoma and how to prevent it (1, 2). Despite this, the rate of diagnoses still increases every year (1–3). The rate of deaths due to melanoma does not show a similar increase due to the many therapeutic treatments discovered each year, ranging from targeted radiation to immunotherapies (3–6). These therapeutics often result in severe side-effects, and the cost of cancer treatment in the United States is notoriously high (1, 2, 7, 8). Though the increasing rate of melanoma diagnoses has not resulted in an increase in deaths, the drawbacks of current treatments have led to research in further therapeutics.

Melanoma

Melanoma is a form of skin cancer that arises in melanocytes. Though not the most common form of skin cancer, the rate of melanoma diagnoses has increased in the United States in the past several decades (1–3). Melanoma incidence rates in the United States doubled through 1982 to 2011 from 9.8 to 19.7 per 100,000 people, and are predicted to increase further through 2030 (4). The incidence of melanoma also differs between sexes, as melanoma has a higher incidence in women ages 14-49 than men (4-6 per 100,000), but there is higher incidence in men than women aged 50 years and older (1, 3, 4, 9–11). After age 55, men have an incidence of anywhere between 23 to 131 per 100,000 higher than women (11). Despite the increase in diagnoses, the death rate for melanoma in the United States has not shown the same increase as the incidence. The death rate for melanoma increased by 2.3% from 1975-1982 but began to slow down with a -0.6% rate of change between 1975-2008 (3). Indeed, the mortality rate has

remained relatively steady with 2.7 per 100,000 people (4). Mortality in melanoma changes with age, increasing significantly after age 65, and gender, with men having an overall rate of 4.0 and women having 1.7 per 100,000 people (4). Though the death rate has not risen over the past few decades as the incidence rate has, melanoma remains a deadly form of cancer and a serious public health concern

Melanoma is known for metastasizing, but the primary melanoma itself can guide the treatment of cancer moving forward. Most primary tumors regardless of cancer are categorized by many indicators, including the size of the tumor, shape, and rate of growth. Unlike other solid tumors, the diameter of malignant melanoma is not an indicator for cancer stage or malignancy: instead, patient prognosis relies on the thickness of the tumor (Figure 1.1). The thickness of the tumor and number of metastases from the melanoma can be directly related to patient survival (3, 6, 10). The diagnostic value of tumor thickness can determine appropriate treatment plans (12, 13).

Melanoma begins at stage 0, also referred to as *in situ* melanoma, in which the "thin" (<1.0 mm) melanoma remains in the epidermis and rarely metastasizes (8). Many melanomas are diagnosed after growing into the "superficial" stage I. Stage I melanoma occurs with radial growth increasing the diameter, while the tumor remains in the epidermis and can be removed via surgery (6). Stage I melanoma is still thin (<2.0 mm) and is unlikely to metastasize but may contain ulcerations on the tumor surface (8). The danger of metastases occurs after the tumor begins vertical growth, as the tumor reaches the dermis (14, 15). Stage II melanoma is not required to have ulceration or metastases, but must have a thickness of up to 4 mm (6, 8).The thicker stage III tumors are associated with small metastases growing in the lymph nodes (8). Stage IV melanoma is, as with many different cancers, diagnosed with metastases in the brain,

lungs, or liver rather than any criteria for the primary tumor itself (8). However, the key associations of primary tumor thickness and likelihood of metastases make identification of the primary tumor essential.

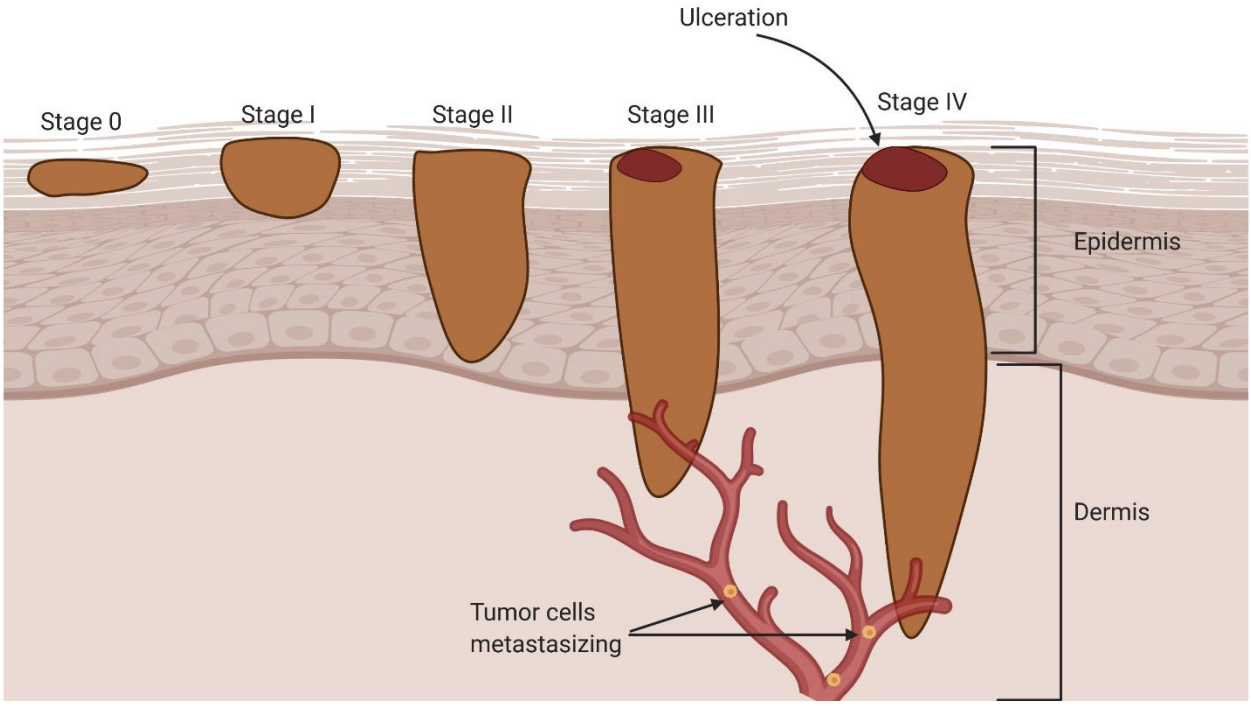

Figure 1.1 Melanoma stages are determined by thickness.

In situ, or stage 0, melanomas are very thin and do not grow beyond the epidermis, similar to stage I melanoma (thickness <2.0 mm). Stage II melanoma, which may have ulceration, is much thicker (<4.0 mm). Stage III melanoma are often ulcerated and have metastasized to local sites or nearby lymph nodes. Stage IV melanoma is often ulcerated, and includes metastases in the lungs, liver, or brain. Figure based on (16), and created with BioRender.com

Melanoma is also known for metastasis and recurring tumors even after the main tumor was removed or treated with chemotherapy (3, 10, 12, 17, 18). This high risk of metastasis is responsible for melanoma's reputation as one of the most aggressive and deadly forms of skin cancer. Primary melanoma tumors >4.0 mm thick have a 62% chance of a second, distinct melanoma occurring in the same area within three years (10, 13, 15, 17). Despite the aggressive nature of melanoma, early detection and specialized treatments have prevented the rate of deaths

from increasing alongside the incidence (1, 3, 4, 7). Nonetheless, patients with metastatic melanoma face a very poor prognosis, with many patients dying within a year of diagnosis and a 25% survival rate after five years (19, 20). Further resistance to surgeries, chemotherapies, and immunotherapies reinforce cutaneous metastatic melanoma as the most deadly skin cancer (21–25).

Melanoma is studied in the lab with a primary cell line or, more commonly, an immortalized cell line. However, like all cancers, each melanoma expresses high heterogeneity between tumors and within the tumor itself (26–28). Immortalized cell lines, though less heterogenous, experiments, and mouse models can help discover possible new treatments and their effects on growth. B16F10 cells are a well-studied immortalized melanoma cell line derived from C57Bl/6 mice with high rates of lung metastases that mimic the metastatic potential of melanoma (29, 30). Regardless of tumor heterogeneity, there are still reoccurring biological targets that can be used to reduce or prevent tumor growth.

Angiogenesis

As they grow beyond stage I, tumors become hypoxic and deprived of nutrients, requiring angiogenesis, the formation of new blood vessels from existing vessels. Angiogenesis is required for the tumor to grow beyond 2 mm in diameter (31), and is absolutely required for tumor survival (31–33). Angiogenesis is promoted by hypoxic cells, which secrete pro-angiogenic factors and chemokines to increase endothelial cell migration and maturation to form blood vessels (34–37). Once oxygen is properly restored to the cells, anti-angiogenic factors are released from endothelial cells to restrict angiogenesis and further vessel growth (38–43). Growth factors such as the essential vascular endothelial growth factor (VEGF) increase

endothelial cell growth and survival and promote new blood vessel growth. Meanwhile, inhibitors such as angiostatin and sFlt-1 prevent excessive angiogenesis.

The constant signaling for angiogenesis results in extreme dysregulation, caused by high concentrations of pro-angiogenic secretions and unsustainable blood vessel growth (Reviewed in 28, 30–32). Not only does the increased angiogenesis lead to the rapid production of new blood vessels, but the vessels produced through tumor angiogenesis are abnormal, often leading to further hypoxia and continuing the process again (Figure 1.2).

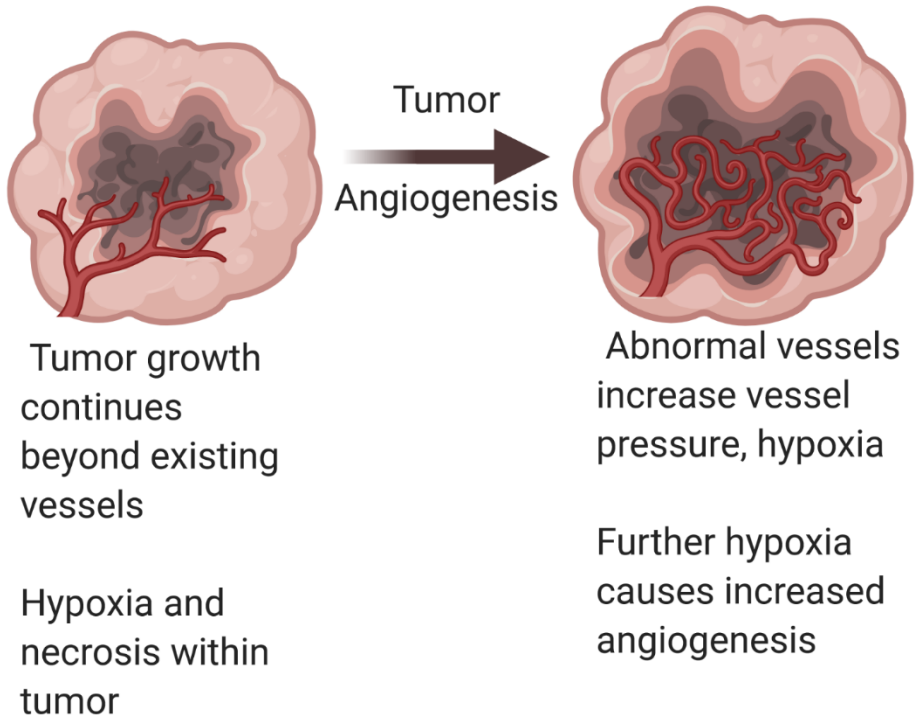

Figure 1.2 Hypoxia and stimulation of angiogenesis in melanoma.

As tumor growth progresses beyond existing blood vessels, the tumor becomes hypoxic. Lack of oxygen causes death of the cells within the tumor and causes signaling of pro-angiogenic cytokines. The vessels that grow from this angiogenesis are disorganized and abnormal, causing increased vessel pressure, leakage of blood vessels, and further hypoxia. Thus, the resulting hypoxia causes signaling of pro-angiogenic cytokines and begins the cycle again. Created with BioRender.com.

Abnormal vasculature

The rapid angiogenesis that leads to tumor progression also produces abnormal vascularization (47, 48). Tumor blood vessels lack pericytes, the stabilizing cells in the lining of the blood vessels and basement membranes, leading to weak, poorly formed blood vessels (49–52). The instability in blood vessels leads to leaking, hemorrhage, and collapsing vessels, further reducing the flow of blood throughout the tumor (47, 49, 53, 54). This lack of blood flow and compression of vessels by the tumor tissue produces high vascular pressure and damages the vessels further (54–56). This forms a cycle of continued hypoxia and increased angiogenesis to restore oxygen to the tumor cells, followed by poor perfusion within the tumor which results in hypoxia again (57–62).

Along with promoting further angiogenesis, these abnormal vessels assist in immune evasion, tumor malignancy, and tumor progression (47, 63). The hypoxia causes an increase in treatment resistance, as the poor perfusion of the blood vessels prevents the dissemination of treatments throughout the tumor (47, 55, 64). However, new cancer treatments have emerged as abnormal tumor angiogenesis has been studied (48, 65, 66). Inhibition of hypoxia normalizes vascularity and inhibit tumor growth (64, 67). Normalization of vascularity results in a lack of hyperpermeable and damaged vessels, allowing for an enhanced immune response and chemotherapeutic response (67, 68). Thus, while abnormal vasculature encourages further tumor progression and survival, targeting tumor angiogenesis can control tumor growth and improve the success of other treatments. *In vitro,* angiogenesis can be studied using primary or immortalized endothelial cell lines. MS1 (Mile Sven 1) cells are an immortalized endothelial cell line derived from pancreatic islet cells of *Mus musculus*. A well-examined endothelial cell line,

MS1 cells secrete VEGF and express its receptor (69, 70), and are used as an experimental model for endothelial cells.

Markers and cytokines involved in angiogenesis

VEGF is a key angiogenesis signaling molecule and mitogen. Originally named vascular permeability factor (71), VEGF-A (usually referred to simply as VEGF) has multiple isoforms ranging from 121 to 206 amino acids. The isoforms are encoded by alternative splicing of the exons of the gene, with the 165 amino acid isoform being the most common and the most associated with angiogenesis (72, 73). As an endothelial-specific mitogen, VEGF-A promotes survival in endothelial cells and is necessary for fetal development (74–77).

The other forms of VEGF, VEGF-B, -C, and -D, are not as well understood. VEGF-B has been associated with myocardial and embryonic angiogenesis in particular (78). VEGF-C and VEGF-D are associated with lymphangiogenesis, though only VEGF-C has a clear relationship with angiogenesis (79–83). VEGF-C in particular is associated with tumorigenesis and tumor growth, and has been used as targets for anti-tumor therapeutics (32, 46, 58, 75, 84). Though VEGF-A is considered the “main” member of the VEGF family, the other members perform varied but essential roles in angiogenesis and vasculogenesis.

The VEGF family also features two main receptors, VEGFR1 (a receptor for VEGF-A and -B) and VEGFR2 (a receptor for VEGF-A and -C), along with VEGFR3, which only binds to VEGF-D and is associated with lymphangiogenesis (Figure 1.3). KDR (also known as VEGFR2 and Flk-1) is a key receptor for VEGF in the context of tumor angiogenesis. A cell surface receptor tyrosine kinase, KDR is necessary for angiogenesis in fetal growth. KDR is essential for angiogenesis in tumors (85, 86) and thus often upregulated in cancer (69, 87).

As a key regulator of VEGF-A and -B, the fms-like tyrosine kinase receptor Flt-1 (also known as VEGFR1) was the first of the VEGF receptors identified (88). At 150 kDa, Flt-1 was originally believed to be a decoy receptor, as the resulting signal was not as strong as KDR, but Flt-1 was later confirmed to promote signaling for angiogenesis. Knockouts of membrane-bound Flt-1 significantly hinder angiogenesis due to its function in VEGF signaling (77, 88, 89). Soluble Flt-1 (sFlt-1) is a truncated form of VEGFR1 that was first discovered as an endogenous inhibitor of VEGF (41). sFlt-1 binds VEGF and prevents it from signaling, restricting endothelial cell activation and angiogenesis (41, 90). Excessive sFlt-1 secretion is associated with endothelial cell dysfunction, and sFlt-1 concentrations are used as a diagnostic for clinically hypoxic conditions such as pre-eclampsia (91, 92). Importantly, increased sFlt-1 reduces cancer growth both by the inhibition of angiogenesis signaling and the reduction of endothelial cell migration (33, 93). While Flt-1 functions in promoting angiogenesis with VEGF signaling, sFlt-1 functions as an endogenous inhibitor of angiogenesis, offering two different but important results with the same protein.

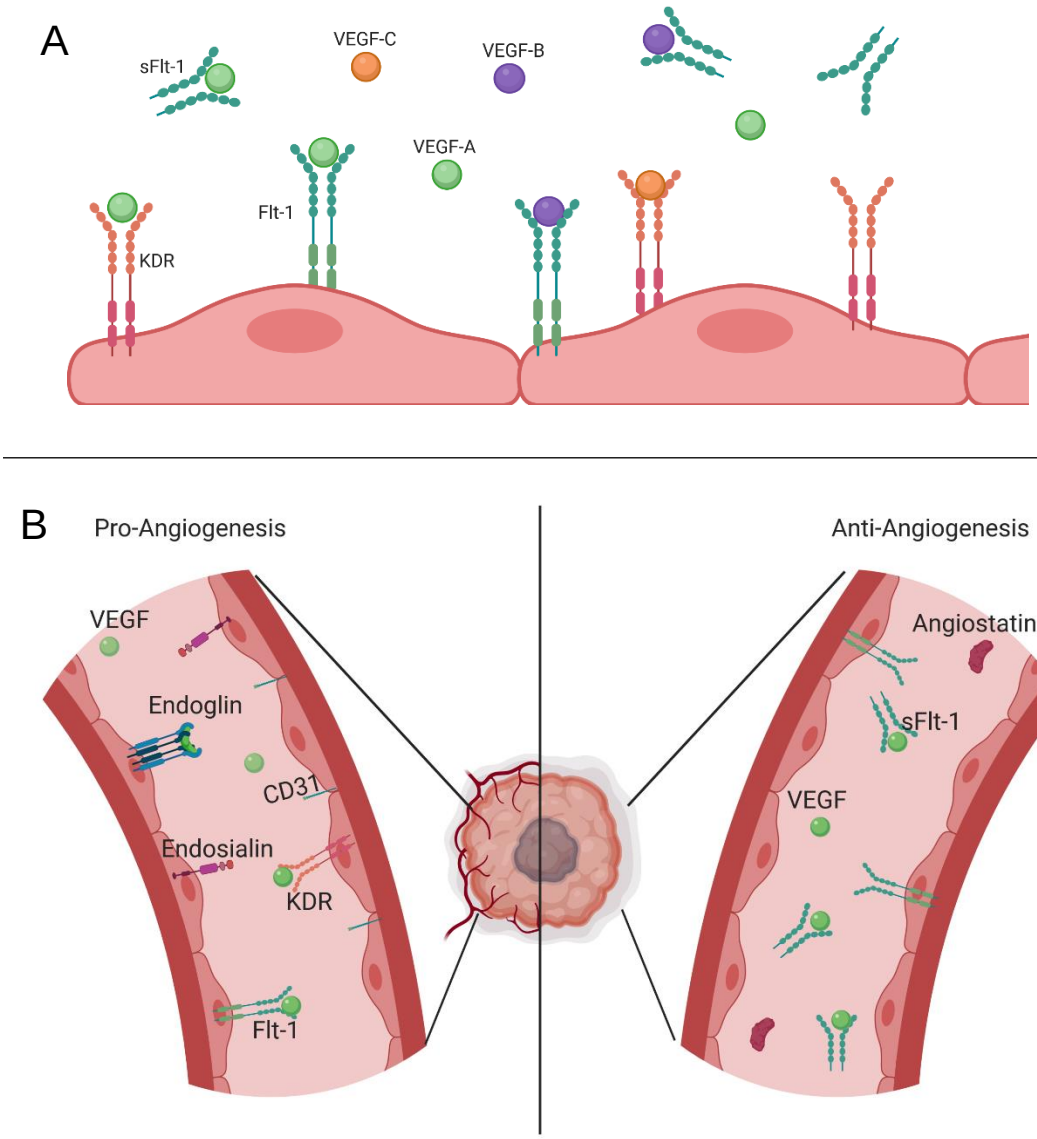

Figure 1.3 Tumor angiogenesis includes multiple VEGF pathways and surface markers.

A. In angiogenesis, VEGF family includes VEGF-A, B, and C, and two receptors Flt-1 (VEGFR1) and KDR (VEGFR2). These proteins are essential for the promotion of angiogenesis, while the soluble Flt-1 (sFlt-1) is an angiogenesis inhibitor.

B. Tumor vascularity is dependent on the presence or absence of pro- and anti-angiogenic proteins. Surface markers such as endoglin and endosialin are used as diagnostic markers for angiogenesis, while the VEGF family increases angiogenesis. sFlt-1 and angiostatin, however, inhibit angiogenesis and restrict tumor growth. Created with BioRender.com.

Tumor blood vessels can be identified through several surface markers present on endothelial cells. Endosialin (CD248; TEM1) was initially identified as a surface protein on

tumor blood vessels (94, 95). Later, endosialin was further characterized as a marker for tumor angiogenesis expressed differentially on human tumor endothelial cells and embryonic cells, but not on normal adult tissues (96, 97). Further investigation found increased expression of endosialin associated with recurrent breast cancer (98) and metastatic melanoma (99), allowing the surface marker to be targeted for tumor treatments (100).

Endoglin (CD105), is an accessory receptor for TGF-β and is highly expressed on vascular endothelial cells (101). In particular, endoglin is expressed on the rapidly multiplying endothelial cells of tumor blood vessels (102). Due to its upregulation in tumor blood vessels, endoglin is used as a diagnostic marker for tumor growth and angiogenesis (101–103). Similarly, endoglin has been used to determine the efficacy of therapeutic cancer treatments (104, 105). However, not all histological markers used to measure tumorigenesis are exclusive to tumor cells. CD31 (PECAM-1) is a 130 kDa membrane glycoprotein expressed on platelets and endothelial cells (106) and is concentrated in endothelial junctions (106, 107). Clinically, CD31 is used in histology and microscopy to both locate blood vessels and measure the progress of angiogenesis within tissues (81). While CD31 is not exclusive to tumor cells, both CD31 and endoglin are key markers in monitoring angiogenesis within tumors.

Angiogenesis is also controlled by negative regulation to prevent excessive blood vessel formation. Angiostatin is an endogenous angiogenesis inhibitor derived from a proteolytic fragment of plasminogen (108). Angiostatin restricts endothelial growth, and reduces tumor growth and metastasis, making it an inhibitor of interest in tumor angiogenesis (42, 43). However, treatments designed to use angiostatin as an anti-tumor therapeutic have not yet been successful (108, 109). In conclusion, angiogenesis is regulated and identified by many pro- and anti-angiogenic proteins.

Beta2 Glycoprotein I

Structure and function

Originally discovered in 1961 (110), Beta2 Glycoprotein I (β2-GPI) is a globular serum protein that naturally occurs in concentrations near 0.2 mg/mL in the blood (111). Also called Apolipoprotein H due to its binding to cardiolipin, β2-GPI is also highly conserved, with 88% homology in mice and 91% in bovines compared to human β2-GPI (112). In particular, there is nearly 100% conservation in the domain I antibody binding site (RGGMR) and the positively-charged phospholipid binding site in domain V (CKNKEKKC) between mice, bovines, and humans (112). A 43-kDa protein with 326 amino acids, β2-GPI contains five sushi, or, complement control protein (CCP) domains and a flexible hydrophobic "tail" of amino acids (113, 114). Domains I-IV of β2-GPI are CCP domains containing about 60 amino acids with two disulfide bonds and a conserved tryptophan. The overall sequence of β2-GPI contains a high percentage of proline residues (8.3%) and cysteine residues (5%) (113). The cysteines form the disulfide bonds conserved in CCP domains that hold together the individual CCP domains (115), and the prolines separate the domain structures within β2-GPI.

Circulating β2-GPI maintains a "closed" globular conformation, concealing the antibody binding epitopes on the interior of the protein (116). In its circulating state, β2-GPI remains mostly inert. After binding to moieties such as negatively charged phospholipids and lipoproteins, β2-GPI "opens", exposing the neoantigens on domains I and II (116, 117) (Figure 1.4). These neoantigens can then be recognized by naturally occurring anti-β2-GPI antibodies

(117–119) which bind to epitopes on domains I and II (117, 120, 121). This antibody binding can then initiate the complement cascade, causing cell lysis and inflammatory response.

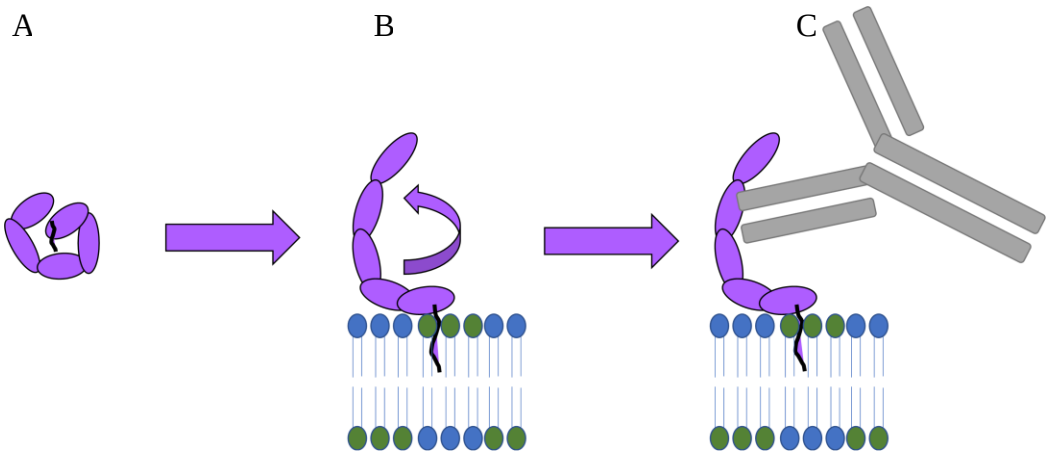

Figure 1.4 Beta2 glycoprotein I circulates in a globular conformation (A), before it opens upon binding (B), allowing antibodies to recognize previously hidden antigens (C)

In contrast to the first four CCP domains, the fifth domain contains a positively charged site that binds to negatively charged moieties such as phospholipids (114, 122, 123). These negatively charged phospholipids include those found on the surface of stressed or damaged cells produced by hypoxia (124). Under hypoxic conditions, negatively charged phospholipids are "flipped" to the surface of the cell and β2-GPI can then bind (124). In addition, the 20 amino acid "tail" extension can be inserted into the lipid bilayer or cleaved by plasmin. Though the "tail" of β2-GPI inserts into the lipid bilayer, it is not necessary for the binding of the protein to the negatively charged phospholipids (114, 125). The cleavage of the tail results in a functional "cleaved" or "nicked" form of β2-GPI (114, 125). Though the tail is not necessary for β2-GPI binding, the fifth domain of the protein contains the binding domain allowing for β2-GPI to bind and change conformation.

β2-GPI normally functions in many systems in vivo. In coagulation, β2-GPI inhibits coagulation through several mechanisms, including the inhibition of thrombin activation and inhibition of factor H (126, 127). While β2-GPI has been well investigated as an anticoagulant (126, 128–130), further research has revealed that it can also function as a procoagulant (131–133). It also inhibits activated protein C, which reduces anticoagulant production (134). With both pro- and anticoagulant functions, β2-GPI is complex in its function within coagulation.

β2-GPI is also associated with autoimmune disorders, particularly anti-phospholipid syndrome (APS). In APS, autoantibodies target proteins associated with phospholipids, resulting in thrombosis and obstetric morbidity and miscarriages. Anti-β2-GPI antibodies are one of the criteria for an APS diagnosis (135). The other two antibodies required for diagnosis, anti-cardiolipin and lupus anticoagulant, are believed to be dependent on β2-GPI as well (136). Anti-cardiolipin, from APS patients binds to β2-GPI on the surface of cells, and lupus anticoagulant was shown to increase β2-GPI sensitivity (120, 137, 138).

Though the protein contains several “complement control” domains, the exact function of β2-GPI in the complement system is unclear. β2-GPI was initially found to be a complement inhibitor (139). It inhibits C3a generation, and enhances C3b cleavage, further limiting complement (139). However, evidence also suggests that β2-GPI can perform the opposite function. In APS, antibodies bound to β2-GPI caused complement activation and deposition (140, 141), suggesting that β2-GPI can initiate and regulate the complement system.

β2-GPI also functions in ischemia and reperfusion (IR), the deprivation of blood flow followed by a reperfusion of blood and oxygen. Ischemia and the subsequent reperfusion result in damage to tissue and further inflammation. However, injury from IR is dependent upon complement activation (142, 143). This complement activation is initiated by β2-GPI after being

bound by anti-β2-GPI antibodies and activating the classical pathway of complement. Domain V of β2-GPI and peptides derived from domain V can prevent complement activation and mitigate damage (144, 145).

Another example of the contrasting functions occurs with β2-GPI and angiogenesis, the growth of new blood vessels. β2-GPI produces opposing effects on angiogenesis that change with both conformation and concentration. In both the native and "nicked" forms, lower (<0.4 μM) concentrations of β2-GPI bind angiostatin, an angiogenesis inhibitor, and allow increased angiogenesis (146). However, both conformations of β2-GPI at higher concentration (>1 μM) reduce angiogenesis by disrupting endothelial cell cycles and suppressing VEGF (147–149). β2-GPI also downregulates KDR expression to limit angiogenesis (150). The contrasting functions regarding angiogenesis may be due to the differences in concentration, but that is unclear.

Peptides

As β2-GPI functions as a neo-antigen during IR, the peptides were designed to compete with β2-GPI for binding and attenuate the damage. Several β2-GPI –derived peptides were derived from the lipid-binding region of Domain V. Multiple peptides, including p296 were derived from overlapping sequences to cover the positively-charged lipid binding domain and the "tail" that inserts into the lipid membrane (145). A scrambled peptide p16ss was designed as a scrambled sequence of amino acids to provide a control for peptide treatments. Peptide p296 (H-IHFYCKNKEKKCYSTVEAHCRDGTI-OH) covered the CKNKEKKC motif responsible for binding negatively charged phospholipids as previously discussed (112, 114, 145). The presence of the motif in the peptide allowed for competition with β2-GPI and resulted in a reduction of IR damage both before and during ischemic events (145, 151).

Peptide p296c-s was derived from the same 26 amino acids as p296c-s, with the cysteines substituted with serines to prevent the formation of disulfide bonds (H-IHFYSKNKEKKSSYTVEAHSRDGTI-OH) (145, 152) (Figure 1.5). From within p296c-s a shorter, more cost-effective peptide p9 (SSYTVEAHS) was designed to provide the same competition. From p9, the retro-inverso peptide RD-p9 (D-SHAEVTYSS) was created utilizing the D form of the amino acids (151). These smaller peptides also significantly reduced IR-related damage when administered before or after the ischemic event (145, 151).

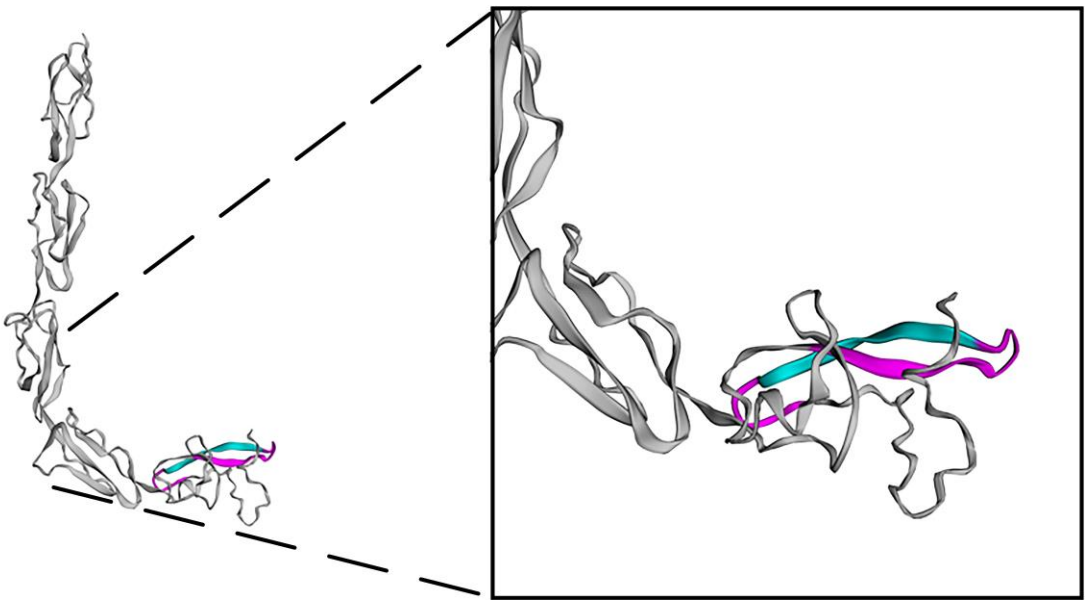

p296 (pink):	H-IHFYCKNKEKKCYSTVEAHCRDGTI-OH
p296c-s:	H-IHFYSKNKEKKSSYTVEAHSRDGTI-OH
p9 (teal):	SSYTVEAHS
RD-p9:	D-SHAEVTYSS

Figure 1.5 Peptides derived from domain V of β2-GPI.

Peptides p296 was derived from domain V of β2-GPI, with p296c-s being the same sequence with each cysteine replaced with serine. p9 was developed from 9 amino acids within p296c-s, and RD-p9 was formed with the D-amino acids of p9 in the reverse order. Protein image made in EZMol (http://www.sbg.bio.ic.ac.uk/ezmol/)

Macrophages

Macrophages are white blood cells that function as part of the innate immune system. Circulating in the blood as monocytes, macrophages phagocytose pathogens, apoptotic cells, and debris. Macrophages also present antigens that have been phagocytosed and secrete distinct cytokines depending on stimulus. When determining the effects of treatments on cell behavior, *in vitro* assays commonly utilize an immortalized cell line for initial experiments. J774A.1 cells are a macrophage-like cell line derived from *Mus musculus* (BALB/cN) generated from fluid-filled ascites from reticulum cell sarcoma. J774A.1 cells continuously secrete IL-1β, are capable of antibody dependent phagocytosis, and their growth is halted by LPS (153–155).

A better metric of macrophage behavior can be determined using bone marrow-derived macrophages (BMDMs). This term includes naïve stem cells that have been removed from the bone marrow of mice that are then differentiated into macrophages in culture. The differentiation of stem cells into monocytes is done by culturing them in media that contains colony-stimulating factor 1 (M-CSF or CSF-1). The addition of the M-CSF, a hematopoietic growth factor, will differentiate the cells into a homogenous population of macrophages (156). These macrophages can then be polarized to different phenotypes for further experimentation.

Macrophage phenotypes

Macrophages can be categorized into different phenotypes. Though these phenotypes were established *in vitro,* they can also be applied in more variable *in vivo* conditions. Macrophage phenotypes are based on their secretions and function within the immune response and can be broadly classified as M1 or M2. There are other smaller subsets of macrophage classification, and subsets within the broader category of M2 as well (Figure 1.6).

M1 macrophages

Originally referred to as classically activated macrophages, M1 macrophages are polarized with LPS and IFNγ and express a pro-inflammatory phenotype. In cancer, these macrophages are associated with tumor cell death and tumor control. Their pro-inflammatory phenotype also helps control angiogenesis and prevent tumors from metastasizing.

One of the hallmarks of M1 macrophages is the expression of inducible nitric oxide synthase (iNOS). iNOS is an enzyme predominantly expressed by macrophages (Reviewed in 136). iNOS breaks down arginine to produce nitric oxide (NO), which then reacts with superoxide and is used to kill foreign cells and increase the inflammatory response (158). iNOS expression and nitric oxide production are associated with M1 pro-inflammatory cytokines (159). High concentrations (>500 nM) of NO are tumoricidal, and can mitigate tumor growth by increasing inflammation and damaging tumor cells (160–164). However, maintaining low (<100nM) concentrations of NO increases angiogenesis and prevents a developed immune response, allowing for continued cancer growth (165–168). This lower concentration of NO is maintained by endothelial nitric oxide synthase (eNOS), present on endothelial cells (168, 169).

M1 macrophages are also identified by their pro-inflammatory cytokine secretion. For instance, IL-1β is an inflammatory cytokine usually associated with autoimmune and autoinflammatory diseases (Reviewed in 155). IL-1β is well known for its anti-tumor function (171–173). Treatments utilizing IL-1β reduced tumor growth in mice, but were less successful in human trials (171, 173, 174). TNFα is a pro-inflammatory cytokine secreted by macrophages. TNFα is a pyrogen associated with systemic inflammation and is upregulated in inflammatory diseases (175–179). Initially, TNFα was discovered as a cytotoxin induced by endotoxin that caused necrosis in tumors (180). Additionally, clinical inhibition of TNFα can lead to

malignancies, particularly melanoma (181–185). Both IL-1β and TNFα can induce low-level inflammation to increase tumor growth but are primarily used by the immune system to prevent tumor growth.

Another cytokine, the interleukin IL-6 is both an anti- and pro-inflammatory cytokine secreted by macrophages. The interactions of IL-6 with various forms of cancer have been extensively investigated, and IL-6 was found to increase rather than reduce tumor growth (Reviewed in 165). IL-6 is highly upregulated in many cancers and has been proven to increase metastasis, angiogenesis, tumor growth, and aid in treatment resistance (186–189). Patient prognosis declines with higher IL-6, and treatments targeting IL-6 have been shown to reduce tumor growth (187, 190–192). IL-6 also polarizes macrophages to an M2, anti-inflammatory phenotype (193–195). Though it is both pro- and anti-inflammatory, IL-6 functions as a pro-tumor cytokine and target for therapeutics.

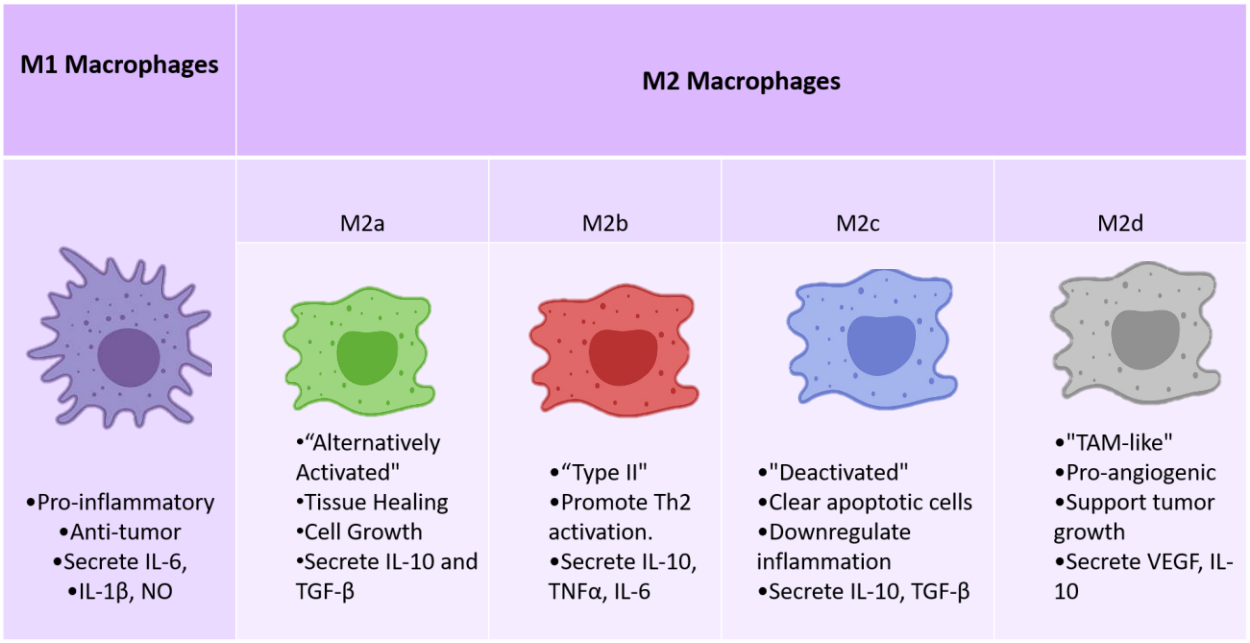

Figure 1.6 Macrophages are categorized into multiple in vitro categories.

Macrophages can be arranged into separate categories in vitro based on the behavior and secretions of the cell. While classically activated M1 macrophages only have one subtype, M2 macrophages have several subtypes that are all generally anti-inflammatory and perform different functions. Created with BioRender.com

M2 macrophages

The other broad phenotype of *in vitro* macrophages is the M2 macrophage. Split into M2a, b, c, and d, these macrophages are generally anti-inflammatory but perform functions ranging from regulating inflammation to promoting wound healing (196–198). M2a macrophages, characterized by stimulation from IL-4 or IL-13, were initially considered the only form of "alternatively activated" macrophages. M2a macrophages secrete increased IL-10 and TGF-β and promote tissue healing and cell growth. Originally called type II macrophages, M2b macrophages are polarized with LPS or IL-1β, through TLR4 or IL-1R (196). M2b macrophages produce increased IL-10, but the secretion of increased TNFα, and IL-6, makes them the "least anti-inflammatory" of the M2 phenotypes (197). M2c macrophages are stimulated by TGFβ, and are sometimes considered "deactivated" macrophages, in that they primarily downregulate inflammation and clear apoptotic cells (199). The illusive M2d phenotype is a more recent characterization that expresses a phenotype similar to tumor-associated macrophages (TAMs). M2d macrophages are polarized with adenosine, and produce IL-10 and VEGF (200).

Overall, TAMs express a primarily anti-inflammatory phenotype to prevent immune destruction of the tumor and encourage angiogenesis (75, 201–203). An increased number of TAMs is also associated with increased tumor survival and metastasis along with poor patient survival prognosis (204–206). The association with patient prognosis allows TAMs to be assessed clinically as a factor of cancer treatment.

Though a concrete phenotype has yet to be established, there are cell surface markers and secretions that are commonly associated with TAMS. Arginase 1 (Arg-1) is an enzyme that breaks down arginine into ornithine and urea, and is one of the primary hallmarks of M2 macrophages (157, 207, 208). Arg-1 prevents the production of pro-inflammatory NO by

limiting available arginine, and thus is associated with the anti-inflammatory macrophages and TAMs.

CD163, originally referred to as M130, is a 150 kDa scavenger receptor expressed only on monocytes and macrophages (209, 210). Though its role in tumor growth and TAM activation has only recently been investigated (211), the high expression of CD163 on TAMs has made it a target for cancer analysis and treatment. High numbers of CD163+ macrophages, and thus TAMS, are associated with poor tumor prognosis in many cancers, including melanoma, bladder cancer, and breast cancer (212–218).

TAMs are also identified by their cytokines and secretions. Originally discovered to suppress CD4+ T-cell proliferation (219), IL-10 is an anti-inflammatory cytokine secreted by monocytes and is considered a hallmark of M2 macrophages (220, 221). It inhibits the secretion of the pro-inflammatory cytokines usually produced by M1 macrophages, such as IL-1β and TNFα, (220, 222, 223). IL-10 secreted by TAMS has been associated with treatment resistance (224). IL-10 in cancer also promotes tumor angiogenesis and metastasis (225–227). However, IL-10 in breast cancer and colorectal cancer can reduce tumor growth and metastases and improve anti-tumor immune response (228–232). Importantly, overexpression of IL-10 in the B16F10 melanoma cell line resulted in tumor destruction by the immune system (233, 234). Secretion of this anti-inflammatory cytokine is one of the hallmarks of TAMs and M2 macrophages but can both improve and inhibit tumor growth.

IL-4 is another cytokine associated with M2 macrophages. IL-4 stimulates B- and T- cell proliferation and decreases production of TH1 cells and macrophages and downregulates IFNγ and IL-12 (Reviewed in 178). It also promotes the differentiation of macrophages into the M2 anti-inflammatory phenotype and prevents the activation of classical M1 macrophages. TGF-β,

another polarizing cytokine, regulates cell growth and proliferation, and promotes angiogenesis. Rather than limiting pro-inflammatory cytokines as IL-10 does, TGF-β restricts the activation of immune cells such as B cells, cytotoxic T cells and macrophages (236–239). TGF-β also polarizes macrophages towards the M2c phenotype, further reducing inflammatory responses. Altogether, while TAMs can produce cytokines that restrict tumor growth, TAMs are primarily M2-like and secrete many cytokines that aid in tumor growth and angiogenesis.

Macrophages and melanoma

Macrophages often make up the largest percentage of immune cells within a tumor (240–242). Originally identified as "monocytic infiltrates", high numbers of macrophages were discovered to aid in tumor progression (240, 243). Early stages of melanomas (Stage I or II) often have a lower density of infiltrated TAMS in the tumor tissue (244, 245). In contrast, a higher density of infiltrated TAMS is associated with poor patient survival and increased tumor thickness (244–246). The importance of TAMs, however, goes beyond the density of macrophages within the melanoma.

TAMs were initially found to differ from the "classically activated" phenotype, and eventually confirmed to be an M2-like, pro-tumor phenotype (247, 248). The resulting anti-inflammatory TAMs support tumor growth and survival (75, 201–203, 249). To benefit from the pro-tumor TAM phenotype, the tumor and endothelial cells secrete cytokines to change macrophage phenotype. This can occur through cytokines that polarize the macrophage such as IL-4, or IL-10 (200, 250–252) (Fig. 1.7 A). Macrophage phenotypes can also be altered through the tumor's hypoxic microenvironment (59, 159, 203). The tumor microenvironment also attracts more macrophages to infiltrate the tumor tissue. Attraction of macrophages occurs through chemokines such as MCP-1 that are secreted by tumor cells (253, 254). More recently, it was

discovered that hypoxia within the tumor both prevents MCP-1 driven macrophage migration and causes a shift towards a pro-angiogenic macrophage phenotype (255–259). The tumor microenvironment utilizes hypoxia, cytokines, and chemokines to attract macrophages and polarize them towards a phenotype that increases melanoma growth.

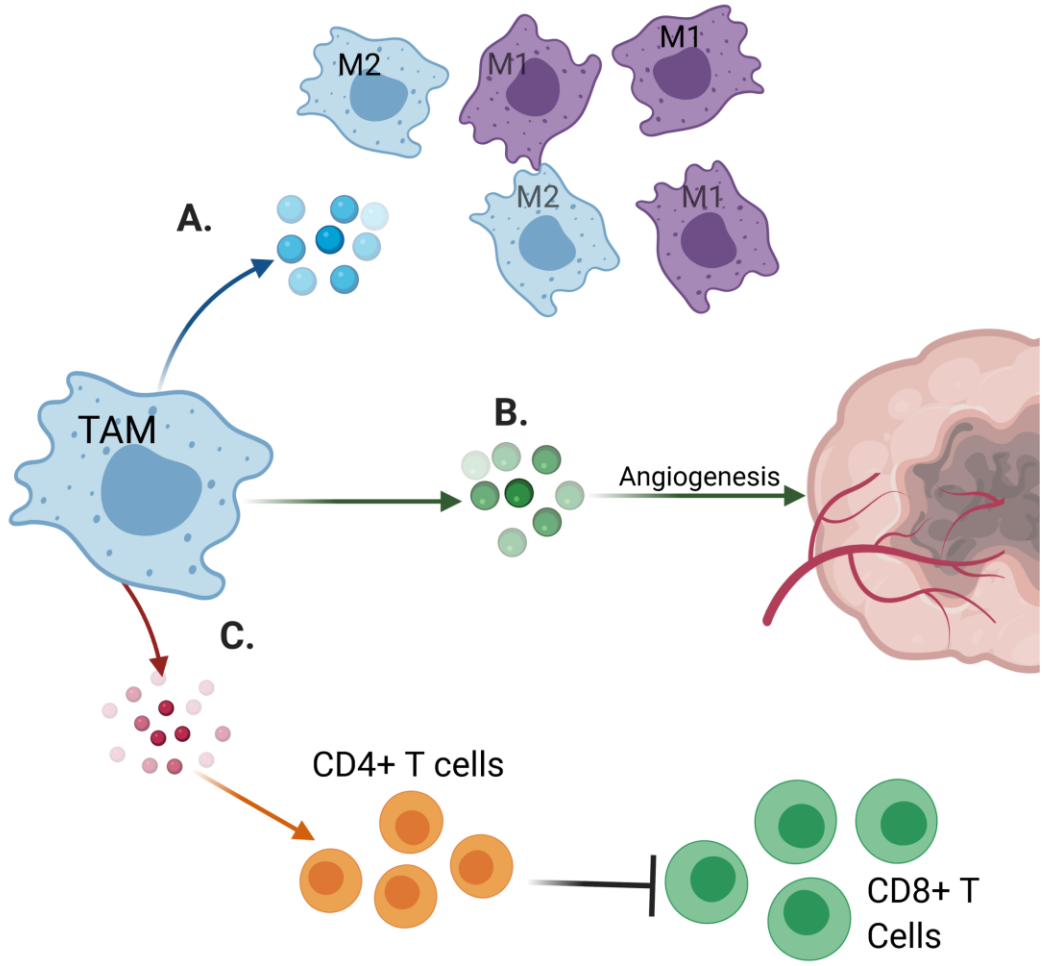

Figure 1.7 TAMs can support melanoma growth through several mechanisms.

TAMs assist in melanoma survival through several mechanisms. This includes the conversion of macrophages to a pro-tumor M2 phenotype through cytokines such as IL-4 and IL-10 (A). TAMs also secrete cytokines such as VEGF-A to increase angiogenesis and tumor cell migration (B). TAMS also utilize cytokines such as TGF β to stimulate CD4+ T cells to suppress CD8+ T cell anti-tumor immune response.

Function of macrophages in melanoma

In melanoma, M2-like macrophages are a key factor in tumor growth and survival (217, 241, 260). Along with an anti-inflammatory phenotype, the macrophages conditioned by melanoma secretions promote tumor cell migration (261, 262). These conditioned M2-like macrophages signal for angiogenesis and promote tumor growth (217, 263–265) (Fig 1.7 B). Thus, a higher number of macrophages in the tumor tissue is clinically associated with increased angiogenesis and the secretion of pro-angiogenic cytokines (264, 266, 267). The tumor supporting functions of the macrophages make TAMs an essential component of tumor survival and tumor progression.

Another essential function of TAMs is the suppression of the anti-tumor immune response. TAMs were originally categorized by their secretion of anti-inflammatory or immune-suppressing cytokines (Reviewed in 265). TAMs reduce the anti-tumor CD8+ T cell response (21, 234, 260, 269, 270). TAMs work in conjunction with CD4+ lymphocytes to suppress the CD8+ T cell-mediated anti-tumor response and increase tumor survival (271–273) (Fig 1.7 C). A low CD8+/TAM ratio is associated with reduced patient survival and increased tumor aggression (213, 244).This immune suppression supported by TAMs can be resolved by targeting the macrophages in question, which then reduces tumor growth and survival (269, 274, 275). Thus, the presence of TAMs benefits the tumor in a myriad of ways that promote and preserve tumor survival.

Unlike the M2-like phenotype exhibited by TAMs, macrophages with an anti-tumor phenotype can prevent tumor growth and improve patient recovery. The addition of M1 macrophages to mouse melanoma can prevent metastases (276, 277). Treatments polarizing TAMs towards an M1 phenotype in melanoma reduce melanoma growth, the growth of

metastases, and treatment resistance (265, 269, 278–281). Similarly, depletion of macrophages in the tumor can improve the effectiveness of radiotherapy and reduce tumor growth (269, 273, 282). Furthermore, a higher number of M1 macrophages is associated with better patient prognosis (213, 283, 284). Altogether, anti-tumor M1 macrophages can combat the tumor-supporting TAM macrophages.

TAMs benefit tumors by increasing angiogenesis and metastasis, as well as suppression of the anti-tumor immune response. These benefits are innately tied to the pro-tumor phenotype that is caused by the tumor microenvironment. Although TAMs support tumor growth and survival, treatments inhibiting the pro-tumor phenotype or increasing M1 macrophages can instead reduce tumor growth. The dual nature of macrophages provides a promising target for future therapeutics.

Conclusion

Melanoma is a rising concern in the United States, with rates of diagnoses increasing every year. Angiogenesis and TAMs are only two of the many facets of tumor growth but are both becoming more evident as possible therapeutic targets. Particularly the interactions between the two; TAMs often increase the rate of tumor angiogenesis while in turn angiogenesis in tumors often leads to hypoxia and signaling that increases the migration of macrophages into the tumors. The involvement of cytokines between TAMs and angiogenesis are complicated and sometimes contradictory. Cytokines such as IL-10 and IL-1β both improve tumor growth and at other times prevent tumor survival altogether. While low concentrations of NO improve angiogenesis and endothelial growth, the higher concentrations produced by iNOS kill tumor cells. Less opposing cytokines such as TGFβ prevent the anti-tumor immune response and polarize macrophages to the more anti-inflammatory phenotype characteristic of TAMs.

In addition, there has been an increased focus on both angiogenesis and TAMs as therapeutic targets in the treatment of cancer. From limiting the growth of blood vessels to the "reprogramming" of TAMs to target tumor cells instead, treatments are focusing on turning pro-tumor functions against cancer in hopes of a more successful treatment. This includes β2-GPI, a protein which was initially used to target angiogenesis only to reveal its dual nature of promotion and inhibition of the growth of new blood vessels.

As this thesis will discuss, a possible therapeutic may still exist in the peptides derived from the binding domain of β2-GPI. We hypothesize that these peptides will compete with β2-GPI for binding and reduce melanoma growth. As the literature indicates β2-GPI can increase and decrease angiogenesis, the peptides may reduce tumor growth by regulating angiogenesis. Furthermore, changes in angiogenesis can also affect TAM phenotype, and the subsequent change may alter the inflammatory response and reduce melanoma growth. If the peptides are successful, we will have a new possible therapeutic in the treatment of melanoma.

Chapter 2 - Beta2 Glycoprotein I Derived Therapeutic Peptides Induce sFlt-1 Secretion to Reduce Melanoma Vascularity and Growth

Haley Smalley[a], Jennifer Rowe[a], Fernando Nieto[a], Jazmin Zeledon[a], Kellyn Pollard[a], John M. Tomich[b] and Sherry D. Fleming[a]

[a] Division of Biology, Kansas State University, [b] Department of Biochemistry and Molecular Biophysics

This chapter will be published *Cancer Letters,* Volume 495:

Smalley, H., J. M. Rowe, F. Nieto, J. Zeledon, K. Pollard, J. M. Tomich, and S. D. Fleming. 2020. Beta2 glycoprotein I-derived therapeutic peptides induce sFlt-1 secretion to reduce melanoma vascularity and growth. *Cancer Lett.* 495: 66–75.

1. Introduction

Melanoma is an aggressive cancer that is rapidly becoming one of the most common cancers in young adults (7). As tumors grow, the microenvironment becomes hypoxic and requires angiogenesis to provide nutrients. Normal angiogenesis forms well-organized, intact blood vessels characterized by CD31 expression, regulated growth factors, and limited vascular permeability (67, 68, 83). However, hypoxia in tumors leads to abnormal vascularization and tumor progression (47, 57, 63). Vascular abnormality is characterized by increased growth factor receptors, endosialin expression, and disorganized blood vessels (47, 57, 68). The disorganized vessels result in increased hypoxia, decreased immune responses, and tumor progression (47, 57, 68). Tumor treatments that reduce hypoxia by normalizing tumor vasculature result in decreased tumor growth with enhanced immune responses and chemotherapeutic responses (68).

Vascular endothelial growth factor (VEGF) and its receptors, VEGF receptor 1 (VEGFR1) (Flt1) and VEGFR2 (KDR) are critical to angiogenesis. However, dysregulated, high concentrations of VEGF and its receptors lead to abnormal angiogenesis (67, 83). VEGF initiates angiogenesis by binding KDR (VEGFR2) and inducing endothelial migration by binding Flt-1 (VEGFR1). In the process, KDR also decreases the endothelial barrier, thus increasing vascular permeability (83). Soluble Flt-1 (sFlt-1) regulates angiogenesis by competitively sequestering VEGF (41), resulting in reduced tumor growth (89, 90). Angiogenic markers that identify the abnormal tumor blood vessels include endosialin (CD248; TEM1) and endoglin (CD105). Endosialin is expressed on endothelial and stromal cells associated with tumor angiogenesis and found only at low levels on normal endothelium (99, 100). Endoglin functions as a co-receptor for TGF-β (101) and is a diagnostic marker for tumor endothelium (103).

Angiostatin and Beta2-glycoprotein I (β2-GPI) are additional serum proteins that regulate angiogenesis. While angiostatin, a cleavage product of plasminogen (43), was not successful as a therapeutic (109), a β2-GPI therapeutic has not yet been developed. β2-GPI contains five complement regulatory domains (285). The 5^{th} domain binds to negatively charged lipid moieties (123, 286, 287) expressed on apoptotic and hypoxic cells (288, 289). β2-GPI binding to endothelial cells regulates angiogenesis (146, 150, 290) and induces antibody (Ab)-mediated, complement activation (145). Upon binding, β2-GPI unfolds (136) and exposes a neoantigen (116) recognized by naturally-occurring antibodies (118). Compared to other domains, the binding domain of native β2-GPI contains an additional 20 amino acid (aa) "tail" (147) that inserts into the lipid bilayer or is cleaved by plasmin resulting in "clipped" β2-GPI (125). With a short half-life, "clipped" β2-GPI is difficult to detect in vivo (136). The literature demonstrates that "clipped" and native β2-GPI can produce opposing angiogenic effects (146, 148, 150, 290).

Multiple studies suggest that the native form of β2-GPI inhibits VEGF signaling by downregulating KDR to block angiogenesis (150, 290). However, additional studies indicate that "clipped" β2-GPI inhibits or enhances angiogenic activity in a concentration-dependent response (146, 150, 290). Thus, the angiogenic activity of β2-GPI is complex.

Our previous studies demonstrated that β2-GPI functions as a neo-antigen during acute ischemia/reperfusion-induced intestinal injury and multiple peptides derived from β2-GPI attenuate the damage (145, 288). Specifically, a large 26 aa peptide derived from the binding domain (p296c-s) and a smaller 9 aa retro-inverso D-amino acid peptide (RD-p9) attenuated intestinal inflammation when administered during ischemia or early in reperfusion (145, 151). Importantly, RD-p9 is derived from within the larger peptide p296c-s suggesting it contains a critical set of amino acids within the larger peptide (151). As β2-GPI is critical in angiogenesis and during hypoxia, we hypothesized that the peptides would limit tumor growth by regulating angiogenesis.

2. Materials and Methods

2.1 Cells

The C57Bl/6-derived, mouse endothelial cell line, MS-1, and melanoma tumor cell line, B16-F10, (American Type Culture Collection, Manassas, VA, USA) were maintained in Dulbecco's modified Eagle medium (DMEM) (Gibco, Grand Island, NY, USA) containing 10% Opti-MEM (Gibco), 5% NuSerum Culture Supplement (Fisher Scientific, Pittsburgh, PA, USA), 5% fetal bovine serum (Atlanta Biologicals, Lawrenceville, GA, USA), and 1% Gluta-MAX (Gibco). All cells were cultured at 37 °C in a humidified 5% CO_2 incubator.

2.2 β2-GPI peptides

β2-GPI-derived peptides p296c-s, RD-p9, and the scrambled control peptide were generated by solid phase synthesis in the KSU Biochemistry Core Laboratory at Kansas State University as previously described (151). Peptide p296c-s was derived from 26 amino acids of the lipid-binding region of Domain V of β2-GPI, (H-IHFYSKNKEKKSSYTVEAHSRDGTI-OH). RD-p9, a retro-inverso D-amino acid p9 is derived from 9 aa within p296c-s (Retro D-p9: D-SHAEVTYSS), and scrambled control peptide contains 16 amino acids in a scrambled order (DEVHYTTSSSKKARGI) (145, 151). The peptides were purified by reversed phase HPLC and characterized by mass spectroscopy. All peptides were lyophilized and stored at -20^{o}C until time of use. Peptides were administered at previously determined concentration of 40 μM (145, 151) unless stated otherwise.

2.3 Cell co-culture

MS-1 mouse endothelial cells (ATCC CRL 2279) were cultured with or without B16-F10 mouse melanoma cells (ATCC CRL 6475). The MS-1 cells were seeded into a 24 well plate at $5x10^5$ cells per well and when co-cultured, B16-F10 cells were seeded into 6.5 mm Transwells with 0.4 μm pores (Sigma Aldrich, Darmstadt, Germany) at $1x10^5$ cells per well in 1 mL of media. Cells were treated with scrambled control peptide, p296c-s, or RD-p9 at 40 μM. After 48 h of treatment, the supernatants were collected and analyzed for endoglin, endothelin, VEGF-C and VEGF-A using a MILLIPLEX® Mouse Angiogenesis Magnetic Bead Panel (Millipore Sigma, Temecula, California). The panel was analyzed according to the manufacturer's protocol using the Luminex® 200™ and data processed using MILLIPLEX® Analyst 5.1 software and data collected as pg/mL of supernatant. Supernatants were also analyzed using a Mouse

sVEGFR1/Flt-1 DuoSet ELISA kit (#DY471, R&D Systems, Minneapolis, MN). The cells were collected in TRIzol for transcript analysis.

2.4 MTT assay

MS-1 or B16-F10 cells (5 x 10^5 cells/mL) were seeded in triplicate in 24 well plates in the presence (40 μM) or absence of p296c-s, RD-p9 or scrambled control peptide. Cells were cultured in hypoxic or normoxic (control) conditions. Hypoxic conditions were simulated by culturing cells in a sealed chamber with 0.1% oxygen for 6 hours at 37ºC. After removal from hypoxia, all cells were treated with scrambled control peptide, peptides p296c-s, RD-p9 (40μM) or left untreated for 2 hours prior to incubation for 4 hr with MTT (3-(4,5-Dimethylthiazol-2-yl)-2,5-diphenyltetrazolium bromide) in PBS (phosphate-buffered saline) at a final concentration of 0.5 mg/mL. The crystals were dissolved, and supernatants read at 550 nm on the spectrometer (Biorad Model 680 Microplate Reader, Biorad, Hercules, California).

2.5 Transepithelial electrical resistance

MS-1 cells (1 x 10^5 cells/mL) were seeded in 6.5 mm inserts containing a 0.4 μm polyester membrane. Cells were cultured in hypoxic or normoxic (control) conditions as above. After 2 h of treatment, transendothelial electrical resistance was determined using an epithelial volt-ohm meter. Measurements were expressed as units of resistance in ohms (Ω) after subtracting mean values of resistance of cell free inserts.

2.6 Migration assay

MS-1 cells (8x10^4 total cells) were seeded into silicone culture inserts (Ibidi, Martinsried, Germany) for 24 h in a humidified 5% CO_2 incubator at 37°C to create a standardized wound.

After removal of the silicone inserts and washing, fresh serum-free media was added to each well to assure that cell proliferation did not skew the migration data (291, 292). The endothelial cells were then treated with 40 μM of scrambled control peptide or RD-p9, or a dose response of 40, 20, 10, or 4 μM p296c-s. In some experiments, 0.5 μM anti-sFlt-1 Ab (Fisher Scientific, Waltham, MA) was added with the peptide. At 0 and 48 h, microphotographs (minimum of 4 per wound per time point) were acquired along the length of the wound with a Nikon DS-5M camera using DS-L2 software at 100x magnification. The area of the wound was calculated using ImageJ and the MRI Wound Healing Tool (http://dev.mri.cnrs.fr/projects/imagej macros/wiki/Wound_Healing_Tool). The endothelial cell migration quantification was based on the amount of regrowth across the area of the wound compared to wound size at the 0-time point.

2.7 *In vivo* tumors

C57Bl/6 mice were bred and maintained in the Division of Biology at Kansas State University. Specific pathogen-free male and female mice were kept in a 12 h light/dark cycle with constant access to rodent food and water. All procedures were approved by the Institutional Animal Care and Use Committee (IACUC) and were in compliance with the Animal Welfare Act. B16-F10 cells ($2x10^6$) in Matrigel (1:1) were subcutaneously injected into mice at 10-18 weeks. Mice (7-10 mice per treatment) were injected intravenously with either saline, scrambled control peptide, or peptides p296c-s, or RD-p9 (40 μM; 3 - 9 mg/kilogram depending on peptide size) on days (d) 1, 2, 3, 4, 6, and 8 after tumor injection. Additional peptide treatment regimens were tested with p296c-s injections on d 1, 3, 5, 7, and 9, d 3, 5, 7, and 9, and d 4, 6, and 8. In the dose response studies, 40, 10, or 4 μM of peptide p296c-s was injected intravenously on d 1-4, 6 and 8. *In vivo* tumor growth was measured and calculated daily (length x $width^2$). Additional animals were injected with tumor cells and peptide p296c-s or scrambled control peptide (40 μM

on d 1-4, and 6) with or without 0.2 μg anti-sFlt-1 Ab (Fisher Scientific, Waltham, MA) on days 2, 4, and 6. Due to tumor size, these animals were euthanized on day 8, in accordance with IACUC guidelines which state tumor growth must not exceed 1.5 cm in diameter. Tumors were removed 8-10 days after injection and *ex vivo* volume and diameter of the tumors measured by calipers, with pictures taken before preparation for PCR, immunohistochemistry, and secretion assays. Tumor secretions were collected by incubating the tumors ex vivo in freshly oxygenated Tyrode's solution at 37°C for 20 min and analyzed using a MILLIPLEX® Mouse Angiogenesis Magnetic Bead Panel (Millipore Sigma, Temecula, California) or a Mouse sVEGFR1/Flt-1 DuoSet ELISA kit (#DY471, R&D Systems, Minneapolis, MN). Final secretions were calculated based on pg/mg of total protein determined by BCA assay using a bovine serum albumin standard.

2.8 Immunohistochemistry (IHC)

Tumors sections flash frozen in OCT embedding compound (Fischer Healthcare, Waltham, MA) (8 μm) were cut, placed on slides, and blocked prior to staining with anti-CD31 antibodies (Clone 390, Isotype Rat IgG2a, Biolegend, San Diego, CA) or anti-pan-endothelium antibodies (Clone MECA-32, Isotype Rat IgG2a, BD Pharmingen, San Jose, CA). Additional sections were incubated with the appropriate Rat IgG2a isotype control antibodies (Clone RTK2758, Purified Rat IgG2a κ Isotype Control, Biolegend, San Diego, CA). After washing, the slides were incubated with the appropriate secondary antibodies, washed again, and examined by fluorescent microscopy using a Nikon 80i microscope equipped with a Photometrics CoolSnap cf camera and MetaVue software. Microphotographs were taken by blinded observers and quantified with ImageJ software (https://imagej.nih.gov/ij/docs/examples/index.html).

2.9 Reverse transcriptase PCR

Total RNA was isolated from TRIzol homogenized tumors or cells and RNA concentration determined by nanodrop at 260 nm. cDNA was synthesized from 1 μg isolated RNA using qScript cDNA Synthesis Kit (Quantbio, Beverly, MA) with M-MLV reverse transcriptase and a combination of oligo and random primers.

Reverse-transcriptase PCR (RT-PCR) was performed using SYBR Green fluorescence. RNA was incubated with gene specific primers (Supplementary Table 4.1) at 90°C for 2 min, followed by 50 cycles of 95°C for 10 s, a primer-specific temperature for 20 s (Supplementary Table 4.1) and 72°C for 10 s, before melt curve analysis from 60°C to 95°C in increments of 0.5 °C. All threshold values were normalized to 18s RNA prior to determining the ΔΔCt fold change of Endoglin, Endosialin, CD31, VEGF-A, KDR, and Flt-1 as compared to scrambled control peptide treated cells or saline-treated tumors.

2.10 Statistics

Data are presented as mean ± SEM and significance ($p<0.05$) determined by non-parametric one-way ANOVA with Dunns post analysis to compare all columns, or by Mann Whitney nonparametric t-test (GraphPad/Instat Software).

3. Results

3.1 Peptides increase sFlt-1 secretion and hypoxia-induced vascular permeability but not endothelial cell growth.

Initial studies examined direct peptide toxicity or stimulation on mouse B16-F10 melanoma cells and a mouse endothelial cell line, MS-1. Each cell line was incubated with 40 μM β2-GPI-derived peptides p296c-s, RD-p9, or a scrambled control peptide (p16ss) for 48 h

prior to performing an MTT assay to determine metabolic activity with normoxic or hypoxic conditions. Compared to normoxia, hypoxia significantly decreased proliferation of both cell lines (Fig. 2.1A, B). However, within either normoxia or hypoxia conditions, the control or β2-GPI-derived peptides did not change proliferation or cellular metabolic activity on either melanoma (Fig. 2.1A) or endothelial cells (Fig. 2.1B). To determine if the peptide treatment affected endothelial barrier function, we evaluated the transendothelial electrical resistance. Similar to the metabolic activity, peptide treatments did not change the resistance compared to the scrambled control peptide-treated cells under normoxic conditions. However, compared to untreated or scrambled control peptide treated hypoxic cells, treatment of hypoxic cells with peptides p296c-s and RD-p9 significantly reduced endothelial resistance (Fig. 2.1C). Together, the peptides do not appear to cause direct toxicity to the tumor or endothelial cells but do reduce the formation of a tight barrier in the hypoxic endothelial cells within 48 h.

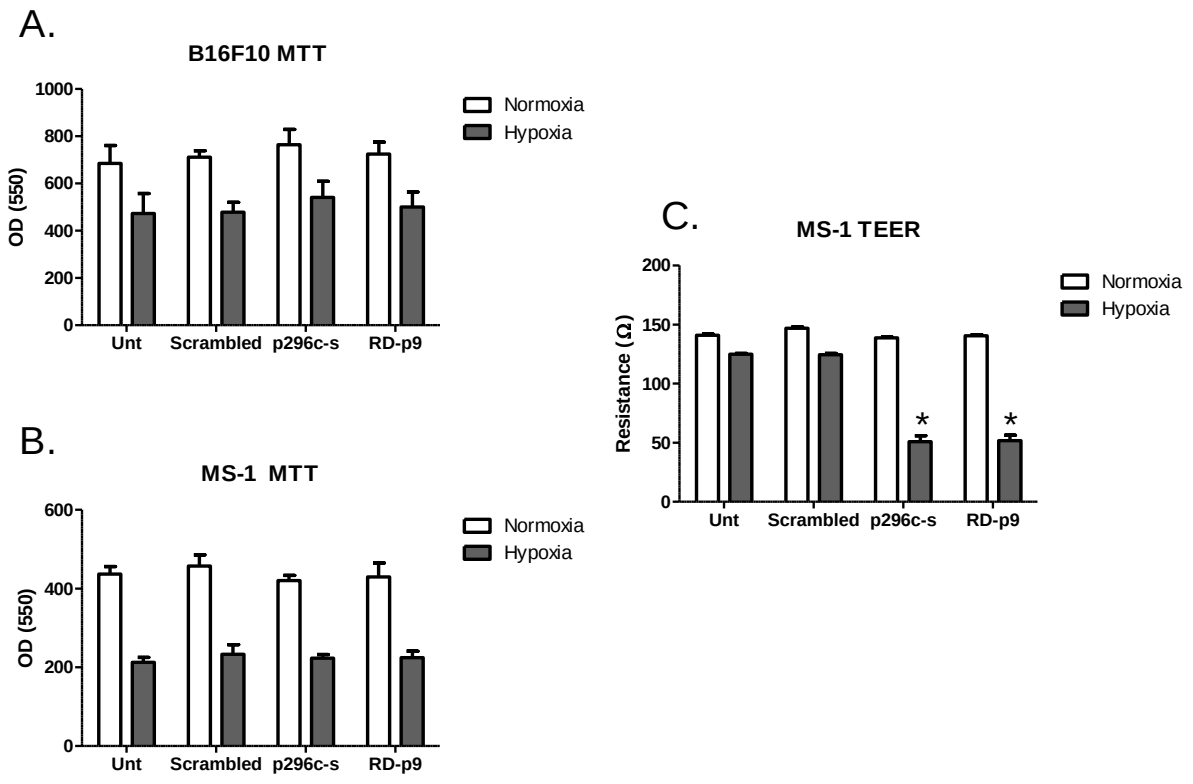

Figure 2.1 The presence of peptides does not alter cell growth or transendothelial resistance.

B16-F10 (A) and MS-1 (B, C) cells were incubated in hypoxic (white) conditions, or normoxic (gray) conditions as a control and treated with 40μM peptides p296c-s, RD-p9, or scrambled control peptide (scrambled) for 2 h prior to adding MTT to determine cell growth (A, B) or measuring resistance by TEER (C). Each bar represents the mean ± SEM of n=3-4 experiments performed in duplicate. * $p<0.05$ compared to p16ss treatment.

To examine the effects of peptide treatment on MS-1 secretion, we determined RNA and protein secretion of specific angiogenic factors. RNA expression of endoglin, endosialin, CD31, VEGF-A, and VEGF receptors, KDR and Flt-1, were not significantly different between peptide treatments (Fig. 2.2A-F). Similarly, secretion of endoglin, endothelin and VEGF-A was not significantly different between peptide treatments or after co-culture with melanoma cells (Fig. 2.3A-C). VEGF-C was not detectable in supernatants from MS-1 or MS-1 co-cultured with B16-F10 melanoma cells (data not shown). However, sFlt-1 secretions were significantly lower in

RD-p9 treated cells and trended lower in p296c-s treated cells ($p=0.11$) compared to the scrambled control peptide (Fig. 2-3D). These data indicate that while peptide treatment did not affect the secretion of other angiogenic factors, it did alter the secretion of the regulatory protein, sFlt-1.

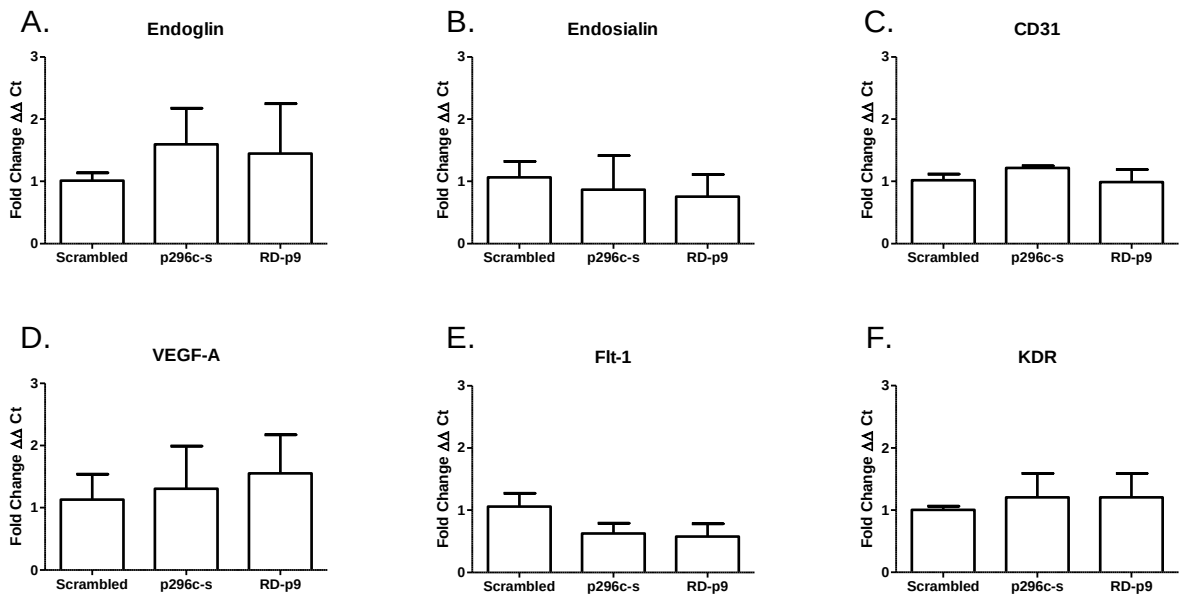

Figure 2.2 Peptides do not affect RNA of angiogenic markers in endothelial cells.

Endothelial cells were cultured with peptides 296c-s, RD-p9, or the scrambled control peptide (40 μM) for 48 h before the cells lysed with TRIzol. Reverse transcriptase PCR of cellular cDNA was normalized to 18s rRNA and ΔΔCt fold change compared to scrambled control peptide-treated cells. MS-1 cells (n=4-6 experiments) were examined for (A) endoglin, (B) endosialin, (C) CD31, (D) VEGF-A, (E) KDR, and (F) Flt-1 RNA. Each bar represents the mean ± SEM. No significance between treatments.

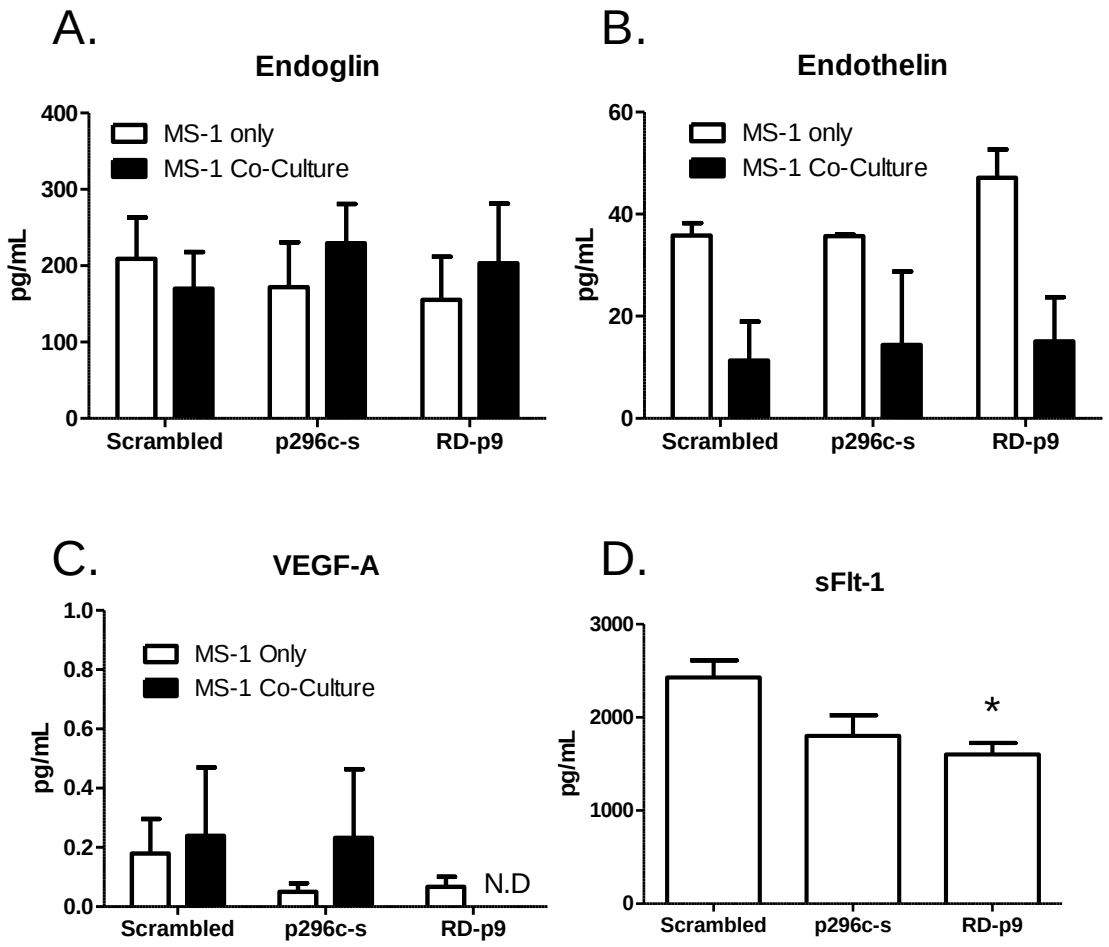

Figure 2.3 Peptides reduce sFlt-1 secretion from endothelial cells.

Endothelial cells were cultured in the presence or absence of B16-F10 melanoma cells and with peptides 296c-s, RD-p9, or the scrambled control peptide (40 μM) for 48 h. Collected supernatants (n=3-5 experiments) were analyzed via Luminex assay to determine levels of endoglin (A), endothelin (B), or VEGF-A (C). Secretion of sFlt-1 (pg/mL) (D) was analyzed via ELISA assay (n=4-5 experiments). All data were standardized to pg/ml supernatant. Each bar represents the mean ± SEM. * $p<0.05$ compared to scrambled control treated cells

3.2 Peptide decreases MS-1 endothelial cell migration in a Flt-1 dependent response

Angiogenesis characteristically induces endothelial migration, which was mimicked in a 48 h wound assay with MS-1 endothelial cells. Initial studies determined that the presence of serum in the assay increased cell replication as well as cell migration (data not shown). Thus, the

assays were performed under serum deprivation conditions to examine only migration and prevent cellular replication from confounding the results (291, 292). All treatment groups had similar wounds sizes at time 0 (Fig. 2.4A). Migration of the scrambled control peptide-treated cells after 48 h resulted in approximately 75% filling of the wound (74.05 ± 2.651 percent regrowth) (Fig 2.4A, B). In contrast, the p296c-s and RD-p9 treated cells significantly reduced regrowth compared to the scrambled control peptide treatment with approximately 40% filling of the wound (p296c-s: 39.95±3.152 percent regrowth, RD-p9:44.75±4.823 percent regrowth) (Fig. 2.4B). In a peptide dose response, lower doses of 20 μM and 10 μM p296c-s also caused a significant reduction in regrowth (39.39±2.865 percent regrowth and 54.794±1.290 percent regrowth, respectively) while 4 μM of p296c-s (77.94±2.951 percent regrowth) was insufficient to alter endothelial migration (Fig. 2.4B). Thus, p296c-s and RD-p9 treatment reduced migration of MS-1 endothelial cells in a dose dependent response. Because peptide reduced secretion of the angiogenic inhibitor, sFlt-1, we tested the hypothesis that wound regrowth was dependent on sFlt-1 secretion. Cells were left untreated or treated with scrambled control peptide or p296c-s (40 μM) with or without 0.5 μM of anti-mouse Flt-1 Ab at 0 h in the wound assay. The presence of anti-Flt-1 Ab significantly increased regrowth of the p296c-s-treated cells from 39.736±8.05 percent regrowth without Ab to 86.661±2.095 percent regrowth in the presence of Ab (Fig. 2.4C). These data indicate that reduced endothelial cell migration caused by β2-GPI-derived peptides is sFlt-1 dependent.

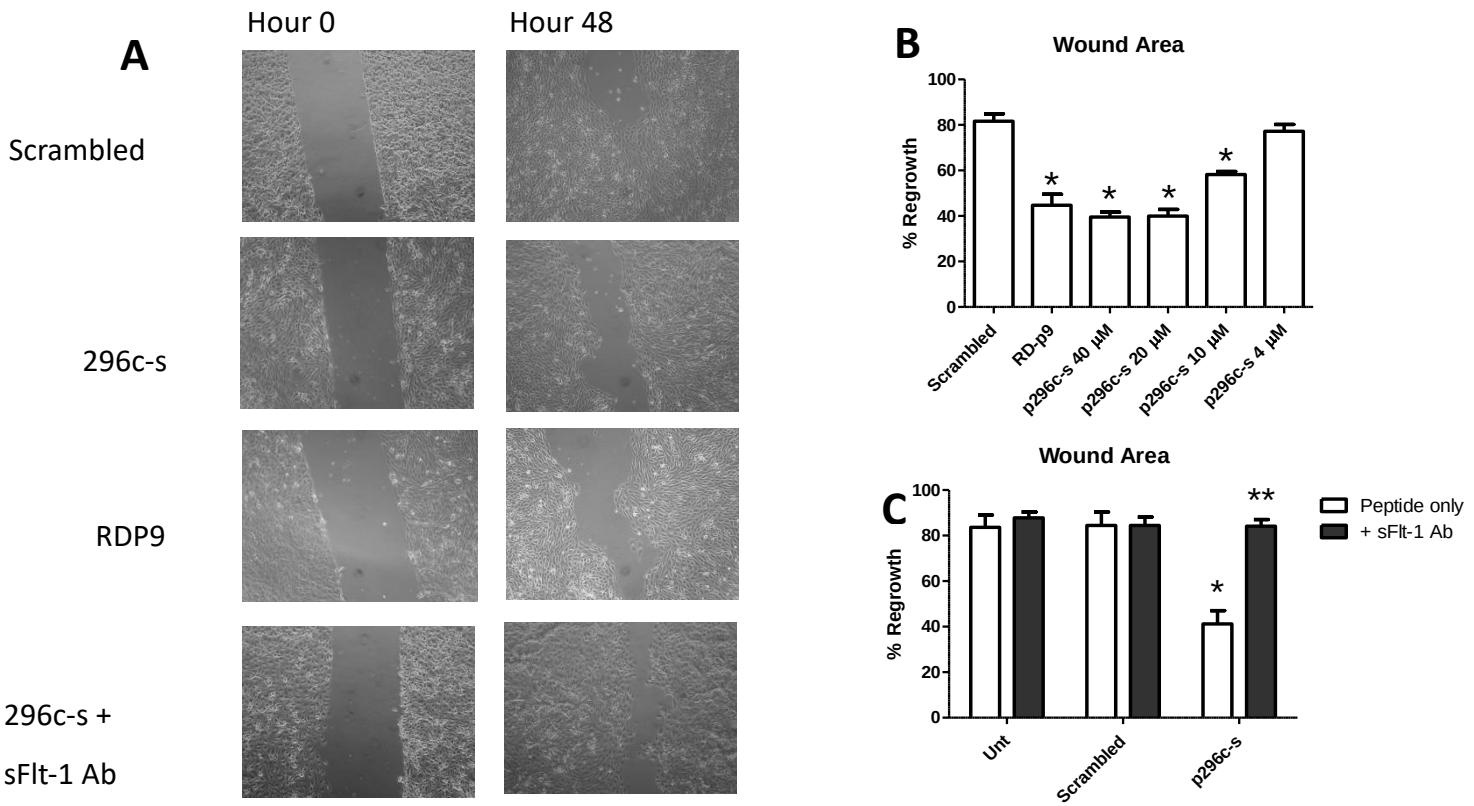

Figure 2.4 Peptides, p296c-s and RD-p9, reduce endothelial cell migration through Flt-1.

MS-1 cells were incubated for 24 h in a 2-chamber silicone insert to create a consistent wound. Cells were treated with the scrambled control peptide (scrambled) (40 μM) RD-p9 (40 μM), or p296c-s (40-4 μM) at time 0. Microphotographs were taken at 0 and 48 h (A) after removal of the insert to determine the rate of cell migration (regrowth) across the wound (B) (n= 5-8 experiments). * $p<0.05$ compared to scrambled control peptide -treated cells. In another study (C) untreated, scrambled or p296c-s peptides cells were incubated with or without anti-mouse Flt-1 Ab (0.5 μM) at time 0 (n=3). Each bar represents the mean ± SEM. ** $p<0.05$ compared to the cells treated without antibody. Each microphotograph is representative of 4 photographs per time point of each wound.

3.3 Peptides result in a dose-dependent, clinically-relevant reduction of mouse melanoma growth.

As β2-GPI can increase angiogenesis and β2-GPI-derived peptides altered the production of the angiogenesis regulator sFlt-1, we hypothesized that peptides p296c-s and RD-p9 would decrease tumor growth in vivo by regulating Flt-1. Tumor growth was measured daily for 10 d after injecting B16-F10 mouse melanoma cells into syngeneic, immunocompetent C57Bl/6 mice. Based on the in vivo, calculated tumor volume, tumors grew more slowly when treated with

p296c-s or RD-p9 treatment than the scrambled control peptide treatment throughout the time course (Fig. 2.5A) (n=7-10 animals per treatment).

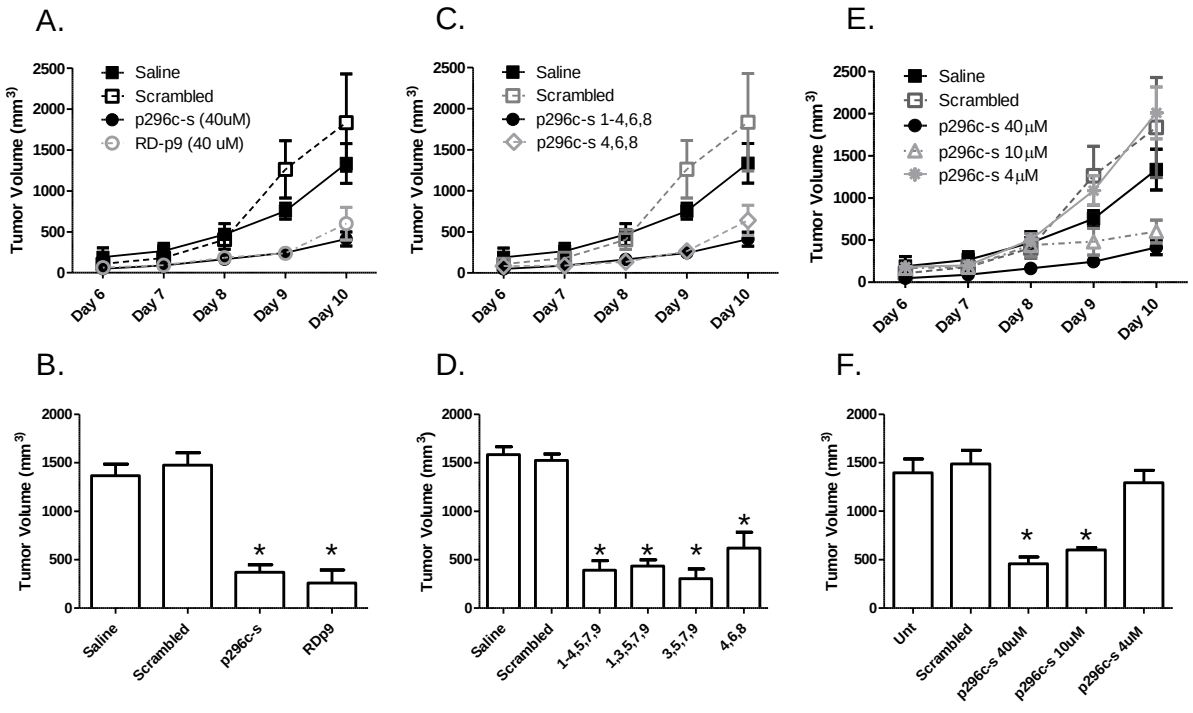

Figure 2.5 Peptide treatments reduce tumor growth.
(A, B) The daily in vivo volume of the tumors treated with saline (■),scrambled control peptide (scrambled) (□) p296c-s (●) or RD-p9 (○) (40 μM) on d1-4, 6, 8 was calculated for 10 days (A.) and excised tumor volume calculated (B) (n=7-10 animals). (C, D) Peptide p296c-s (40 μM) was also measured over multiple treatment regimens (● p296c-s d1-4,6,8; ◊ p296c-s d4,6,8) (C) (n=6-10 animals), with excised tumor volume calculated in (D) (n=6-10 animals). The x-axis numbers in (D) indicate the days of injection. (E,F) A dose response of p296c-s treatment on d1-4,6,8 with 40 μM (●), 10 μM (Δ), or 4 μM (*) (E) and the excised tumor volume calculated in (F) (n=3-6 animals). Treatment with saline (■) or scrambled control peptide (scrambled) (□) are consistent throughout the figure. Each bar represents the mean ± SEM. * $p<0.05$ compared to saline and scrambled control peptide treated tumors.

Measurements of excised tumors confirmed these data. The p296c-s and RD-p9 peptide treatment significantly decreased tumor volume *ex vivo* (Fig. 2.5B). Saline and scrambled peptide-treated tumor volumes averaged 1366±120.1 mm^3 and 1476±128.1 mm^3, respectively. In contrast, p296c-s and RD-p9 peptide treated tumors were 66-75% smaller with average volumes of 370.6±77.04 mm^3 and 260.4 ± 133.8 mm^3, respectively (Fig. 2.5B). Similarly, p296c-s and

RD-p9 peptide treatment reduced *ex vivo* tumor diameter ~25% and 50%, respectively compared to tumors from control mice. Average diameters were 10.35 ±0.6988 mm and 6.437±1.306 mm in p296c-s and RD-p9 peptide, respectively, compared to 14.06±1.093 mm and 14.77±0.6498 mm, saline and scrambled control peptide, respectively.

To explore more therapeutic treatments, additional treatment regimens were tested with peptide 296c-s. Cohorts of animals were treated with peptide p296c-s on days 1,3,5,7, and 9, days 3,5,7,9 or on days 4,6, and 8 after tumor injection. Importantly, tumor growth slowed across all treatments (Fig. 2.5C) with average day 10 in vivo tumor volume of 486±95.317 mm^3 for treatment on d 1,3,5,7,9, 527±139.470 mm^3 d 3,5,7, 9 and 639.144±184.209 mm^3 for d 4,6,8. The calculated volume of the excised tumors was significantly reduced by each treatment regimen analyzed (Fig. 25D). Treatments on d 1,3,5,7,9 (433.9±64.50 mm^3), d 3,5,7,9 (303.9±101.7 mm^3), and d 4,6,8 (621.4±163.5 mm^3) were similar to the 75% reduced tumor volume seen in the d 1-4, 6, and 8 regimen (393±95.65 mm^3). These data suggest the peptide treatment may be clinically relevant.

To determine the optimal peptide dose, a dose response of 40 μM, 10 μM, and 4 μM 296c-s peptide treatment was measured using the original treatment regimen of intravenous injection on d 1-4, 6, and 8 (Fig. 2.5E-F). Treatment with 10 μM p296c-s (601.5±23.72 mm^3 on day 10) reduced tumor growth similar to 40 μM p296c-s (458±71.4 mm^3) and tumor volume significantly differed compared to control treatments (1396±142.7 mm^3 for saline and 1488±140 mm^3 for scrambled control peptide). In contrast, treatment with 4 μM p296c-s did not reduce tumor growth or volume (1294±128.3 mm^3) (Fig. 2.5E,F). The saline or scrambled control peptide treated animals developed large, multi-lobed tumors, while the peptide treated tumors remained small and compact. These significant reductions in tumor volume and diameter

indicate peptides derived from β2-GPI decreased tumor growth in a dose-dependent response and across multiple treatment regimens.

3.4 *In vivo* peptides reduce tumor vessel markers and upregulate sFlt-1 secretion

After identifying a clear reduction in tumor size, we examined tumor RNA and angiogenic secretions. The tumors from mice treated on days 1-4,6,8 with saline, control peptide, p296c-s or RD-p9 peptides (40 μM) were analyzed for RNA expression similar to *in vitro* studies above. Tumors from mice treated with p296c-s and RD-p9 resulted in significant increases of endosialin, endoglin, and VEGF-C RNA compared to the saline control (Fig. 2.6A, B, D). In addition, CD31 and KDR RNA expression was significantly decreased with RD-p9 treatment. In contrast, CD31 expression in p296c-s treated tumor trended downward ($p=0.07$) while KDR expression was not different as compared to the saline treated tumors (Fig. 2.6C, F). Similar to the *in vitro* experiments, Flt-1 RNA was not significantly different between treatments (Fig. 2.6E). Thus, β2-GPI-derived peptides p296c-s and RD-p9 significantly changed angiogenic markers, either up or down but, importantly, Flt-1 RNA was not changed.

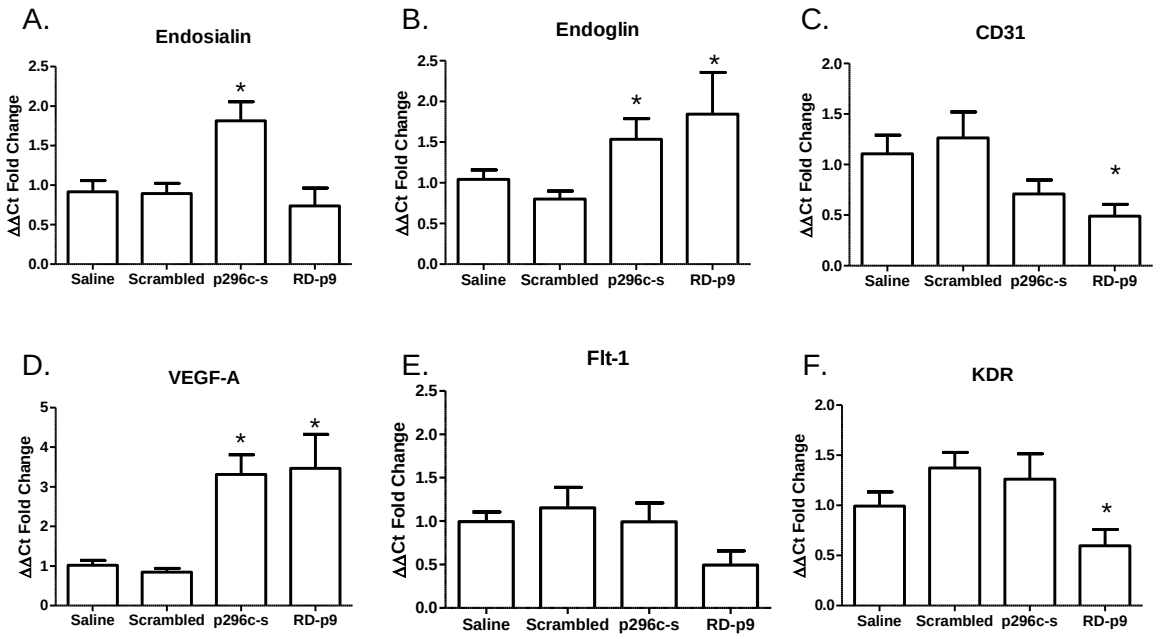

Figure 2.6 Peptide treatments increase VEGF-A, endosialin and endoglin transcription.

Tumors excised from mice treated with or without peptides were homogenized in TRIzol for RNA isolation. Reverse transcriptase PCR of tumor cDNA was normalized to 18s rRNA and ΔΔCt fold change determined by comparison to saline treated tumors. Tumor RNA (n=4-7) was examined for (A) endoglin, (B) endosialin, (C) CD31, (D) VEGF-A, (E) Flt-1, and (F) KDR expression. Each bar represents the mean ± SEM. * $p<0.05$ compared to saline-treated tumors

After identifying the reduction in tumor growth and vascular markers, we examined tumor vasculature using immunohistochemistry (IHC). Tumors from mice treated with either p296c-s or RD-p9 peptide expressed significantly less CD31 (Fig. 2.7A, B) and pan-endothelium (Fig. 2.7A, C) compared to saline or scrambled control peptide treated mice. This reduction in CD31 correlates with the reduced CD31 RNA in Figure 2.6. KDR staining revealed very low levels on tissue with no changes between treatments (data not shown). These data indicate that peptides derived from the binding domain of β2-GPI decrease blood vessel markers in B16F10

melanoma tumors. The decreased tumor blood vessel markers after treatment with β2-GPI-derived peptides suggests that the peptides change vascularity.

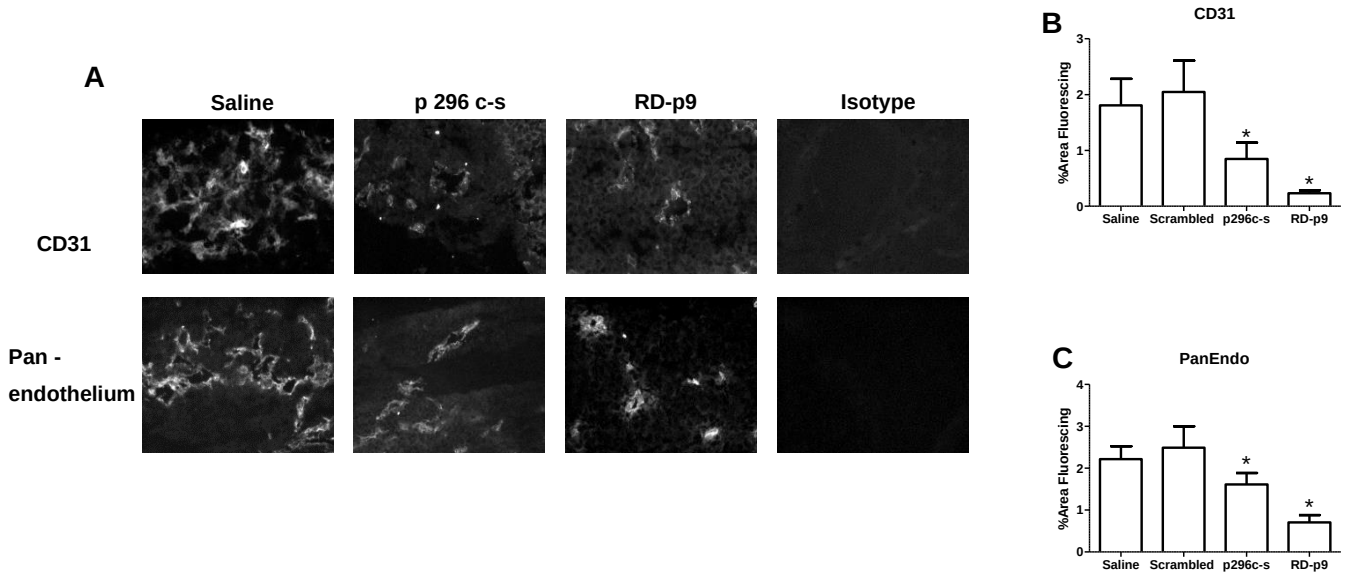

Figure 2.7 p296c-s and RD-p9 reduced deposition of CD31 and Pan-endothelium in tumor tissues.

Tumor tissues from mice treated with and without peptide were stained with anti-CD31, Pan Endothelium, or Isotype control. Slides (8 μm) were prepared from tumors excised on d 10. Microphotographs (A) (200X) are representative of 6-8 photographs from at least 5 different animals. Quantitation of anti-CD31 (B), and pan endothelium (C), staining performed with ImageJ software. Each bar represents the mean ± SEM of 3-6 animals, * $p<0.05$ compared to saline-treated tumors

After identifying a clear reduction in tumor size and vascular markers of peptide-treated mice, we examined tumor angiogenic secretions. Figure 2.8 demonstrates protein secretions varied by specific peptide treatments. Compared to control treatments, endoglin (Fig. 2.8A) significantly increased in both p296c-s and RD-p9 treated tumors, after 10 days. However, endothelin secretion only increased in tumors from RD-p9-treated mice (Fig. 2.8B) and VEGF-C increased only in p296c-s treated tumors (Fig. 2.8C). Importantly, sFlt-1 secretion significantly increased in both the p296c-s and RD-p9 treated mice compared to the control treatments (Fig. 2.8D). These data suggest that peptides change vascularity and regulate sFlt-1 secretion.

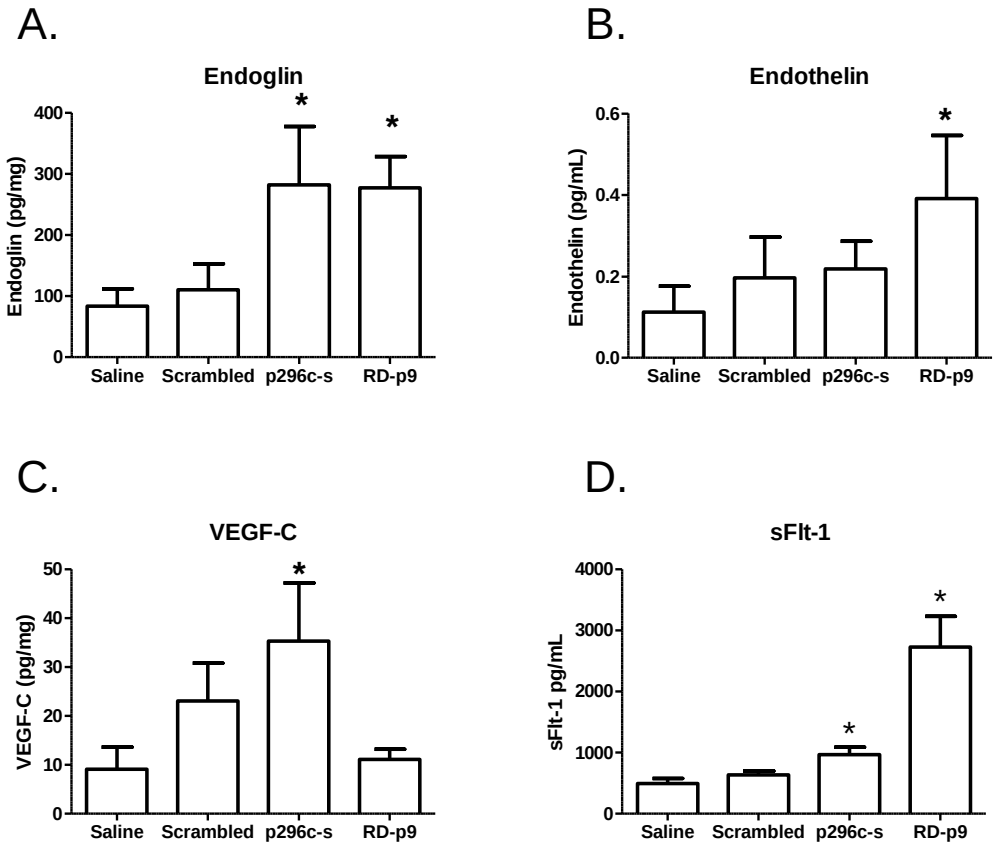

Figure 2.8 Peptide treatments increase VEGF-A, endosialin, endoglin and sFlt-1 protein secretions. Tumors excised from mice treated with or without peptides were incubated for 20 min in Tyrodes buffer at 37 °C for protein secretion calculated as pg/mg tissue. Tumor secretions (n=6-10) were analyzed via LUMINEX assay for (A) endoglin, (B) endothelin, and (C) VEGF-C. Secretion of sFlt-1 (pg/mL) (D) was analyzed via ELISA assay (n=4-5 tumors). * $p<0.05$ compared to saline-treated tumors

3.5 Blockade of sFlt-1 increases mouse melanoma growth

Previous studies indicate that sFlt-1 restricts endothelial cell migration and angiogenesis [9, 10, 11]. To determine if peptide treatment was sFlt-1 dependent, 40 μM peptide p296c-s or scrambled control peptide-treated mice were administered 0.2 μg anti-sFlt-1 Ab or control. In vivo tumor measurements demonstrated that p296c-s with anti-sFlt-1 Ab treatment did not differ from the scrambled control peptide treatment (Fig. 2.9A). Excised tumor volume (Fig. 2.9B)

indicated that treatment with p296c-s and anti-sFlt-1 produced significantly larger tumors (426.3±59.63 mm3) than treatment with p296c-s alone (155±38.79 mm3). The diameter (Fig. 2.9C) of the excised tumor from the p296c-s treated mouse was significantly lower than the scrambled control (4.495±0.941 mm and 11.68±0.4463 mm, respectively). However, peptide 296c-s treatment with sFlt-1 antibody (9.254±0.82 mm) was not significantly smaller than the control treatments. The differences in size are also visible in the photographs of the excised tumors (Fig. 2.9D). These data indicate β2-GPI-derived peptides are sFlt-1 dependent in limiting tumor growth and angiogenesis.

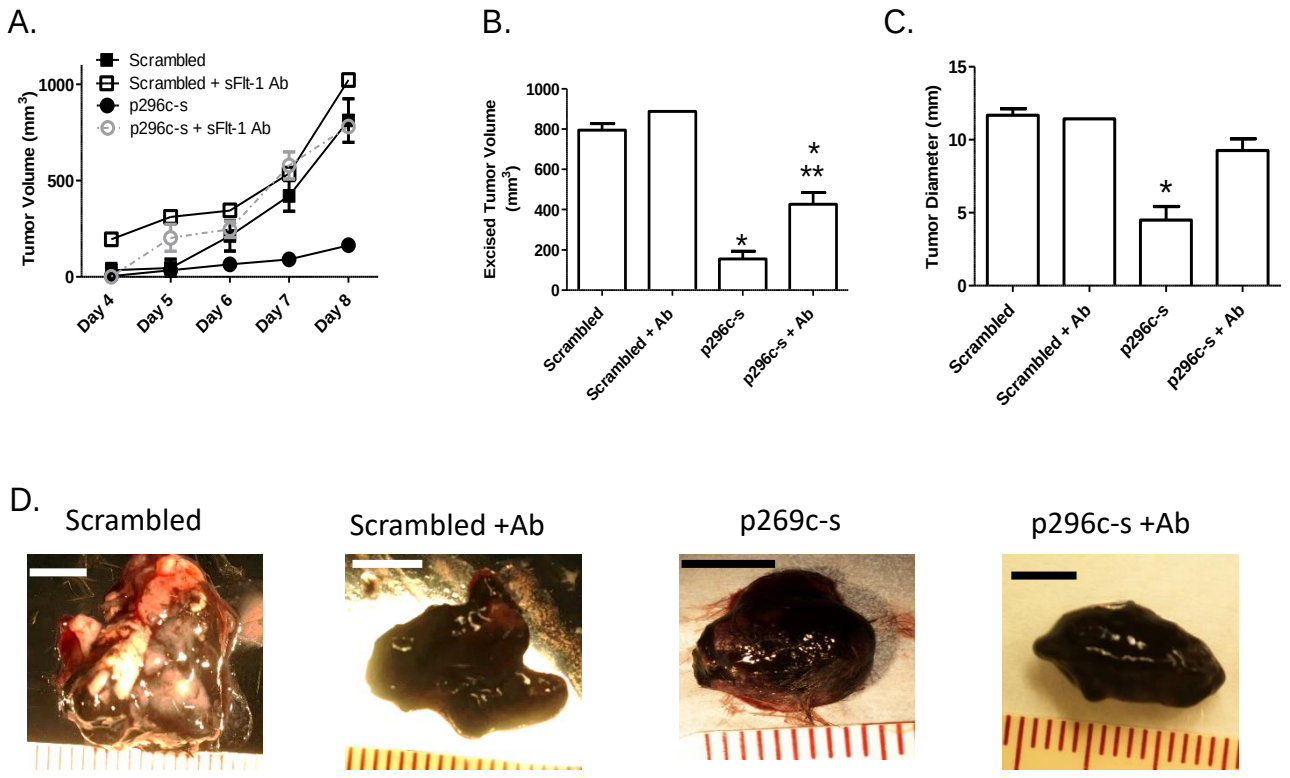

Figure 2.9 Peptide reduction of tumor growth is sFlt-1 dependent.

Tumors were treated on d1-4, 6, 8, with scrambled control peptide (scrambled) (■), scrambled peptide with anti-sFlt-1 antibody (Ab) (□), p296c-s (40 μM) (●), or p296c-s with the anti-sFlt-1(○). The in vivo volumes of the tumors were calculated daily for 8 d (A). After excision on day 8, the tumor diameter (B) and volume (C) were calculated for all four treatments (n=1-4). The scrambled control + sFlt-1 Ab treatment is n=1 as the other tumors had to be harvested earlier due to their size. Photographs were taken of excised tumors (D). Images are representative of 3-4 pictures per tumor. Each bar represents the mean ± SEM. * $p<0.05$ compared to scrambled peptide treated tumors. **$p<0.05$ compared to p296c-s treatment without antibody.

Discussion

Beta2 Glycoprotein I is a highly complex serum protein with a wide range of functions. While the protein has angiogenic properties, (146, 148, 150, 290) the mechanism was unclear. Previous murine studies indicated that β2-GPI-derived peptides, p296c-s and RD-p9, decreased intestinal damage in response to an acute ischemia/reperfusion injury (151). However, the role of the peptides in decreasing tumor growth was unknown. This study demonstrates that peptides p296c-s and RD-p9 induce sFlt-1 secretion to limit B16F10 melanoma growth. The peptide effects were dose dependent and crossed multiple, clinically-relevant treatment regimens.

RD-p9 and p296c-s peptide treatment increased angiogenic markers, specifically sFlt-1 secretion, suggesting that experimental but not control peptides alter the vasculature to reduce tumor growth. Previous studies indicate that in response to hypoxia, increased sFlt-1 reduces angiogenesis by competing with KDR for VEGF binding (41, 293). The increased sFlt-1 also reduces endothelial cell survival and migration resulting in decreased tumor growth (89, 90). While sFlt-1 secretion was decreased in the immortalized cell line, MS-1, it is possible that immortalization or growth conditions may change the cell's responses compared to *in vivo* cells. Anti-sFlt-1 Ab studies indicated that the peptide reduction of endothelial migration (Fig. 2.4C) and in vivo tumor growth are sFlt-1 dependent (Fig. 2.9 A-C). Thus p296c-s and RD-p9 limited tumor angiogenesis and growth by increasing sFlt-1 production.

Recent studies demonstrated that β2-GPI alters VEGF to inhibit endothelial cell migration (148, 149). Our *in vitro* serum-free data indicate the peptides p296c-s and RD-p9 increased sFlt-1 secretion and reduce endothelial cell migration with no change in VEGF-A or VEGF-C (data not shown). Importantly, sFlt-1 secretion sequesters VEGF to decrease

endothelial cell migration and survival (41, 88). Importantly, endothelial migration for the peptide-treated cells was restored completely after the addition of an sFlt-1 antibody, indicating that the sFlt-1 secretion is responsible for the reduction in cell migration. Serum-free media prevented complications due to cell proliferation (291, 292) and avoided addition of native serum β2-GPI. Although addition of serum may skew the results, the lack of growth factors in the serum may also change cell response and cause differences between studies (291, 294).

Tumor hypoxia forms a feedback loop. Hypoxia induces increased abnormal vasculature (60, 62, 295). The abnormal growth and maturation of tumor vasculature compresses vessels resulting in hypoxia within the tumors that assists with tumor immune evasion [3, 6, 43], tumor malignancy (61), tumor progression (47, 61, 295), and treatment resistance (47, 62). It is likely that this hypoxic cycle changes the activity of β2-GPI. Previous studies showed β2-GPI binds to negatively charged moieties expressed on the stressed cell surfaces during hypoxic conditions (124, 145). Other studies demonstrated that "clipped" β2-GPI decreased angiogenesis using *in vitro* studies (146, 149) and *in vivo* (147) matrigel assays. In addition, larger B16-F10 tumors developed the absence of β2-GPI in β2-GPI-deficient mice (290). It was hypothesized that "clipped" β2-GPI may limit or repair the abnormal vasculature, leading to normal vessels for increased immune responses and subsequently limiting tumor growth (47, 57).

Different concentrations of native B2-GPI and its clipped form resulted in opposing effects on angiogenesis through a range of mechanisms (146, 149, 150, 290). Normal circulating levels of β2-GPI are approximately 4 μM (296). Low concentrations (<0.4 μM β2-GPI) of both native and "clipped" forms of β2-GPI prevent the angiostatin inhibition of angiogenesis (146). However, at higher concentrations (>1 μM β2-GPI) native β2-GPI reduces angiogenesis via endothelial cell cycle disruption, plasminogen binding, and VEGF suppression (147–149).

Importantly, higher concentrations (>1 μM β2-GPI) of the "clipped" form of β2-GPI bound to annexin II to mitigate the anti-angiogenic effect (147–149). At 3-10 times the normal B2-GPI concentration, 40 and 10 μM peptide treatments appear to decrease tumor growth similarly, suggesting that a lower, more clinically relevant dose may be sufficient. Together these data suggest β2-GPI concentration differences may induce distinct activity and be responsible for the apparent conflicting literature.

Previous studies showed a reduction in tumor size when increased β2-GPI and "clipped" β2-GPI were injected directly to or close to the tumor environment (290). However, β2-GPI is known to affect a wide range of conditions ranging from pregnancy to stroke and even obesity. Thus, increasing β2-GPI concentrations may result in other off target effects. The current peptide allows for enhanced inflammation and immune response to the tumor by regulation of the vasculature without the addition of increased β2-GPI. Future studies are required to determine the efficacy of β2-GPI-derived peptides delivery routes, such as intra- or peri-tumor, as well as delivering intra-peritoneal or subcutaneous rather than intravenously as in the current study.

In conclusion, peptide inhibition of β2-GPI decreased tumor growth by changing endothelial cell migration and regulating tumor angiogenesis by inducing sFlt-1. Importantly, treatment with anti-sFlt-1 Ab blocked the peptide activity. Furthermore, the peptides functioned in a dose response and in a clinically relevant treatment regimen. Further studies will utilize the β2-GPI-derived peptides to further understand the function of β2-GPI within cancer and the clinical application of the peptides.

Chapter 3 - Beta2 Glycoprotein I Derived Peptides Alter Tumor Associated Macrophages

Introduction

Melanoma is an aggressive cancer that develops from melanocytes in the skin. Over the past several decades, the rate of melanoma diagnoses has steadily increased (3, 4). However, the rate of deaths due to melanomahas not risen due to new treatments targeting different aspects of melanoma survival such as immune evasion (4, 9, 11). Melanoma, like other cancers, manipulates the host immune system to benefit the tumor. The tumor microenvironment attracts macrophages to invade the tumor tissue (203, 249, 297). Furthermore, the tumor microenvironment also manipulates macrophages towards an anti-inflammatory phenotype to increase tumor growth and metastasis (207, 250, 298).

Macrophages are often categorized into two phenotypes, the pro-inflammatory M1 phenotype and anti-inflammatory M2 phenotypes. Macrophages are polarized towards the M1, or “classically activated”, phenotype with LPS and IFNγ, and express surface markers such as CD68 (208, 247). The “alternative” activation of macrophages to an M2 phenotype can be achieved through IL-4, causing the expression of surface markers such as CD206 (200, 299, 300).

The M1, pro-inflammatory phenotype increases inflammation and reduces tumor growth (200, 298). These macrophages secrete pro-inflammatory cytokines and molecules such as IL-1β, IL-6, TNFα, and reactive oxygen species such as NO (250, 301). In particular, the breakdown of arginine leading to NO secretion through the macrophage-specific iNOS is considered a hallmark of the M1 phenotype (248, 302). Secreted NO is used to kill target cells (159, 303), and high (>0.5μM) concentrations of NO are known to be tumoricidal (159, 207, 304). M1 macrophages

can also secrete soluble Flt-1 (sFlt-1), an angiogenesis inhibitor (33, 93). IL-1β, a potent pyrogen, is predominently known as an anti-cancer cytokine, and can limit cancer growth and destroy tumor cells (171, 173). Another pro-inflammatory cytokine, TNFα can polarize macrophages towards an M1 phenotype and upregulate the inflammatory immune response to kill tumor cells (177, 305, 306). Increased numbers of pro-inflammatory M1 macrophages in tumors have been associated with better cancer survival and are reported to be anti-angiogenic and tumoricidal.

The majority of macrophages in a tumor, however, do not express a pro-inflammatory phenotype. Tumor-associated macrophages (TAMs) primarily utilize an M2-like anti-inflammatory phenotype to reduce inflammation and increase angiogenesis within the tumor (249, 299, 307, 308). High numbers of anti-inflammatory TAMs present in tumors are also associated with increased tumor growth and tumor reoccurence (59, 207, 214, 309).

TAMs secrete a range of anti-inflammatory molecules to assist in tumor survival, including Transforming Growth Factor Beta (TGF-β), IL-10 and Vascular Endothelial Growth Factor A (VEGF-A). TGF-β is essential in the growth of new blood vessels (Reviewed in (310)) and restricts the activation and function of the adaptive immune response in cancer (238, 311, 312). IL-10 produced by TAMs increases the growth of cancer cells at low concentrations (299), but upregulated IL-10 can reduce cancer growth and improve the anti-tumor immune response (229, 230). VEGF-A is an endothelial growth factor that, along with its receptors Flt-1 and KDR, is required for tumor angiogenesis and development (32, 44, 313, 314). Rather than producing NO from arginine, TAMs break down arginine to produce urea, allowing the nitrogen to remain within the biomass of the tumor through arginase-1 (Arg-1) (207). CD163 is a surface marker heavily associated with TAMs (203, 211, 214) and increased CD163+ macrophages in a patient

have been used to indicate a poor prognosis (211, 300, 308). Another surface marker, CD206 is also associated with M2 macrophages and poor patient prognosis (315–317). IL-6, a cytokine that can polarize macrophages towards an M2 phenotype (193–195), increases angiogenesis, treatment resistance, and leads to a poor patient prognosis (Reviewed in (186, 190, 192, 318)).An increase in these anti-inflammatory or TAM-associated secretions allows the tumor to both prevent the apoptosis of tumor cells and encourage angiogenesis and further tumor growth.

Our previous data indicated a significant reduction in tumor growth after the treatment with Beta2 Glycoprotein I (β2-GPI)-derived peptides p296c-s and RD-p9 (319). The peptides reduction of tumor growth was marked by a significant increase in soluble Flt-1 (sFlt-1), which is secreted by M1 macrophages, and a significant increase in NO production in the tumors. These results suggest that our peptides are reducing tumor growth and vasculature by altering the macrophage immune response. We hypothesize that the β2-GPI-derived peptides reduce tumor growth by altering TAM phenotype.

Methods

Cell culture

The C57Bl/6-derived, melanoma tumor cell, B16-F10, and the BALB/cN derived mouse macrophage cell line J774A.1 (American Type Culture Collection, Manassas, VA, USA) were maintained in Dulbecco's modified Eagle medium (Gibco, Grand Island, NY, USA) containing 10% Opti-MEM (Gibco), 5% fetal bovine serum (FBS) (Atlanta Biologicals, Lawrenceville, GA, USA, 5% NuSerum Culture Supplement (Fisher Scientific, Pittsburgh, PA, USA), and 1% Gluta-MAX (Gibco). All cells were cultured with 5% CO_2 at 37 °C in a humidified incubator. Cells were split three times a week at 1:5 ratios the first two times, and a 1:10 ratio for the third time.

For experiments, cells were collected from confluent plates rather than splitting the plates. For polarizing experiments, J774A.1 cell were left unpolarized, treated with IFNγ (100 U/mL) and LPS (100 ng/mL), treated with IL-4 (20 ng/mL), or treated with 10% B16F10 melanoma cell supernatants.

β2-GPI peptides

β2-GPI-derived peptides p296c-s, RD-p9 and the scrambled peptide p16ss were produced by solid phase synthesis as previously described at Kansas State University in the KSU Biochemistry Core Laboratory. Peptides p296c-s (H-IHFYSKNKEKKSSYTVEAHSRDGTI-OH) was derived from the lipid binding region of Domain V. From within p296c-s, RD-p9 was created from nine D-amino acids RD-p9 (D-SHAEVTYSS). The scrambled control peptide p16ss contains a scrambled 16 amino acids (DEVHYTTSSSKKARGI). All peptides were purified by reversed phase HPLC and characterized by mass spectroscopy, before lyophilization and storage at -20°C. Peptides were administered at 40 μM unless otherwise specified.

Bone marrow derived macrophage collection and culture

Femurs were collected from 4-6-month-old male C57Bl/6 mice. Bone marrow was then extracted by flushing the marrow from leg bones with serum free media using a 23 ½ gauge needle. Collected marrow was flushed into serum free medium, centrifuged, and resuspended in ACK (ammonium-chloride-potassium) lysing buffer (1.5 M ammonium chloride, 100 mM potassium bicarbonate, 1 mM EDTA) for five minutes on ice to remove red blood cells. The remaining cells were centrifuged at 1400 revolutions per minute (rpm) and resuspended in serum-free medium before counting. Cells ($2x10^5$ cells/well) were seeded into a 24 well plate in 1 mL of Complete Macrophage Medium (DMEM/F12 (1:1) (Gibco, Grand Island, NY, USA), 10 mM L-glutamine, 10% FBS, and 20% LM929 supernatant for GM-CSF). After 72 hours, an

additional 1 mL of Complete Macrophage Medium was added to replenish available nutrients for the cells. At 5 days after initial cell seeding, the medium was removed and replaced with fresh media (DMEM, 10% Opti-MEM (Gibco), 5% FBS, 5% NuSerum and 1% Gluta-MAX) and the bone marrow derived macrophages (BMDMs) were simultaneously treated with polarizing agents and peptides. BMDMs were left unpolarized, treated with IFNγ (100 U/mL) and LPS (100 ng/mL), treated with IL-4 (20 ng/mL), or treated with 10% B16F10 melanoma cell supernatant. BMDMs with and without polarizing cytokines were also left untreated or treated with 40 μM peptides p16ss, p296c-s, or RD-p9. After 24 h, the supernatants were then collected and frozen at 80 °C. The cells were collected in TRIzol for future RNA isolation. Collected supernatants were analyzed for IL-1β, IL-6, IL-10 and TNFα using a MILLIPLEX® Mouse Cytokine/Chemokine Magnetic Bead Panel (Millipore Sigma, Temecula, California). Analysis of the panel used the Luminex® 200™ according to manufacturer's protocol before processing with MILLIPLEX® Analyst 5.1 software. The final data was collected as pg/mL of supernatant (2 x 10^5 BMDM). Concentration of sFlt-1 (pg/mL) in the supernatant was determined with a Mouse sVEGFR1/Flt-1 DuoSet ELISA kit (#DY471, R&D Systems, Minneapolis, MN).

In vivo tumors

C57Bl/6 mice at 8-12 weeks of age were bred and maintained in the specific pathogen free Laboratory Animal Care Service (LACS) facility in the Division of Biology at Kansas State University. All animals had constant access to rodent food and water in a 12 h light/dark cycle and all procedures were approved by the Institutional Animal Care and Use Committee (IACUC) and were in compliance with the Animal Welfare Act. Mice were subcutaneously injected with B10-F10 cells ($2x10^6$) in Matrigel (1:1). Mice were injected intravenously with saline or peptide (40 μM, 3 – 9 mg/kg dependent on peptide size) on days 1, 2, 3, 4, 6, and 8 after injection.

Tumor growth in vivo was measured and calculated daily (length x width^2) and animals were euthanized if tumor size surpassed 1.5 cm in diameter. Tumors were removed 10 days after injection, measured with calipers, and pictures taken before the tumor was prepared for PCR and TAM isolation.

TAM isolation

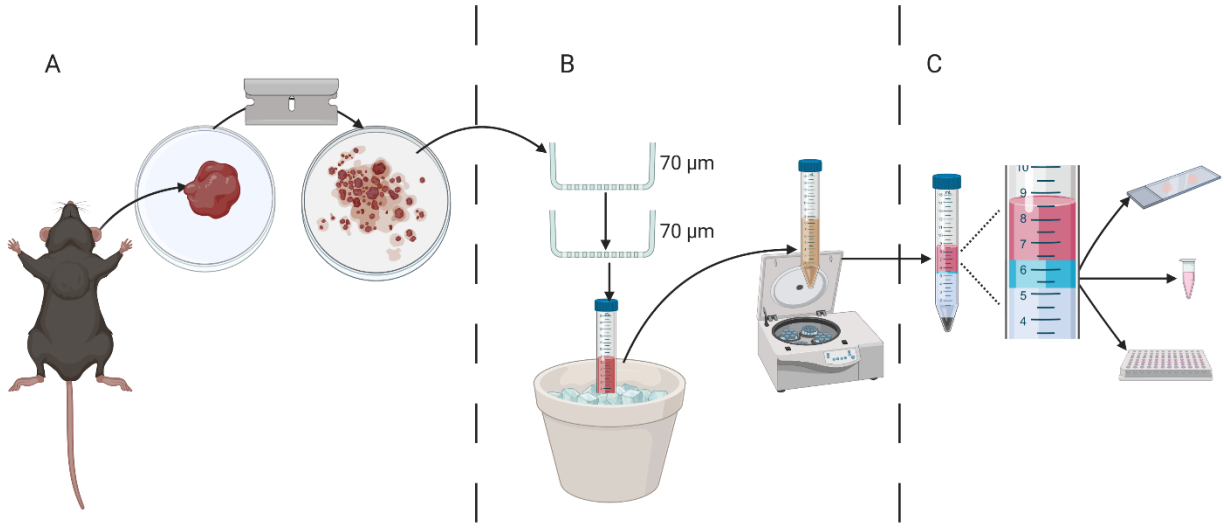

Figure 3.1 Extraction of tumor associated macrophages

A. Tumor tissue is extracted from the mouse after 10 days of growth, minced into fine pieces and collected in serum free media. B. The serum-free medium is pipetted through the minced tissue on 70 µm filters twice, before being incubated with AKC lysis buffer on ice. The cells were then resuspended in fresh medium and layered on top of Lympholyte-M solution and centrifuged. C. After centrifugation, the cell layer (blue) is removed from the tube, counted, and seeded for immunocytochemistry, RNA isolation, or secretions.

Tumor tissue was extracted on day 10 and immediately placed into serum-free media. After dicing and placing the tissue on a 70 µm filter, a single cell suspension was obtained by flushing the tissue with serum-free media twice. The suspension was then incubated in ACK lysing buffer for five minutes on ice to remove red blood cells. To isolate monocytes from the tumor cell suspension, the cells were isolated using Lympholyte-M (CedarLane, Burlington,

NC). According to manufacturer's protocol, the cell solution was brought to $2x10^7$ cells/mL, and pipetted in a layer over an equal volume of Lympholyte-M in a 15 mL tube. The tube was then centrifuged at 1250xg for 20 mins at room temperature. The TAMs were pipetted out from the second layer (blue layer in Figure 3.1), centrifuged, and resuspended in DMEM media containing 5% FBS before being counted for immunocytochemistry, PCR, and secretion assays.

NO assay

Tumor secretions were collected by incubating tumor tissue in oxygenated Tyrode's solution at 37 °C for 20 mins. The top well of the first two columns was filled with 25 μM $NaNO_2$, and a standard curve of 1:2 dilutions was made down the columns. Collected supernatants (150 μL) and two Tyrode's solution blanks were added to a 96 well plate. After the standards and diluted samples were added, an additional 150 μL of Greiss Reagent was added to all wells and incubated at room temperature for 10 mins. After incubation, plates were read on a spectrophotometer at 550 nm (Biorad Model 680 Microplate Reader, Biorad, Hercules, California).

RNA isolation

Total RNA was isolated from TRIzol (Thermofisher, Waltham, MA) homogenized tumors or cells. Tumor tissue was homogenized in 1 mL and cells were suspended in 0.5 mL TRIzol and kept in 1.5 mL capped tubes at -80 °C until isolation. After thawing, 0.2X starting volume of chloroform was added to the tube before shaking for 1 min, followed by 4 mins of rest. After the tube rested at room temperature, the tubes were centrifuged at 13,500 RPM for 15 mins at 4°C. After centrifugation, the separated aqueous phase was pipetted into a new RNase-free 1.5mL tube. An additional 0.5X starting volume of isopropanol was added into the tube before shaking and incubated at room temperature for 10 mins. The mixture was then centrifuged

at 13,000 RPM for 10 mins at 4°C. After centrifugation, the liquid was carefully pipetted off and the remaining pellet was washed twice by adding 0.5X starting volume of 75% ethanol, vortexed briefly, and centrifuged at 10,000 RPM for 5 minutes at 4 °C. After washes, the supernatant was removed and the remaining pellet was air dried for approximately 15 minutes. The pellet was then resuspended in nuclease-free water (100 μL for tumor tissue, 20 μL for cells), and frozen at -80 °C until PCR.

Reverse-Transcriptase PCR

Prior to analysis, RNA concentration and purity was determined by nanodrop at 260 nm. cDNA was synthesized from 1 μg isolated RNA using qScript cDNA Synthesis Kit (Quantbio, Beverly, MA) with M-MLV reverse transcriptase and a combination of oligo and random primers. Reverse-Transcriptase PCR (RT-PCR) was performed using SYBR Green fluorescence as previously described. RT-PCR was performed as follows: RNA was incubated with gene specific primers (Supplementary Table 4.2) at 90°C for 2 min, followed by 50 cycles of 95°C for 10 s, a primer-specific temperature for 20 s (Supplementary Table 4.2) and 72°C for 10 s. The primer-specific temperature was determined by the melting temperature of the specific primers. We then determined the ΔΔCt of iNOS, Arg-1, VEGF-A, TNFα, IL-10, IL-6, IL-1B, Flt-1, and CD163 as compared to saline-treatment.

Immunocytochemistry

BMDM cells and isolated tumor cells ($1x10^4$ cells in 100μL media) were cytocentrifuged at room temperature for 5 minutes at 600 rpm onto glass microscope slides, with two sections per slide. After the centrifugation, the slides were fixed in cold methanol (100%) for 3 minutes, followed by two 5-minute incubations in PBS to wash off excess methanol. Slides were then incubated in a PBS blocking solution with 10% serum for 30 minutes in at 37 °C. After

incubation, slides were placed in PBS to remove excess blocking solution for an additional 5 minutes before removal from PBS and placement in a container with wet paper towels. Primary antibodies for F4/80 (10 nM Anti-mouse IgG2a, Alexa Fluor 594, Biolegend) and M1 marker CD68 (20 nM Anti-mouse IgG2b, FITC, Caltag) or M2 marker CD206 (10 nM Anti-mouse IgG2b, FITC, CALTAG) and isotypes (Mouse IgG2a FITC, Mouse IgG2 Alexa Fluor 594 Biolegend) incubated on the slide overnight at 4 °C. The next day, slides were incubated three times in PBS for 5 minutes each, before a final incubation in purified water for 3 minutes. After removal from the water, slides were dried and coverslips affixed with Prolong Gold mounting reagent with DAPI (Thermofisher, Waltham, MA). Slides were then stored at 4 °C in a dark container until pictures were taken. Fluorescent microscopy images were taken blinded using a Nikon 80i microscope equipped with a camera and MetaVue software. Each section had 6-8 photographs taken.

Statistics

Data are presented as mean ± SEM and significance ($p<0.05$) determined by parametric one-way ANOVA with Dunn's post analysis to compare all columns, or by parametric t-test (GraphPad/Instat Software). Experiments counted in n refer to the number of independent experiments performed separately.

Results

Polarization tests for J774A.1 Cells

We hypothesized that our peptide treatment was affecting the phenotype of macrophages present in the tumor. Initially, we examined the peptides' effects *in vitro* on J774A.1 cells. We established a protocol to polarize the macrophages towards an M1, M2, or TAM phenotype by incubating J774A.1 cells with cytokines. The cells were left untreated or polarized to an M1-like

(with IFNγ and LPS), M2-like (with IL-4), or TAM-like (with B16F10 supernatant) phenotype 24 hours prior to collection of supernatants and cells in TRIzol. The J774A.1 cells treated with IFNγ and LPS had significantly higher iNOS mRNA than the other treatments (Fig. 3.2 A) and secreted significantly more NO than the other treatments (Fig. 3.2 B). RT-PCR also demonstrated that Arg-1 mRNA expression significantly increased with IL-4 treatment compared to the untreated controls (Fig. 3.2 C). The TNFα mRNA did not change regardless of the treatment, though TNFα secretion is increased in TAMs. These data suggest that though our TAM-like polarization did not produce a distinct phenotype, our M1-like and M2-like treatments successfully polarized the macrophages towards the desired phenotypes.

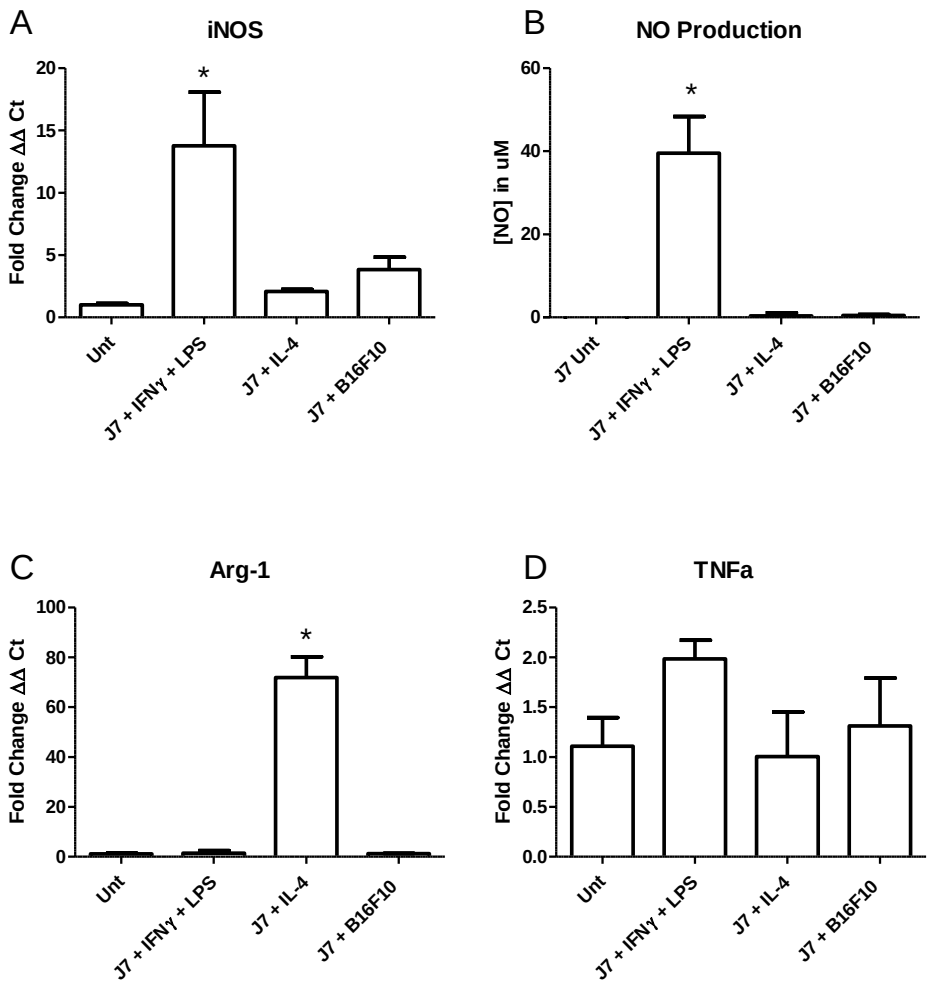

Figure 3.2 M1-like and M2-like phenotypes polarized in J774A.1 cells.

J774A.1 cells were cultured with a treatment of IFNγ (100 U/mL) and LPS (100 ng/mL), IL-4 (20ng/mL), or treated with 10% B16F10 melanoma cell supernatant for 24 h before collecting supernatants and lysing cells with TRIzol. RT-PCR of cellular cDNA was normalized to 18s rRNA and ΔΔCt fold change determined by comparison to untreated cells. J774A.1 cells (n=2-4 experiments) were examined for (A) iNOS, (B) NO secretion, and (C) Arg-1 and (D) TNFα RNA. Each bar represents the mean ± SEM. * $p<0.05$ compared to untreated cells.

Further tests were performed to determine whether the immunocytochemistry protocol would work for future experiments. In a preliminary experiment, J774A.1 cells on microscope slides were stained for the macrophage marker F4/80 (red), the M1 marker CD68 (green), and nuclei (blue) (Figure 3.3). The J774A.1 cells were polarized as demonstrated above, while

simultaneously treated with scrambled control peptide p16ss, or peptides p296c-s or RD-p9 or untreated. The fluorescence showed consistent F4/80 expression across all treatments, and slightly increased CD68 in the M1-like phenotype (Fig. 3.3). These preliminary data indicate that our immunocytochemistry protocol resulted in adhesion of the cells to the slide as well as intact markers that could be detected by IHC.

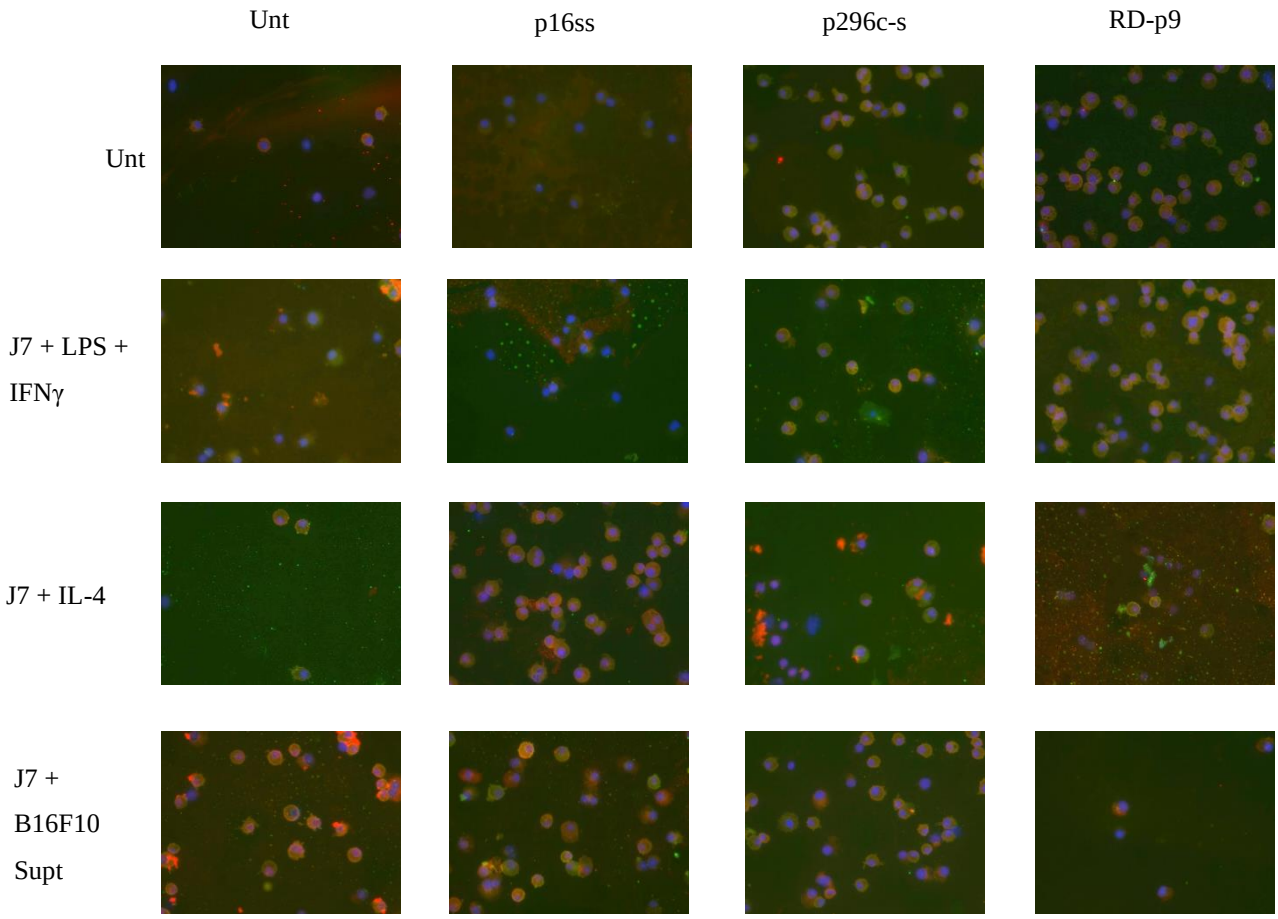

Figure 3.3 Peptide treatment increases CD68 expression in J774A.1 cells.

J774A.1 cells (J7, $1x10^4$) were polarized to M1- M2- or TAM-like phenotypes (left column) and left untreated, or treated the scrambled peptide (p16ss), p296c-s, or RD-p9 for 24 hours. Peptides were then centrifuged down onto microscope slides and stained with anti-F4/80 (Red, Alexa Fluor 594), anti-CD68 (Green, FITC) and DAPI. Microphotographs (A) (200X) are representative of 6-8 pictures per section.

Treatment with peptides alters inflammatory markers in BMDMs.

After we had confirmed our method to polarize macrophages to an M1- or M2-like phenotype and the immunocytochemistry protocol suggests that the markers could be successfully examined through immunocytochemistry, we examined the effects of the peptides p296c-s and RD-p9 on macrophage phenotype with BMDMs. We determined mRNA expression of both pro- and anti-inflammatory markers to see shifts in phenotype after peptide treatment. In initial studies, BMDMs were treated with a scrambled control peptide (p16ss), p296c-s or RD-p9

before being collected in TRIzol and analyzed with RT-PCR. Treatment of BMDMs with only RD-p9 reduced RNA expression of all the anti-inflammatory cytokines or TAM-associated surface marker CD163 (Fig. 3.4 A-F). Treatment with just p296c-s also significantly reduced IL-10 mRNA expression compared to the control treatments (Fig. 3.4 B). However, treatment with p296c-s significantly increased RNA of VEGF and its receptors (Fig. 3.4 D-F). These data suggest that peptide treatments reduce the mRNA expression of anti-inflammatory cytokines.

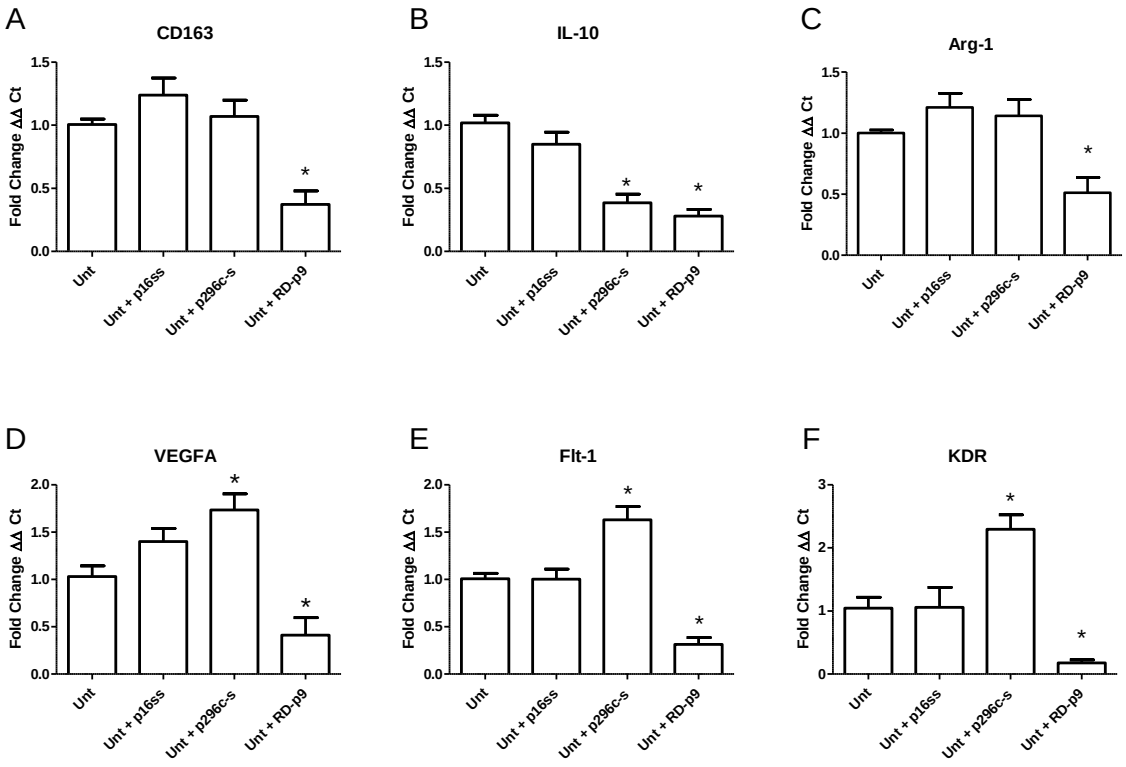

Figure 3.4 Treatment with RD-p9 reduces anti-inflammatory and TAM-like mRNA expression in unpolarized bone marrow derived macrophages.

BMDMs were left untreated or incubated with 40μM peptides p296c-s, RD-p9 or scrambled control peptide p16ss for 24 h prior to collection of cells in TRIzol for RT-PCR. RT-PCR of cDNA was normalized to 18s rRNA and ΔΔCt fold change determined by comparison to untreated BMDMs. Collected RNA was examined for (A) CD163, (B) IL-10, (C) Arg-1, (D) VEGFA, (E) Flt-1, and (F) KDR. Each bar represents the mean ± SEM of n=4-6 experiments. * $p < 0.05$ compared to untreated controls.

We also examined the effects of the peptides on macrophage phenotype with macrophages that were co-treated with polarizing cytokines. We performed RT-PCR for macrophages with or without peptides in addition to IL-4. Treatment with p296c-s and RD-p9 significantly reduced the mRNA expression of CD163 (Fig. 3.5 A) compared to untreated controls. p296c-s treatment also reduced mRNA expression for IL-10 and Arg-1 compared to untreated controls (Fig 3.5 B, C). Treatment with either p296c-s or RD-p9 increased mRNA expression for VEGF-A compared to untreated cells (Fig. 3.5 D), though peptide treatments had no effect on Flt-1 or KDR (Fig. 3.5 E, F). These data indicate that co-treating macrophages with polarizing cytokines and peptides also alters mRNA expression of the macrophage.

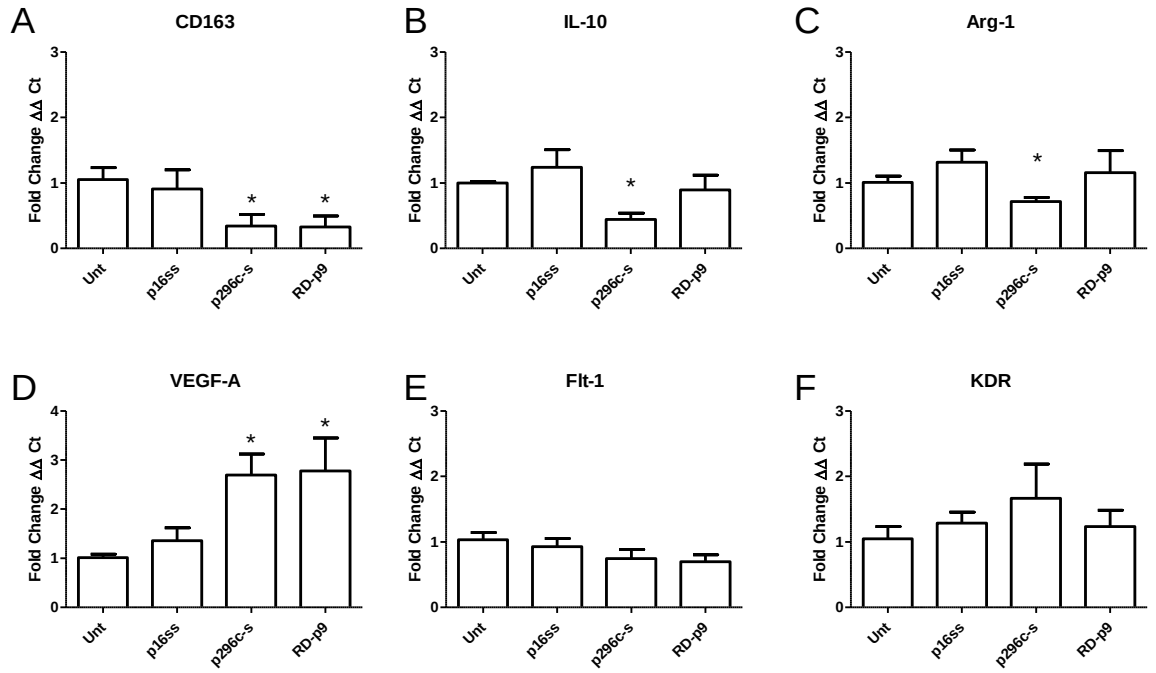

Figure 3.5 Treatment with peptides alters the anti-inflammatory markers in IL-4 treated bone marrow-derived macrophages.
BMDMs treated with IL-4 (20 ng/mL) were left untreated or co-treated with 40μM peptides p296c-s, RD-p9 or scrambled control peptide p16ss for 24 h prior to collection of cells in TRIzol for RT-PCR. RT-PCR of cDNA was normalized to 18s rRNA and ΔΔCt fold change determined by comparison to untreated BMDMs. Collected RNA was examined for (A) CD163, (B) IL-10, (C) Arg-1, (D) VEGFA, (E) Flt-1, and (F) KDR. Each bar represents the mean ± SEM of n=4-6 experiments. * $p < 0.05$ compared to untreated controls

As we determined a shift in the mRNA expression of anti-inflammatory markers, we also investigated changes in pro-inflammatory markers and secretions. When examining the pro-inflammatory markers, RNA for iNOS decreased after p296c-s treatment, compared to controls, but was unchanged with RD-p9 treatment (Fig. 3.6 A). TNFα and IL-6 RNA showed an increase with p296c-s, and a reduction with RD-p9 treatment (Fig. 3.6 B, D). Treatment with RD-p9 and p296c-s both reduced IL-1β expression compared to controls, (Fig. 3.6 C). While mRNA expression of IL-6 increased after treatment with p296c-s, the expression decreased after treatment with RD-p9 (Fig. 3.6 D) The shift in inflammatory markers with RD-p9 treatment suggests that the peptides alter the inflammatory response in macrophages.

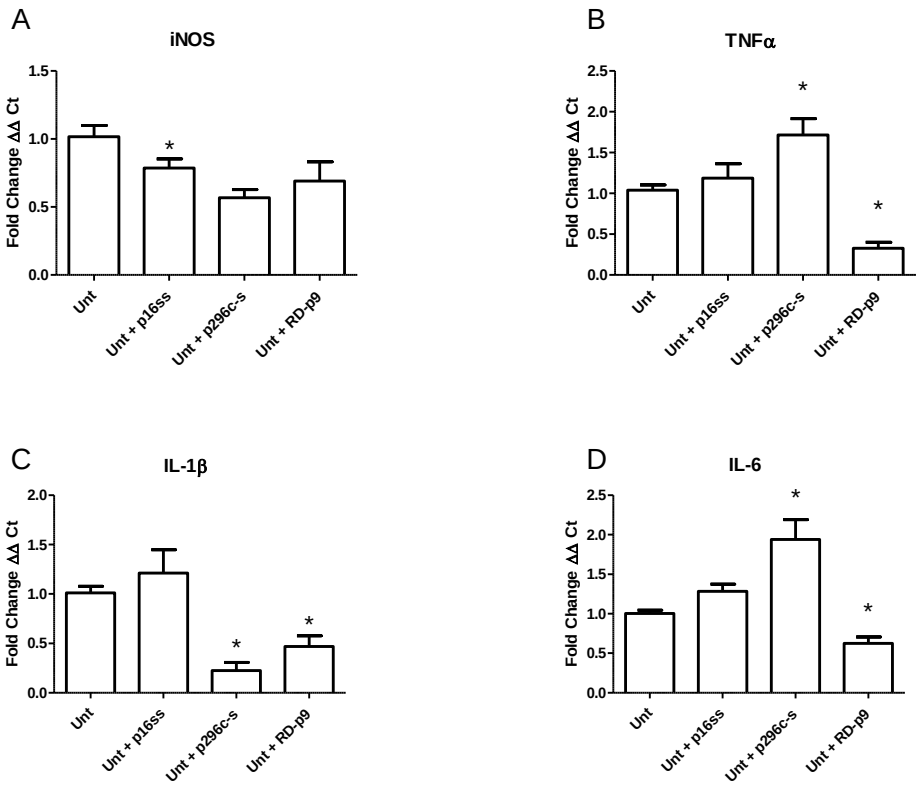

Figure 3.6 Treatment with p296c-s and RD-p9 alter pro-inflammatory markers in bone marrow derived macrophages.

BMDMs were left untreated or incubated with 40μM peptides p296c-s, RD-p9 or scrambled control peptide p16ss for 24 h prior to collection of cells in TRIzol for RT-PCR. RT-PCR of cDNA was normalized to 18s rRNA and ΔΔCt fold change determined by comparison to untreated BMDMs. Collected RNA was examined for (A) iNOS, (B) TNFα, (C) IL-1β, and (D) IL-6. Each bar represents the mean ± SEM of n=4-6 experiments. * $p < 0.05$ compared to untreated controls.

We also determined the changes in mRNA expression of macrophages that had been co-treated with peptides and M1 polarizing cytokines, IFNγ and LPS. RD-p9 reduced mRNA expression for all of the four M1 genes examined; iNOS, TNFα, IL-1β and IL-6 (Fig. 3.7, A-D). In contrast, p296c-s treatment only reduced mRNA expression of TNFα (Fig. 3.7 B).

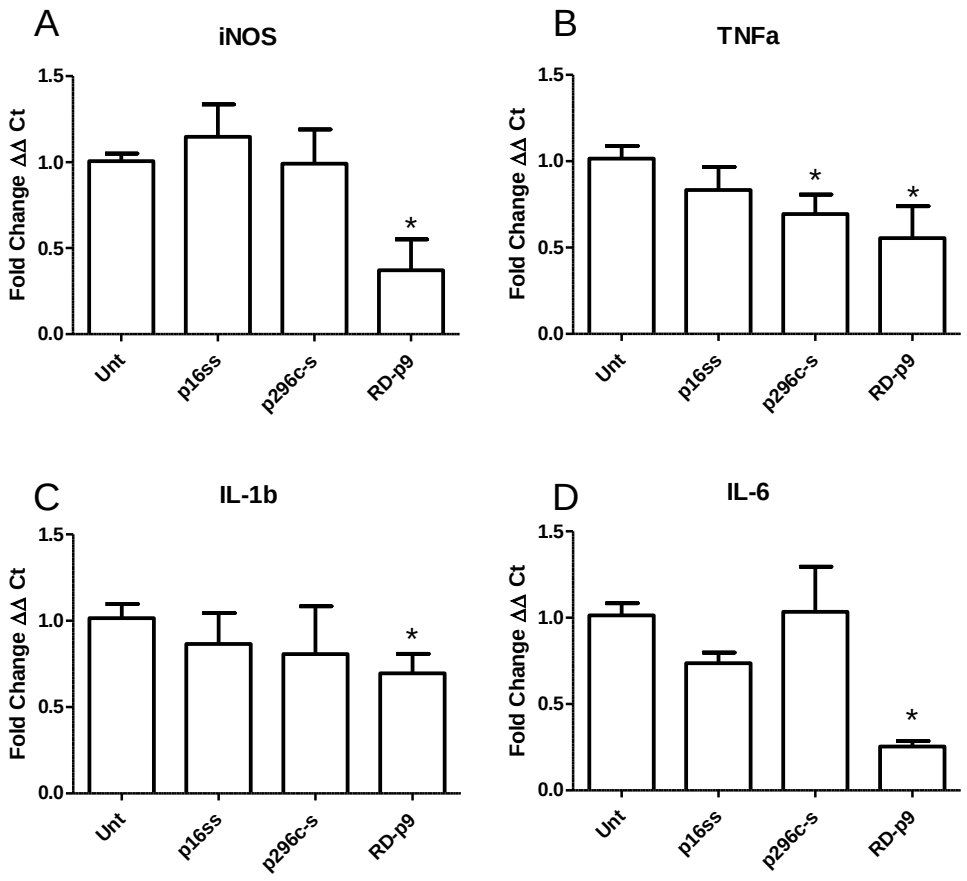

Figure 3.7 Treatment with p296c-s and RD-p9 alter pro-inflammatory markers of macrophages treated with IFNγ and LPS.

M1-like BMDMs treated with IFNγ (100 U/mL) and LPS (100 ng/mL) were simultaneously left untreated or incubated with 40μM peptides p296c-s, RD-p9 or scrambled control peptide p16ss for 24 h prior to collection of cells in TRIzol for RT-PCR. RT-PCR of cDNA was normalized to 18s rRNA and ΔΔCt fold change determined by comparison to untreated BMDMs. Collected RNA was examined for (A) iNOS, (B) TNFα, (C) IL-1β, and (D) IL-6. Each bar represents the mean ± SEM of n=4-6 experiments. * $p < 0.05$ compared to untreated controls.

After observing a change in RNA expression of pro- and anti-inflammatory markers, we determined whether the secreted protein changed as well. Using a LUMINEX assay, we examined the secretion of IL-1β, IL-6, TNFα and IL-10 by unpolarized and cytokine-treated BMDMs treated with peptides. Secretion of IL-1β did not change in the untreated BMDMs but co-treatment of IFNγ and LPS with p296c-s significantly increased the secretion of IL-1β (Fig.

3.8 A). Both IL-6 and TNFα secretion by unpolarized and IFNγ and LPS co-treatment did not change between treatments (Fig. 3.8 B, C). Secretion of IL-10 increased in the unpolarized macrophages after treatment with p296c-s and RD-p9 (Fig. 3.8 D). These data indicate that treatment of unpolarized BMDMs and co-treatment polarizing cytokines with p296c-s and RD-p9 alters the secretion of pro- and anti-inflammatory cytokines.

As we had previously determined that peptides controlled tumor growth in an sFlt-1 dependent manner (320), we examined sFlt-1 secretion by macrophages treated with the peptides. After leaving macrophages untreated or co-treating with IL-4 and the control peptide, p296c-s or RD-p9, we determined the concentration of sFlt-1 in the cell supernatants with an ELISA. Though the concentration of sFlt-1 did not change between treatments of the unpolarized macrophages, the concentration of sFlt-1 in the supernatant was significantly higher in the p296c-s and RD-p9 treatment of macrophages with added IL-4 (Fig. 3.8 E). These data indicate that treatment of BMDMs with IL-4 in addition to peptides results in an increase of sFlt-1 secretion by macrophages.

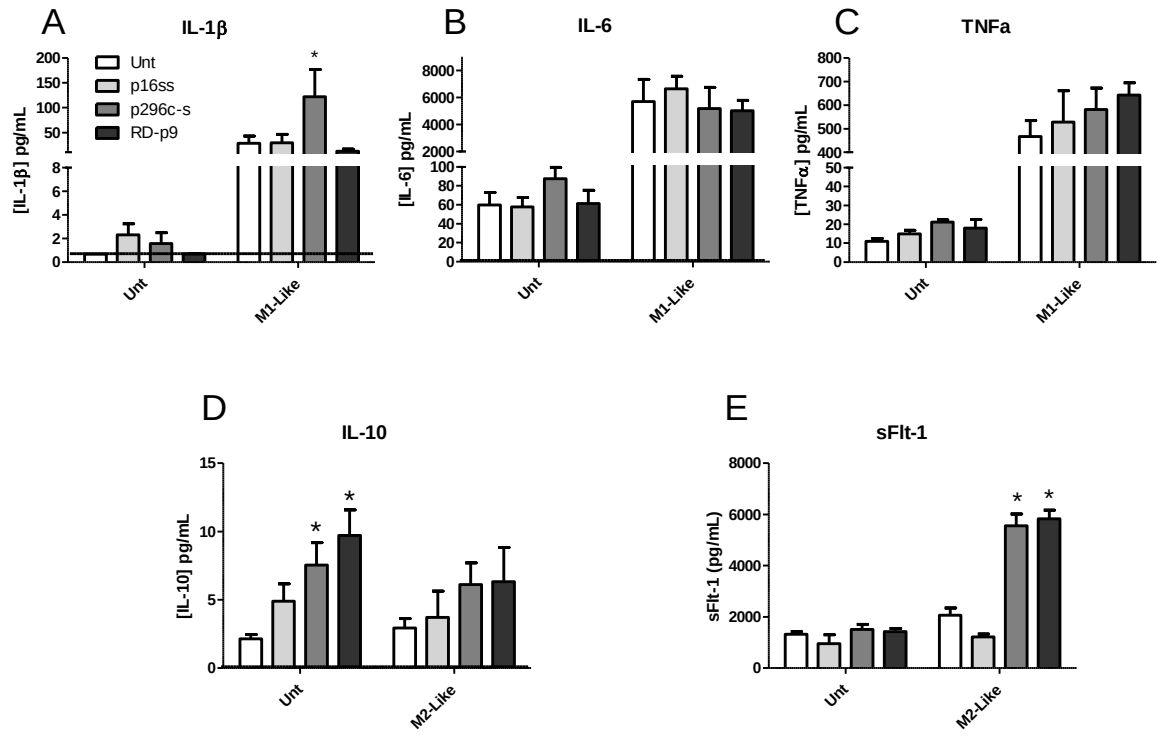

Figure 3.8 Peptide treatment alters secretion of pro- and anti- inflammatory cytokines in BMDMs. Unpolarized BMDMs or BMDMs with added IL-4 (20n g/mL) were left untreated or incubated with 40μM peptides p296c-s, RD-p9 or scrambled control peptide p16ss for 24 h prior to collection supernatants. Collected supernatants (n=4 experiments) were analyzed via Luminex assay to determine levels of IL-1β (A), IL-6 (B), TNFα (C), or IL-10 (D). Secretion of sFlt-1 (pg/mL) (E) was analyzed via ELISA assay (n=4-5 experiments). All data were standardized to pg/ml supernatant. Each bar represents the mean ± SEM. * $p<0.05$ compared to untreated cells

Peptide treatment reduces tumor growth and alters inflammatory response

Mice were injected with B16F10 melanoma cells and measured daily for 10 days. During the course of tumor growth, mice were left untreated, treated with p16ss, or p296c-s (40 μM) on days 1-4, 6 and 8. On day 10, excised tumors were measured with calipers, and tumor tissue was incubated in Tyrode's solution to collect secretions or in TRIzol for RNA isolation. Previously collected and frozen tumors treated with RD-p9 were also analyzed for their secretions and RNA. The daily and excised tumor volumes (Fig. 3.9 A, B) of p296c-s treated mice were

significantly lower than the volumes of saline-treated mice. NO secretion was significantly higher in the p296c-s and previously harvested RD-p9 treated tumors compared to the saline treated mice (Fig. 3.9 C).

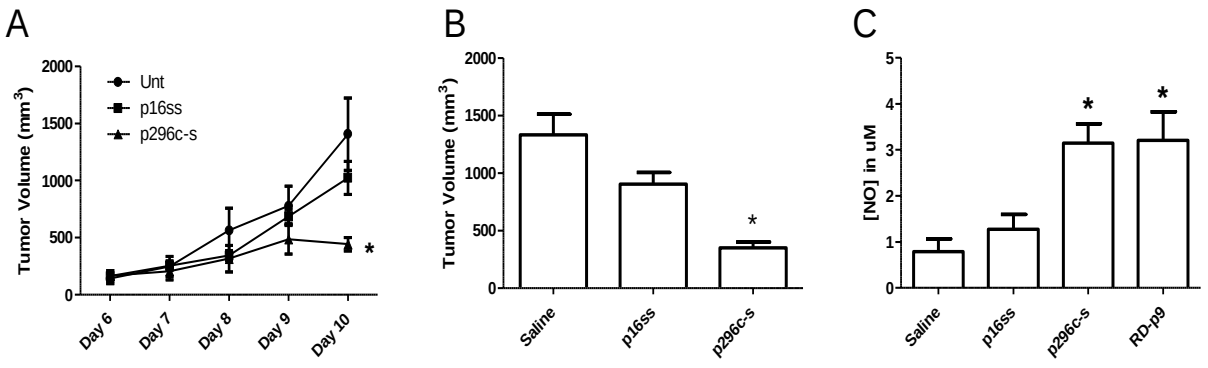

Figure 3.9 Peptide treatment reduces tumor growth and increases NO production in tumors.

The daily in vivo volume of the tumors treated with saline, scrambled control peptide p16ss (p16ss), or p296c-s, (40 μM) on d1-4, 6, 8 was calculated for 10 days (n=4-5 animals) (A) and excised tumor volume calculated (B) (n=5-7 animals). Excised tumors were incubated for 20 min in Tyrodes buffer at 37 °C. Collected secretions were analyzed for NO concentration(C). Each bar represents the mean ± SEM. * $p<0.05$ compared to saline treated tumors

After noting the increase in NO production by the tumors, we examined the changes in RNA for other pro- and anti-inflammatory cytokines. RT-PCR for CD163 and F4/80 showed a significant decrease in the RD-p9 treated tumors compared to controls, but no change in p296c-s treated tumors (Fig 3.10 A, B). In contrast, TNFα and IL-10 RNA significantly increased in the p296c-s and RD-p9 treated tumors compared to the control treatments (Fig 3.10 C, D). IL-6 was significantly reduced in the p296c-s and RD-p9 treated tumors compared to the control. (Fig 3.10 E). RNA of IL-1β significantly increased in the RD-p9 treated tumors compared the control but

did not change in the p296c-s treated tumors (Fig 3.10 F). These data indicate that peptide treatment alters the inflammatory response in tumors.

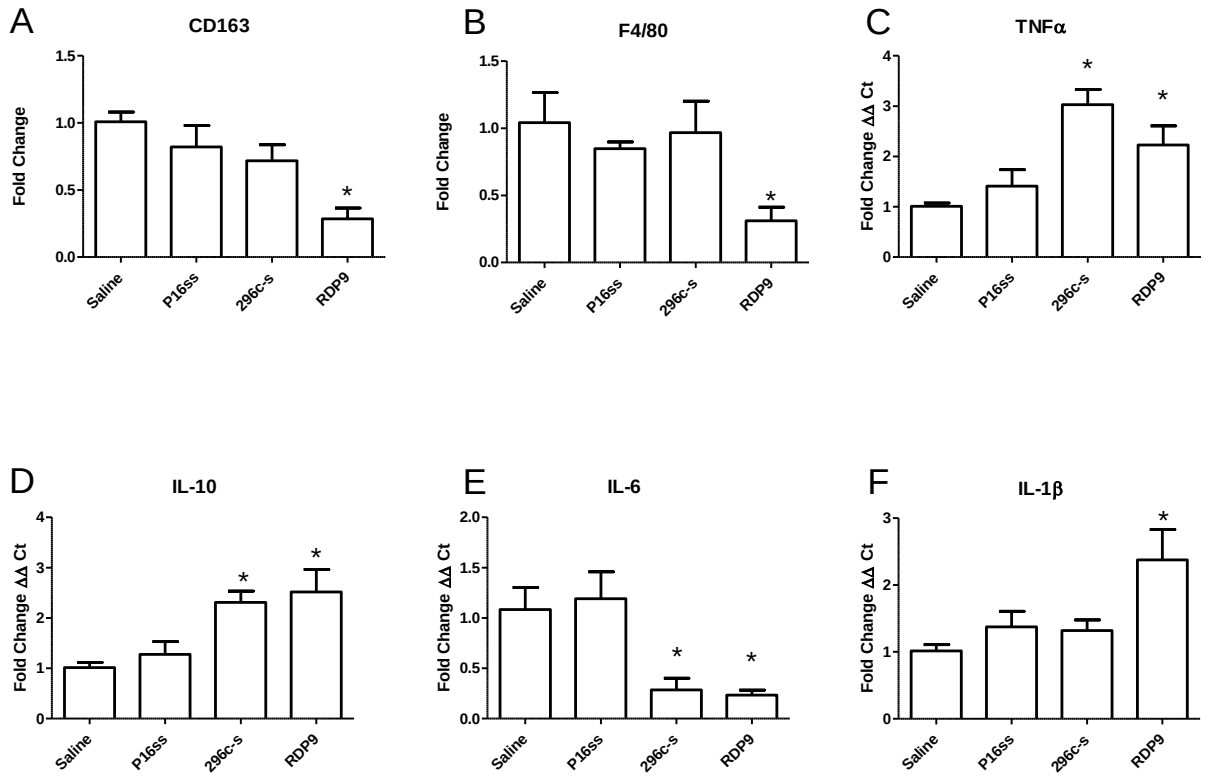

Figure 3.10 Treatment with p296c-s and RD-p9 alters inflammatory response in tumors.

Tumors excised from mice treated with or without peptides were either homogenized in TRIzol for RNA isolation. RT-PCR of tumor cDNA was normalized to 18s rRNA and ΔΔCt fold change determined by comparison to saline treated tumors. Tumor RNA (n = 3-6) was examined for (A) CD163, (B) F4/80, (C) TNFα, (D) IL-10, (E) IL-6, and (F) IL-1β. Each bar represents the mean ± SEM. * $p<0.05$ compared to saline-treated tumors

Tumor associated macrophage isolation

With the changes in inflammatory cytokines in the overall tumor, we planned to examine the changes in TAMs. To do this, we isolated cells from the tumor and examined them with Diff-Quik cell staining reagent. The morphological appearance of the cells indicated that macrophages had been isolated from the tumor tissue (Fig. 3.11 A)**.** Isolated cells fixed onto

microscope slides were also examined with anti-F4/80 (red) antibodies to identify macrophages and CD206 (green) antibodies to identify M2 macrophages. The red fluoresent staining suggests that several F4/80+ cells, likely macrophages, were isolated from the tumor tissue (Fig. 3.11 B). However, the fluoresence also indicates that the only a minority of isolated cells were macrophages (Fig. 3.11 B). These data indicate that while our method of TAM isolation produced macrophages in the p16ss and p296c-s treated tumors, many of the isolated cells are not TAMs. This could be due in part to the collection of the cells from the Lympholyte, indicating that each withdrawal of collected cells for their respective assays does not collect an equal number of macrophages.

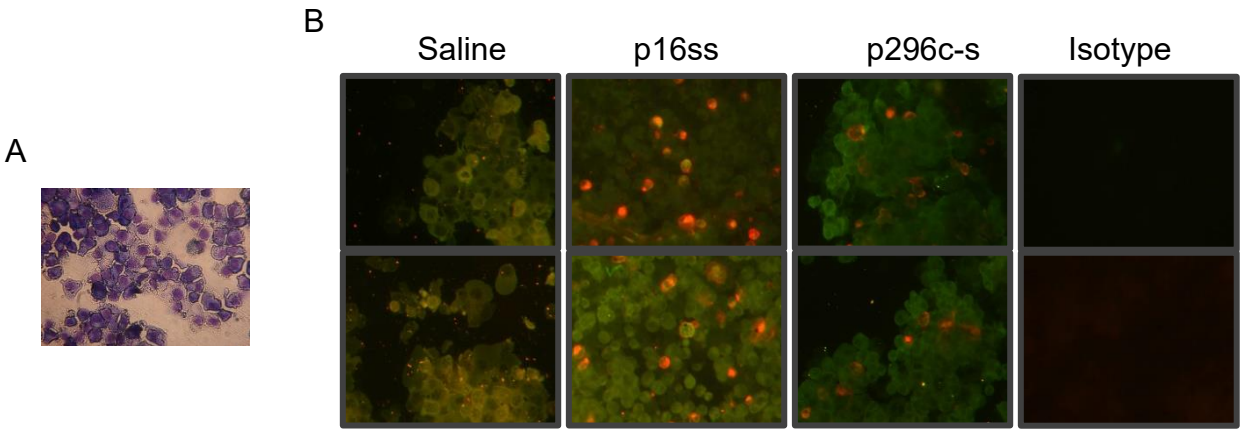

Figure 3.11 Macrophages isolated from mouse tumors.

Cells isolated from excised tumors were spun down onto microscope slides. Cells were stained with Diff-Quik for morphology (A) (n=4). Cells were also stained for anti-F4/80(Alexa Fluor 594) and anti-CD206 (FITC) fluorescent antibodies or an isotype control (B) (n=6). Microphotographs (40X) are representative of 6-8 photographs per section.

Discussion

Tumor survival *in vivo* relies in part on the immune response to the tumors, including TAMs. The phenotype and number of TAMs in a tumor influence the growth of the tumor and survival of the patient (203, 212, 215–218, 321). Our previous study with the β2-GPI-derived peptides discovered an sFlt-1-dependent reduction of tumor growth after treatment with peptides p296c-s and RD-p9 (319). As sFlt-1 can be secreted by M1 macrophages, we examined the effects of our peptide on macrophage phenotype. Though further experiments must be conducted, our initial data suggests that the peptide treatment polarizes TAMs towards an anti-tumor phenotype.

The initial experiments in this chapter focused on establishing protocols and methods to test changes in macrophage phenotype. Initial testing experiments for the immunocytochemistry method resulted in cells clearly adhered to the slides and possessing intact surface markers identifiable through IHC. While M1 and M2 macrophages produce a multitude of cytokines and markers, NO and Arg-1 are often used as a standard of pro- versus anti-inflammatory macrophage phenotype (159, 198, 208, 247). Initial studies using J774A.1 cells focused on the changes in iNOS and Arg-1, as well as NO production. However, our preliminary immunocytochemistry of J774A.1 cells did not indicate a phenotypic change. As this could be due to the low numbers of cells and that this was only one preliminary experiment, future experiments must confirm changes in phenotypic surface markers. With the shifts in iNOS and Arg-1 RNA and NO secretion, our polarization of the J774A.1 cells produced distinct phenotypes similar to M1 and M2. These results confirmed the methods used for further experiments.

The p296c-s and RD-p9 treatment of the tumors resulted in a reduction of tumor size and volume, as previously discussed. The shift in macrophage phenotype is less clear. The *in vitro* BMDM data did not produce consistent results between treatments. The mRNA expression after RD-p9 treatment was lower than the untreated control in most of the examined cytokines. In contrast, mRNA expression of examined cytokines after treatment with p296c-s was often unchanged or significantly higher than the untreated control. This may be due to *in vitro* conditions lacking hypoxic microenvironment and cell signaling present in the tumor.

Treatment with p296c-s and RD-p9 also altered mRNA expression of macrophages when co-treated with polarizing cytokines. RD-p9 treatment reduced mRNA expression of all of the pro-inflammatory cytokines examined in macrophages co-treated with IFNγ and LPS. The macrophages treated with p296c-s in addition to IL-4 resulted in reduced mRNA expression of CD163, IL-10 and Arg-1, though RD-p9 only caused a reduction in CD163 expression. Examination of protein secretion through Luminex assay also indicated a shift in pro- and anti-inflammatory cytokines. The increase of IL-10 secretion in untreated BMDMs was opposite of what the mRNA data would suggest. This could imply that after 24 h had passed, enough IL-10 had been secreted that further IL-10 was not necessary to produce. Similarly, the increased IL-1β secretion in macrophages co-treated with IFNγ and LPS along with p296c-s may not need increased mRNA expression. Importantly, while sFlt-1 secretion did not change in the unpolarized macrophages, treatment with p296c-s and RD-p9 in addition to IL-4 significantly increased sFlt-1 secretion. Together, these data indicate that the peptides can alter the inflammatory response of both unpolarized macrophages and macrophages co-treated with polarizing cytokines.

In contrast, the *in vivo* data was more consistent between peptide treatments but did not align exclusively with M1 or M2 phenotypes. This was expected, as *in vivo* phenotypes often express aspects of both pro- and anti-inflammatory phenotypes (Reviewed in 251, 253). While the mRNA expression for many pro-inflammatory markers increased with peptide treatment, many anti-inflammatory markers also showed a significant increase compared to the controls. Looking beyond the broad M1 and M2 categories for the cytokines, however, the peptide treatment still results in an anti-tumor shift in inflammation.

The increase in NO secretion by the tumors indicates a shift towards an anti-tumor inflammatory response. NO can promote tumor progression as well as inhibit tumor growth (Reviewed in 163). These two functions rely on the concentration of NO present. A low (<0.1 μM) concentration of NO sustained by endothelial nitric oxide synthase (eNOS) is beneficial to cancer, increasing angiogenesis, tumor growth, and metastasis (169, 306, 322–325). NO concentrations are slightly elevated in several forms of cancer, including cervical and lung cancer (326, 327). However, "high" (>0.5μM) concentrations of NO prevent angiogenesis, improve the anti-cancer immune response, treatment response, and induce apoptosis of tumor cells (159, 328–330). The significant increase in NO secretion with p296c-s and RD-p9 treatment by the tumors may reach "high" NO concentrations, indicating an anti-tumor effect.

Similar to NO, low concentrations of TNFα and IL-10 have been shown to increase tumorigenesis, angiogenesis, and tumor resistance (62, 224, 305, 331–333). However, high concentrations of TNFα destabilize blood vessel formation, kill tumor cells, and increase immune cell invasion into the tumor (334–336). In colorectal cancer, breast cancer, and B16F10 melanoma, overexpression of IL-10 improves the anti-tumor immune response to kill tumor cells (228–230, 232, 233) possibly due to the inhibition of regulatory CD4+ T cells (311, 337). The

significantly higher expression of IL-10 and TNFα in the p296c-s and RD-p9 treated tumors indicates that peptide treatment may upregulate these cytokines to reduce tumor growth.

However, other markers and cytokines do not have both pro- and anti-tumor functions. Pro-inflammatory cytokines IL-1β and IL-6 function as opposites within tumors. Increased IL-6 promotes tumor growth and treatment resistance (186, 189, 191, 192), while IL-1β kills tumor cells, increases anti-tumor immune response, and reduces tumor growth (171, 172, 338). The peptide treatment resulted in significantly lower IL-6 and significantly higher IL-1β mRNA expression compared to the controls, which could contribute to the reduction in tumor growth. The treatment with RD-p9 also resulted in a reduction of CD163 and F4/80 expression in tumors. CD163 is a clinical TAM marker, and increased numbers of CD163+ macrophages in tumors can indicate poor patient prognosis (213, 218, 283, 300). The peptides also reduced expression of F4/80, and though the marker is not specific to TAMs, a reduction of macrophages in tumor tissue leads to improved treatment response and a reduction of tumor growth (241, 339–341). Altogether, though both pro- and anti- inflammatory markers shifted after treatment with the peptides, they could all contribute to the inhibition of tumor growth.

Though initial tests with TAMs indicate that the protocol successfully isolated macrophages, there are many experiments to perform. The percent yield of TAMs with the protocol must be verified in each single cell suspension. While this can be done by examining morphology as in this experiment, mouse TAM verification often examines surface markers such as CD11b+, F4/80+, or Ly6G/C+ cells through IHC or flow cytometry (342–344). Similarly, using a density gradient for the isolation of TAMs can be replaced with cell sorting and flow cytometry for the same target surface markers or antibody-based macrophage sorting kits (342–

344). While this would change the processing of the tumor tissue, these methods would produce a higher percentage of collected TAMs.

After verifying the number of macrophages collected from the tumor, further experiments will be conducted with the TAMs. RT-PCR for the TAMs will examine the same pro- and anti-inflammatory cytokines previously examined in whole tumor tissue. Importantly, a LUMINEX assay will examine the pro- and anti-inflammatory cytokines secreted from tumor tissue and extracted TAMs. These will confirm that the changes in RNA caused by the peptides also result in changed protein secretion. Immunohistochemistry for the tumor tissue will also examine the distribution of TAMs within the tumor as well as the phenotype they expressed. The IHC will not only confirm the changes in the inflammatory response but also examine whether the peptides changed the infiltration of the macrophages into the tumor tissue.

While the data collected in this chapter provides insight into the changes in inflammatory response, further investigation is needed. RT-PCR of both BMDMs and tumor tissue revealed a shift towards an anti-tumor inflammatory response after p296c-s and RD-p9 treatment. If the shift towards an anti-tumor immune response is confirmed with LUMINEX or IHC, it could be another mechanism of tumor control caused by these peptides. Future research could confirm our data, which suggests that our peptide treatments result in a change of the inflammatory phenotype of the tumor.

Chapter 4 - Concluding Remarks

The overarching purpose of these studies was to examine the mechanism behind the β2-GPI-derived peptides' reduction of tumor growth. While the protein itself can promote and reduce angiogenesis, the function of β2-GPI appears dependent on both concentration and conformation of the protein (146–149). The reported mechanisms of β2-GPI regulation of angiogenesis involved the control of endothelial cell growth, cleavage of angiostatin, and prevention of VEGF signaling. However, in our experiments, the β2-GPI-derived peptides regulated angiogenesis through sFlt-1, a mechanism not previously associated with β2-GPI.

The literature examining the involvement of β2-GPI with angiogenesis has produced conflicting results. It is possible that the peptides high concentrations may be the cause of reduced angiogenesis and tumor growth, which is then mimicked with our peptides. The established disruption of VEGF signaling through β2-GPI addressed changes in KDR rather than Flt-1. Regardless, the sFlt-1 dependent reduction of tumor growth is very clear. The increase in sFlt-1 secretion could be related to the previously mentioned VEGF signaling or through the cells that secrete sFlt-1 such as macrophages. In addition, through this regulation of angiogenesis other factors may arise to assist in tumor control as well.

Few publications have focused on the interaction of β2-GPI and macrophages. This interaction could be worthwhile, considering the involvement of macrophages in pre-eclampsia, angiogenesis, and autoimmune disorders. However, our research must investigate further regarding TAMs and the β2-GPI-derived peptides. Our PCR data indicated a reduction in M2 markers after treatment with p296c-s and RD-p9. This could be due to VEGF, as it is reported to increase M2 macrophage polarization, and treatments targeting VEGF reduced M2 polarization. Given that chapter 2 indicates a control of angiogenesis in an sFlt-1 dependent manner, the

peptides may be preventing the polarization of TAMs to M2. This may not mean that blockage of M2 macrophage polarization immediately increases the M1 macrophage population. However, the RT-PCR data of the whole tumor tissue clearly indicates a shift promoting the production of anti-tumor cytokines.

The growth of new blood vessels in the tumor can directly alter the tumor immune response. As previously mentioned, factors secreted during angiogenesis such as VEGF can polarize existing macrophages to an anti-inflammatory, pro-tumor M2 phenotype. In addition, VEGF can promote macrophage invasion into the tumor tissue. Limiting the growth of abnormal vasculature allows for further immune response to the tumor, which may be responsible for the shift in the tumor inflammatory markers that did not occur in the *in vitro* studies. The tumor microenvironment that influences macrophage phenotype and invasion is in turn influenced by the angiogenesis that occurs during tumor growth.

Future Directions

Questions on the β2-GPI-derived peptide of tumor control still remain. Though our data suggests a shift in TAM phenotype with peptide treatment, this needs to be confirmed through further studies. The immune response to tumor growth is multifaceted and complex, leaving many questions to be addressed. In addition to TAM manipulation of the tumor microenvironment, other cells such as tumor-associated neutrophils can alter inflammation. Beyond the immune response, tumor studies should examine the other consequences of the peptides' regulation of angiogenesis. Studies on the route of injection or more efficient ways to treat melanoma will allow for a better understanding of the limits of the peptide treatment. Longer studies also must be performed to examine the effects of the peptide beyond the 10 days

examined in this study. These studies will determine the long-term effectiveness of the peptide, whether the peptide will continue to reduce tumor growth or the tumor response to the peptide will change. Additional experiments will also examine changes in the formation of metastases after treatment with peptides. The β2-GPI-derived peptides may offer a possible therapeutic to combat the growth of melanoma. While the treatments do not kill the existing tumors, they prevent further growth and allow for other interventions to eliminate the tumor. Further studies can go beyond melanoma to study other forms of cancer such as breast cancer to establish a new cancer therapeutic.

Bibliography

1. Centers for Disease Control and Prevention, and US Department of Health and Human Services. 2019. *Melanoma Incidence and Mortality, United States–2012–2016*,.

2. Guy, G. P., S. R. Machlin, D. U. Ekwueme, and K. R. Yabroff. 2015. Prevalence and costs of skin cancer treatment in the U.S., 2002-2006 and 2007-2011. *Am. J. Prev. Med.* 48: 183–187.

3. Rastrelli, M., S. Tropea, C. R. Rossi, and M. Alaibac. 2014. Melanoma: Epidemiology, risk factors, pathogenesis, diagnosis and classification. *In Vivo (Brooklyn).* 28: 1005–1012.

4. Guy, G. P., C. C. Thomas, T. Thompson, M. Watson, G. M. Massetti, and L. C. Richardson. 2015. Vital signs: Melanoma incidence and mortality trends and projections — United States, 1982–2030. *Morb. Mortal. Wkly. Rep.* 64: 591–596.

5. Banerjee, S., K. Halder, S. Ghosh, A. Bose, and S. Majumdar. 2015. The combination of a novel immunomodulator with a regulatory T cell suppressing antibody (DTA-1) regress advanced stage B16F10 solid tumor by repolarizing tumor associated macrophages in situ. *Oncoimmunology* 4: 1–12.

6. Goldsmith, L. A., F. B. Askin, A. E. Chang, C. Cohen, J. P. Dutcher, R. S. Gilgor, S. Green, E. L. Harris, S. Havas, J. K. Robinson, N. A. Swanson, M. A. Tempero, A. B. Ackerman, C. M. Balch, N. Cascinelli, W. H. Clark, E. R. Farmer, D. Guerry, A. N. Houghton, H. K. Koh, A. W. Kopf, K. H. Kraemer, R. M. MacKie, J. C. Maize, F. L. Meyskens, D. A. Perednia, M. W. Piepkorn, D. S. Rigel, G. S. Rogers, R. W. Sagebiel, A. J. Sober, M. A. Tucker, M. R. Wick, J. J. Zone, A. N. Moshell, E. Blume, E. Bray, J. M. Elliott, J. H. Ferguson, M. B. Gregg, W. H. Hall, D. E. Henson, S. I. Katz, M. T. Lotze, J. Maize, K. H. Safavi, and A. Sober. 1992. Diagnosis and Treatment of Early Melanoma: NIH Consensus Development Panel on Early Melanoma. *JAMA J. Am. Med. Assoc.* 268: 1314–1319.

7. Lorimer, P. D., R. L. White, K. Walsh, Y. Han, R. C. Kirks, J. Symanowski, M. R. Forster, T. Sarantou, J. C. Salo, and J. S. Hill. 2016. Pediatric and Adolescent Melanoma: A National Cancer Data Base Update. *Ann. Surg. Oncol.* 23: 4058–4066.

8. Swetter, S. M., H. Tsao, C. K. Bichakjian, C. Curiel-Lewandrowski, D. E. Elder, J. E. Gershenwald, V. Guild, J. M. Grant-Kels, A. C. Halpern, T. M. Johnson, A. J. Sober, J. A. Thompson, O. J. Wisco, S. Wyatt, S. Hu, and T. Lamina. 2019. Guidelines of care for the management of primary cutaneous melanoma. *J. Am. Acad. Dermatol.* 80: 208–250.

9. Weinstock, M. A. 1993. Epidemiology of melanoma. *Cancer Treat. Res.* 65: 29–56.

10. Balch, C. M., S. J. Soong, J. E. Gershenwald, J. F. Thompson, D. S. Reintgen, N. Cascinelli, M. Urist, K. M. McMasters, M. I. Ross, J. M. Kirkwood, M. B. Atkins, J. A. Thompson, D. G. Coit, D. Byrd, R. Desmond, Y. Zhang, P. Y. Liu, G. H. Lyman, and A. Morabito. 2001. Prognostic factors analysis of 17,600 melanoma patients: Validation of the

American Joint Committee on Cancer melanoma staging system. *J. Clin. Oncol.* 19: 3622–3634.

11. Yuan, T. A., Y. Lu, K. Edwards, J. Jakowatz, F. L. Meyskens, and F. Liu-Smith. 2019. Race-, age-, and anatomic site-specific gender differences in cutaneous melanoma suggest differential mechanisms of early-and late-onset melanoma. *Int. J. Environ. Res. Public Health* 16: 908.

12. Balch, C. M., M. M. Urist, C. P. Karakousis, T. J. Smith, W. J. Temple, K. Drzewiecki, W. R. Jewell, A. A. Bartolucci, M. C. Mihm, R. Barnhill, and H. J. Wanebo. 1993. Efficacy of 2-cm surgical margins for intermediate-thickness melanomas (1 to 4 mm): Results of a multi-institutional randomized surgical trial. In *Annals of Surgery* vol. 218. Ann Surg. 262–269.

13. Balch, C. M., T. M. Murad, S. Soong, A. L. Ingalls, P. C. Richards, and W. A. Maddox. 1979. Tumor thickness as a guide to surgical management of clinical stage I melanoma patients. *Cancer* 43: 883–888.

14. Breslow, A. 1970. Thickness, cross-sectional areas and depth of invasion in the prognosis of cutaneous melanoma. *Ann. Surg.* 172: 902–908.

15. Greene, M. H., D. E. Elder, D. Guerry, M. N. Epstein, M. H. Greene, and M. Van Horn. 1984. A study of tumor progression: The precursor lesions of superficial spreading and nodular melanoma. *Hum. Pathol.* 15: 1147–1165.

16. PDQ Adult Treatment Editorial Board. 2002. *Melanoma Treatment (PDQ®): Patient Version,*. National Cancer Institute (US).

17. Duncan, L. M. D. 2009. The Classification of Cutaneous Melanoma. *Hematol. Oncol. Clin. North Am.* 23: 501–513.

18. Bedrosian, I., M. B. Faries, D. P. Guerry IV, R. Elenitsas, L. Schuchter, R. Mick, F. R. Spitz, L. P. Bucky, A. Alavi, D. E. Elder, D. L. Fraker, and B. J. Czerniecki. 2000. Incidence of sentinel node metastasis in patients with thin primary melanoma (≤1 mm) with vertical growth phase. *Ann. Surg. Oncol.* 7: 262–267.

19. Wasif, N., S. P. Bagaria, P. Ray, and D. L. Morton. 2011. Does metastasectomy improve survival in patients with stage IV melanoma? a cancer registry analysis of outcomes. *J. Surg. Oncol.* 104: 111–115.

20. Howlander, N., A. M. Noon, M. Krapcho, D. Miller, A. Brest, M. Yu, J. Ruhl, Z. Tatalovich, A. Mariotto, D. R. Lewis, H. S. Chen, E. J. Feuer, and K. A. Cronin. 2020. SEER Cancer Statistics Review, 1975-2016. *Natl. Cancer Inst.* .

21. Smith, M. P., B. Sanchez-Laorden, K. O'brien, H. Brunton, J. Ferguson, H. Young, N. Dhomen, K. T. Flaherty, D. T. Frederick, Z. A. Cooper, J. A. Wargo, R. Marais, and C. Wellbrock. 2014. The immune microenvironment confers resistance to MAPK pathway inhibitors through macrophage-derived TNF—. *Cancer Discov.* 4: 1214–1229.

22. Solit, D. B., and N. Rosen. 2011. Resistance to BRAF inhibition in melanomas. *N. Engl. J. Med.* 364: 772–774.

23. Zaretsky, J. M., A. Garcia-Diaz, D. S. Shin, H. Escuin-Ordinas, W. Hugo, S. Hu-Lieskovan, D. Y. Torrejon, G. Abril-Rodriguez, S. Sandoval, L. Barthly, J. Saco, B. Homet Moreno, R. Mezzadra, B. Chmielowski, K. Ruchalski, I. P. Shintaku, P. J. Sanchez, C. Puig-Saus, G. Cherry, E. Seja, X. Kong, J. Pang, B. Berent-Maoz, B. Comin-Anduix, T. G. Graeber, P. C. Tumeh, T. N. M. Schumacher, R. S. Lo, and A. Ribas. 2016. Mutations Associated with Acquired Resistance to PD-1 Blockade in Melanoma. *N. Engl. J. Med.* 375: 819–829.

24. Wagle, N., C. Emery, M. F. Berger, M. J. Davis, A. Sawyer, P. Pochanard, S. M. Kehoe, C. M. Johannessen, L. E. MacConaill, W. C. Hahn, M. Meyerson, and L. A. Garraway. 2011. Dissecting Therapeutic Resistance to RAF Inhibition in Melanoma by Tumor Genomic Profiling. *J. Clin. Oncol.* 29: 3085–3096.

25. Mishra, H., P. K. Mishra, A. Ekielski, M. Jaggi, Z. Iqbal, and S. Talegaonkar. 2018. Melanoma treatment: from conventional to nanotechnology. *J. Cancer Res. Clin. Oncol.* 144: 2283–2302.

26. O'Connell, M. P., K. Marchbank, M. R. Webster, A. A. Valiga, A. Kaur, A. Vultur, L. Li, M. Herlyn, J. Villanueva, Q. Liu, X. Yin, S. Widura, J. Nelson, N. Ruiz, T. C. Camilli, F. E. Indig, K. T. Flaherty, J. A. Wargo, D. T. Frederick, Z. A. Cooper, S. Nair, R. K. Amaravadi, L. M. Schuchter, G. C. Karakousis, W. Xu, X. Xu, and A. T. Weeraratna. 2013. Hypoxia induces phenotypic plasticity and therapy resistance in melanoma via the tyrosine kinase receptors ROR1 and ROR2. *Cancer Discov.* 3: 1378–1393.

27. Roesch, A., M. Fukunaga-Kalabis, E. C. Schmidt, S. E. Zabierowski, P. A. Brafford, A. Vultur, D. Basu, P. Gimotty, T. Vogt, and M. Herlyn. 2010. A Temporarily Distinct Subpopulation of Slow-Cycling Melanoma Cells Is Required for Continuous Tumor Growth. *Cell* 141: 583–594.

28. Yancovitz, M., A. Litterman, J. Yoon, E. Ng, R. L. Shapiro, R. S. Berman, A. C. Pavlick, F. Darvishian, P. Christos, M. Mazumdar, I. Osman, and D. Polsky. 2012. Intra- and inter-tumor heterogeneity of BRAF V600E mutations in primary and metastatic melanoma. *PLoS One* 7: Online.

29. Fidler, I. J. 1975. Biological Behavior of Malignant Melanoma Cells Correlated to Their Survival in Vivo. *Cancer Res.* 35: 218–224.

30. Briles, E. B., and S. Kornfeld. 1978. Isolation and metastatic properties of detachment variants of B16 melanoma cells. *J. Natl. Cancer Inst.* 60: 1217–1222.

31. Folkman, J., K. Watson, D. Ingber, and D. Hanahan. 1989. Induction of angiogenesis during the transition from hyperplasia to neoplasia. *Nature* 339: 58–61.

32. Ellis, L. M. 2000. Vascular Endothelial Growth Factor in Human Colon Cancer: Biology and Therapeutic Implications. *Oncologist* 5: 11–15.

33. Jinjun, W., W. Zhaowei, L. Qiang, X. Zhijun, Z. Juanzi, L. Lin, and J. Guixi. 2017. SFLT-1 inhibits proliferation, migration, and invasion of colorectal cancer SW480 cells through vascular mimicry formation suppression. *Tumor Biol.* 39: Online.

34. Madden, S. L., B. P. Cook, M. Nacht, W. D. Weber, M. R. Callahan, Y. Jiang, M. R. Dufault, X. Zhang, W. Zhang, J. Walter-Yohrling, C. Rouleau, V. R. Akmaev, C. J. Wang, X. Cao, T. B. St. Martin, B. L. Roberts, B. A. Teicher, K. W. Klinger, R. V. Stan, B. Lucey, E. B. Carson-Walter, J. Laterra, and K. A. Walter. 2004. Vascular gene expression in nonneoplastic and malignant brain. *Am. J. Pathol.* 165: 601–608.

35. Du, R., K. V. Lu, C. Petritsch, P. Liu, R. Ganss, E. Passegué, H. Song, S. VandenBerg, R. S. Johnson, Z. Werb, and G. Bergers. 2008. HIF1α Induces the Recruitment of Bone Marrow-Derived Vascular Modulatory Cells to Regulate Tumor Angiogenesis and Invasion. *Cancer Cell* 13: 206–220.

36. Diez, H., A. Fischer, A. Winkler, C. J. Hu, A. K. Hatzopoulos, G. Breier, and M. Gessler. 2007. Hypoxia-mediated activation of Dll4-Notch-Hey2 signaling in endothelial progenitor cells and adoption of arterial cell fate. *Exp. Cell Res.* 313: 1–9.

37. Phng, L. K., and H. Gerhardt. 2009. Angiogenesis: A Team Effort Coordinated by Notch. *Dev. Cell* 16: 196–208.

38. Isozaki, T., A. S. Arbab, C. S. Haas, M. A. Amin, M. D. Arendt, A. E. Koch, and J. H. Ruth. 2013. Evidence that CXCL16 is a potent mediator of angiogenesis and is involved in endothelial progenitor cell chemotaxis: Studies in mice with K/BxN serum-induced arthritis. *Arthritis Rheum.* 65: 1736–1746.

39. Bodnar, R. J., C. C. Yates, and A. Wells. 2006. IP-10 blocks vascular endothelial growth factor-induced endothelial cell motility and tube formation via inhibition of calpain. *Circ. Res.* 98: 617–625.

40. Bodnar, R. J. 2015. Chemokine Regulation of Angiogenesis During Wound Healing. *Adv. Wound Care* 4: 641–650.

41. Kendall, R. L., G. Wang, and K. A. Thomas. 1996. Identification of a natural soluble form of the vascular endothelial growth factor receptor, FLT-1, and its heterodimerization with KDR. *Biochem. Biophys. Res. Commun.* 226: 324–328.

42. O'Reilly, M. S., L. Holmgren, Y. Shing, C. Chen, R. A. Rosenthal, M. Moses, W. S. Lane, Y. Cao, E. H. Sage, and J. Folkman. 1994. Angiostatin: A novel angiogenesis inhibitor that mediates the suppression of metastases by a lewis lung carcinoma. *Cell* 79: 315–328.

43. Cao, Y., A. Chen, S. S. An, R. W. Ji, D. Davidson, M. Llinás, and M. Llinás. 1997. Kringle 5 of plasminogen is a novel inhibitor of endothelial cell growth. *J. Biol. Chem.* 272: 22924–22928.

44. Masood, R., J. Cai, T. Zheng, D. L. Smith, D. R. Hinton, and P. S. Gill. 2001. Vascular endothelial growth factor (VEGF) is an autocrine growth factor for VEGF receptor-positive human tumors. *Blood* 98: 1904–1913.

45. Boucher, Y., M. Leunig, and R. K. Jain. 1996. Tumor angiogenesis and interstitial hypertension. *Cancer Res.* 56: 4264–4266.

46. Su, J. L., P. C. Yang, J. Y. Shih, C. Y. Yang, L. H. Wei, C. Y. Hsieh, C. H. Chou, Y. M. Jeng, M. Y. Wang, K. J. Chang, M. C. Hung, and M. L. Kuo. 2006. The VEGF-C/Flt-4 axis promotes invasion and metastasis of cancer cells. *Cancer Cell* 9: 209–223.

47. Hagendoorn, J., R. Tong, D. Fukumura, Q. Lin, J. Lobo, T. P. Padera, L. Xu, R. Kucherlapati, and R. K. Jain. 2006. Onset of abnormal blood and lymphatic vessel function and interstitial hypertension in early stages of carcinogenesis. *Cancer Res.* 66: 3360–3364.

48. Viallard, C., and B. Larrivée. 2017. Tumor angiogenesis and vascular normalization: alternative therapeutic targets. *Angiogenesis* 20: 409–426.

49. Baluk, P., S. Morikawa, A. Haskell, M. Mancuso, and D. M. McDonald. 2003. Abnormalities of Basement Membrane on Blood Vessels and Endothelial Sprouts in Tumors. *Am. J. Pathol.* 163: 1801–1815.

50. Abramsson, A., P. Lindblom, and C. Betsholtz. 2003. Endothelial and nonendothelial sources of PDGF-B regulate pericyte recruitment and influence vascular pattern formation in tumors. *J. Clin. Invest.* 112: 1142–1151.

51. Beckers, C. M. L., V. W. M. Van Hinsbergh, and G. P. Van Nieuw Amerongen. 2010. Driving Rho GTPase activity in endothelial cells regulates barrier integrity. *Thromb. Haemost.* 103: 40–55.

52. Greenberg, J. I., D. J. Shields, S. G. Barillas, L. M. Acevedo, E. Murphy, J. Huang, L. Scheppke, C. Stockmann, R. S. Johnson, N. Angle, and D. A. Cheresh. 2008. A role for VEGF as a negative regulator of pericyte function and vessel maturation. *Nature* 456: 809–814.

53. Padera, T. P., B. R. Stoll, J. B. Tooredman, D. Capen, E. Di Tomaso, and R. K. Jain. 2004. Cancer cells compress intratumour vessels. *Nature* 427: 695.

54. Boucher, Y., and R. K. Jain. 1992. Microvascular Pressure Is the Principal Driving Force for Interstitial Hypertension in Solid Tumors: Implications for Vascular Collapse. *Cancer Res.* 52: 5110–5114.

55. Boucher, Y., J. M. Kirkwood, D. Opacic, M. Desantis, and R. K. Jain. 1991. Interstitial Hypertension in Superficial Metastatic Melanomas in Humans. *Cancer Res.* 51: 6691–6694.

56. Leunig, M., R. K. Jain, A. E. Goetz, K. Messmer, and E. Kastenbauer. 1992. Interstitial Hypertension in Head and Neck Tumors in Patients: Correlation with Tumor Size. *Cancer Res.* 52: 1993–1995.

57. Palazon, A., P. A. Tyrakis, D. Macias, P. Veliça, H. Rundqvist, S. Fitzpatrick, N. Vojnovic, A. T. Phan, N. Loman, I. Hedenfalk, T. Hatschek, J. Lövrot, T. Foukakis, A. W. Goldrath, J. Bergh, and R. S. Johnson. 2017. An HIF-1α/VEGF-A Axis in Cytotoxic T Cells Regulates Tumor Progression. *Cancer Cell* 32: 669–683.

58. Shweiki, D., A. Itin, D. Soffer, and E. Keshet. 1992. Vascular endothelial growth factor induced by hypoxia may mediate hypoxia-initiated angiogenesis. *Nature* 359: 843–845.

59. Lewis, C., and C. Murdoch. 2005. Macrophage responses to hypoxia: Implications for tumor progression and anti-cancer therapies. *Am. J. Pathol.* 167: 627–635.

60. Carmeliet, P., Y. Dor, J. M. Herber, D. Fukumura, K. Brusselmans, M. Dewerchin, M. Neeman, F. Bono, R. Abramovitch, P. Maxwell, C. J. Koch, P. Ratcliffe, L. Moons, R. K. Jain, D. Collen, and E. Keshet. 1998. Role of HIF-1α in hypoxiamediated apoptosis, cell proliferation and tumour angiogenesis. *Nature* 394: 485–490.

61. Pennacchietti, S., P. Michieli, M. Galluzzo, M. Mazzone, S. Giordano, and P. M. Comoglio. 2003. Hypoxia promotes invasive growth by transcriptional activation of the met protooncogene. *Cancer Cell* 3: 347–361.

62. Facciabene, A., X. Peng, I. S. Hagemann, K. Balint, A. Barchetti, L. P. Wang, P. A. Gimotty, C. B. Gilks, P. Lal, L. Zhang, and G. Coukos. 2011. Tumour hypoxia promotes tolerance and angiogenesis via CCL28 and T reg cells. *Nature* 475: 226–230.

63. Carmeliet, P., and R. K. Jain. 2011. Principles and mechanisms of vessel normalization for cancer and other angiogenic diseases. *Nat. Rev. Drug Discov.* 10: 417–427.

64. Tong, R. T., Y. Boucher, S. V. Kozin, F. Winkler, D. J. Hicklin, and R. K. Jain. 2004. Vascular normalization by vascular endothelial growth factor receptor 2 blockade induces a pressure gradient across the vasculature and improves drug penetration in tumors. *Cancer Res.* 64: 3731–3736.

65. Cheng, S. Y., H. J. S. Huang, M. Nagane, X. D. Ji, D. Wang, C. C. Y. Shih, W. Arap, C. M. Huang, and W. K. Cavenee. 1996. Suppression of glioblastoma angiogenicity and tumorigenicity by inhibition of endogenous expression of vascular endothelial growth factor. *Proc. Natl. Acad. Sci. U. S. A.* 93: 8502–8507.

66. Ferrara, N., and R. S. Kerbel. 2005. Angiogenesis as a therapeutic target. *Nature* 438: 967–974.

67. Huang, Y., J. Yuan, E. Righi, W. S. Kamoun, M. Ancukiewicz, J. Nezivar, M. Santosuosso, J. D. Martin, M. R. Martin, F. Vianello, P. Leblanc, L. L. Munn, P. Huang, D. G. Duda, D. Fukumura, R. K. Jain, and M. C. Poznansky. 2012. Vascular normalizing doses of

antiangiogenic treatment reprogram the immunosuppressive tumor microenvironment and enhance immunotherapy. *Proc. Natl. Acad. Sci. U. S. A.* 109: 17561–17566.

68. Martin, J. D., G. Seano, and R. K. Jain. 2019. Normalizing Function of Tumor Vessels: Progress, Opportunities, and Challenges. *Annu. Rev. Physiol.* 81: 505–534.

69. Arbiser, J. L., H. Larsson, L. Claesson-Welsh, X. Bai, K. LaMontagne, S. W. Weiss, S. Soker, E. Flynn, and L. F. Brown. 2000. Overexpression of VEGF 121 in immortalized endothelial cells causes conversion to slowly growing angiosarcoma and high level expression of the VEGF receptors VEGFR-1 and VEGFR-2 in vivo. *Am. J. Pathol.* 156: 1469–1476.

70. Arbiser, J. L., M. A. Moses, C. A. Fernandez, N. Ghiso, Y. Cao, N. Klauber, D. Frank, M. Brownlee, E. Flynn, S. Parangi, H. R. Byers, and J. Folkman. 1997. Oncogenic H-ras stimulates tumor angiogenesis by two distinct pathways. *Proc. Natl. Acad. Sci. U. S. A.* 94: 861–866.

71. Folkman, J., E. Merler, C. Abernathy, and G. Williams. 1971. Isolation of a tumor factor responsible for angiogenesis. *J. Exp. Med.* 133: 275–288.

72. Tischer, E., R. Mitchell, T. Hartman, M. Silva, D. Gospodarowicz, J. C. Fiddes, and J. A. Abraham. 1991. The Human Gene for Vascular Endothelial Growth Factor. Multiple Protein Forms Are Encoded Through Alternative Exon Splicing - PubMed. *J. Biol. Chem.* 266: 11947–11954.

73. Houck, K. A., N. Ferrara, J. Winer, G. Cachianes, B. Li, and D. W. Leung. 1991. The vascular endothelial growth factor family: Identification of a fourth molecular species and characterization of alternative splicing of RNA. *Mol. Endocrinol.* 5: 1806–1814.

74. Leung, D. W., G. Cachianes, W. J. Kuang, D. V. Goeddel, and N. Ferrara. 1989. Vascular endothelial growth factor is a secreted angiogenic mitogen. *Science (80-.).* 246: 1306–1309.

75. Alon, T., I. Hemo, A. Itin, J. Pe'er, J. Stone, and E. Keshet. 1995. Vascular endothelial growth factor acts as a survival factor for newly formed retinal vessels and has implications for retinopathy of prematurity. *Nat. Med.* 1: 1024–1028.

76. Gerber, H. P., A. McMurtrey, J. Kowalski, M. Yan, B. A. Keyt, V. Dixit, and N. Ferrara. 1998. Vascular endothelial growth factor regulates endothelial cell survival through the phosphatidylinositol 3'-kinase/Akt signal transduction pathway: Requirement for Flk-1/KDR activation. *J. Biol. Chem.* 273: 30336–30343.

77. Carmeliet, P., V. Ferreira, G. Breier, S. Pollefeyt, L. Kieckens, M. Gertsenstein, M. Fahrig, A. Vandenhoeck, K. Harpal, C. Eberhardt, C. Declercq, J. Pawling, L. Moons, D. Collen, W. Risaut, and A. Nagy. 1996. Abnormal blood vessel development and lethality in embryos lacking a single VEGF allele. *Nature* 380: 435–439.

78. Li, X., M. Tjwa, I. Van Hove, B. Enholm, E. Neven, K. Paavonen, M. Jeltsch, T. D. Juan, R. E. Sievers, E. Chorianopoulos, H. Wada, M. Vanwildemeersch, A. Noel, J. M. Foidart, M. L. Springer, G. Von Degenfeld, M. Dewerchin, H. M. Blau, K. Alitalo, U. Eriksson, P. Carmeliet, and L. Moons. 2008. Reevaluation of the role of VEGF-B suggests a restricted role in the revascularization of the ischemic myocardium. *Arterioscler. Thromb. Vasc. Biol.* 28: 1614–1620.

79. Oh, S. J., M. M. Jeltsch, R. Birkenhäger, J. E. G. McCarthy, H. A. Weich, B. Christ, K. Alitalo, and J. Wilting. 1997. VEGF and VEGF-C: Specific induction of angiogenesis and lymphangiogenesis in the differentiated avian chorioallantoic membrane. *Dev. Biol.* 188: 96–109.

80. Balboa-Beltran, E., M. J. Fernández-Seara, A. Pérez-Muñuzuri, R. Lago, C. García-Magán, M. L. Couce, B. Sobrino, J. Amigo, A. Carracedo, and F. Barros. 2014. A novel stop mutation in the vascular endothelial growth factor-C gene (VEGFC) results in Milroy-like disease. *J. Med. Genet.* 51: 475–478.

81. Baluk, P., and D. M. McDonald. 2008. Markers for microscopic imaging of lymphangiogenesis and angiogenesis. *Ann. N. Y. Acad. Sci.* 1131: 1–12.

82. Baldwin, M. E., M. M. Halford, S. Roufail, R. A. Williams, M. L. Hibbs, D. Grail, H. Kubo, S. A. Stacker, and M. G. Achen. 2005. Vascular Endothelial Growth Factor D Is Dispensable for Development of the Lymphatic System. *Mol. Cell. Biol.* 25: 2441–2449.

83. Roskoski, R. 2007. Vascular endothelial growth factor (VEGF) signaling in tumor progression. *Crit. Rev. Oncol. Hematol.* 62: 179–213.

84. Siegfried, G., A. Basak, J. A. Cromlish, S. Benjannet, J. Marcinkiewicz, M. Chrétien, N. G. Seidah, and A.-M. Khatib. 2003. The secretory proprotein convertases furin, PC5, and PC7 activate VEGF-C to induce tumorigenesis. *J. Clin. Invest.* 111: 1723–1732.

85. Millauer, B., S. Wizigmann-Voos, H. Schnürch, R. Martinez, N. P. H. Møller, W. Risau, and A. Ullrich. 1993. High affinity VEGF binding and developmental expression suggest Flk-1 as a major regulator of vasculogenesis and angiogenesis. *Cell* 72: 835–846.

86. Shalaby, F., R. Janet, T. P. Yamaguchi, M. Gertsenstein, X. F. Wu, M. L. Breitman, and A. C. Schuh. 1995. Failure of blood-island formation and vasculogenesis in Flk-1-deficient mice. *Nature* 376: 62–66.

87. Rezaei, F. M., S. Hashemzadeh, R. R. Gavgani, M. H. Feizi, N. Pouladi, H. S. Kafil, L. Rostamizadeh, V. K. Oskooei, M. Taheri, and E. Sakhinia. 2019. Dysregulated KDR and FLT1 gene expression in colorectal cancer patients. *Reports Biochem. Mol. Biol.* 8: 208–217.

88. De Vries, C., J. A. Escobedo, H. Ueno, K. Houck, N. Ferrara, and L. T. Williams. 1992. The fms-like tyrosine kinase, a receptor for vascular endothelial growth factor. *Science (80-.).* 255: 989–991.

89. Sako, A., J. Kitayama, H. Koyama, H. Ueno, H. Uchida, H. Hamada, and H. Nagawa. 2004. Transduction of soluble Flt-1 gene to peritoneal mesothelial cells can effectively suppress peritoneal metastasis of gastric cancer. *Cancer Res.* 64: 3624–3628.

90. Hasumi, Y., H. Mizukami, M. Urabe, T. Kohno, K. Takeuchi, A. Kume, M. Momoeda, H. Yoshikawa, T. Tsuruo, M. Shibuya, Y. Taketani, and K. Ozawa. 2002. Soluble FLT-1 Expression Supresses Carcinomatous Ascites in Nude Mice Bearing Ovarian Cancer. *Cancer Res.* 58: 2594–2600.

91. Herraiz, I., E. Llurba, S. Verlohren, A. Galindo, J. L. Bartha, M. De La Calle, J. L. Delgado, C. De Paco, A. I. Escudero, F. Moreno, J. A. Garcia-Hernandez, A. Romero-Requejo, B. Marcos-Puig, A. Perales, and M. Mendoza. 2018. Update on the Diagnosis and Prognosis of Preeclampsia with the Aid of the sFlt-1/PlGF Ratio in Singleton Pregnancies. *Fetal Diagn. Ther.* 43: 81–89.

92. Maynard, S. E., J. Y. Min, J. Merchan, K. H. Lim, J. Li, S. Mondal, T. A. Libermann, J. P. Morgan, F. W. Sellke, I. E. Stillman, F. H. Epstein, V. P. Sukhatme, and S. A. Karumanchi. 2003. Excess placental soluble fms-like tyrosine kinase 1 (sFlt1) may contribute to endothelial dysfunction hypertension, and proteinuria in preeclampsia. *J. Clin. Invest.* 111: 649–658.

93. Hao, D., Y. Li, G. Zhao, and M. Zhang. 2019. Soluble fms-like tyrosine kinase-1-enriched exosomes suppress the growth of small cell lung cancer by inhibiting endothelial cell migration. *Thorac. Cancer* 10: 1962–1972.

94. Rettig, W. J., P. Garin-Chesa, J. H. Healey, S. L. Su, E. A. Jaffe, and L. J. Old. 1992. Identification of endosialin, a cell surface glycoprotein of vascular endothelial cells in human cancer. *Proc. Natl. Acad. Sci. U. S. A.* 89: 10832–10836.

95. Christian, S., H. Ahorn, A. Koehler, F. Eisenhaber, H. P. Rodi, P. Garin-Chesa, J. E. Park, W. J. Rettig, and M. C. Lenter. 2001. Molecular Cloning and Characterization of Endosialin, a C-type Lectin-like Cell Surface Receptor of Tumor Endothelium. *J. Biol. Chem.* 276: 7408–7414.

96. St. Croix, B., C. Rago, V. Velculescu, G. Traverso, K. E. Romans, E. Montegomery, A. Lal, G. J. Riggins, C. Lengauer, B. Vogelstein, and K. W. Kinzler. 2000. Genes expressed in human tumor endothelium. *Science (80-.).* 289: 1197–1202.

97. Carson-Walter, E. B., D. N. Watkins, A. Nanda, B. Vogelstein, K. W. Kinzler, and B. St. Croix. 2001. Cell surface tumor endothelial markers are conserved in mice and humans. *Cancer Res.* 61: 6649–6655.

98. Davies, G., G. H. Cunnick, R. E. Mansel, M. D. Mason, and W. G. Jiang. 2004. Levels of expression of endothelial markers specific to tumour-associated endothelial cells and their correlation with prognosis in patients with breast cancer. *Clin. Exp. Metastasis* 21: 31–37.

99. Kiyohara, E., N. Donovan, L. Takeshima, S. Huang, J. S. Wilmott, R. A. Scolyer, P. Jones, E. B. Somers, D. J. O'Shannessy, and D. S. B. Hoon. 2015. Endosialin Expression in Metastatic Melanoma Tumor Microenvironment Vasculature: Potential Therapeutic Implications. *Cancer Microenviron.* 8: 111–118.

100. Guo, Y., J. Hu, Y. Wang, X. Peng, J. Min, J. Wang, E. Matthaiou, Y. Cheng, K. Sun, X. Tong, Y. Fan, P. J. Zhang, L. E. Kandalaft, M. Irving, G. Coukos, and C. Li. 2018. Tumour endothelial marker 1/endosialin-mediated targeting of human sarcoma. *Eur. J. Cancer* 90: 111–121.

101. Wong, S. H., L. Hamel, S. Chevalier, and A. Philip. 2000. Endoglin expression on human microvascular endothelial cells association with betaglycan and formation of higher order complexes with TGF-β signalling receptors. *Eur. J. Biochem.* 267: 5550–5560.

102. Wikström, P., I. F. Lissbrant, P. Stattin, L. Egevad, and A. Bergh. 2002. Endoglin (CD105) is expressed on immature blood vessels and is a marker for survival in prostate cancer. *Prostate* 51: 268–275.

103. Miller, D. W., W. Graulich, B. Karges, S. Stahl, M. Ernst, A. Ramaswamy, H. -Haral. Sedlacek, R. Müller, and J. Adamkiewicz. 1999. Elevated expression of endoglin, a component of the TGF-β-receptor complex, correlates with proliferation of tumor endothelial cells. *Int. J. Cancer* 81: 568–572.

104. Burrows, F. J., E. J. Derbyshire, P. L. Tazzari, P. Amlot, A. F. Gazdar, S. W. King, M. Letarte, E. S. Vitetta, and P. E. Thorpe. 1995. Up-regulation of endoglin on vascular endothelial cells in human solid tumors: implications for diagnosis and therapy. *Clin. Cancer Res.* 1: 1623–1634.

105. Ollauri-Ibáñez, C., J. M. López-Novoa, and M. Pericacho. 2017. Endoglin-based biological therapy in the treatment of angiogenesis-dependent pathologies. *Expert Opin. Biol. Ther.* 17: 1053–1063.

106. Albelda, S. M., M. Daise, E. M. Levine, and C. A. Buck. 1989. Identification and characterization of cell-substratum adhesion receptors on cultured human endothelial cells. *J. Clin. Invest.* 83: 1992–2002.

107. Albelda, S. M., W. A. Muller, C. A. Buck, and P. J. Newman. 1991. Molecular and cellular properties of PECAM-1 (endoCAM/CD31): A novel vascular cell-cell adhesion molecule. *J. Cell Biol.* 114: 1059–1068.

108. O'Reilly, M. S., L. Holmgren, Y. Shing, C. Chen, R. A. Rosenthal, M. Moses, W. S. Lane, Y. Cao, E. H. Sage, and J. Folkman. 1994. Angiostatin: a novel angiogenesis inhibitor that mediates the suppression of metastases by a Lewis lung carcinoma. *Cell* 79: 315–328.

109. Hutzen, B., H. K. Bid, P. J. Houghton, C. R. Pierson, K. Powell, A. Bratasz, C. Raffel, and A. W. Studebaker. 2014. Treatment of medulloblastoma with oncolytic measles viruses

expressing the angiogenesis inhibitors endostatin and angiostatin. *BMC Cancer* 14: 206–217.

110. Schultze, H. E., K. Heide, and H. Haupt. 1961. Über ein bisher unbekanntes niedermolekulares β2-Glubulin des Humanserums. *Naturwissenschaften* 48: 719.

111. Willems, G. M., M. P. Janssen, M. M. A. L. Pelsers, P. Comfurius, M. Galli, R. F. A. Zwaal, and E. M. Bevers. 1996. Role of divalency in the high-affinity binding of anticardiolipin antibody-β2-glycoprotein I complexes to lipid membranes. *Biochemistry* 35: 13833–13842.

112. Ağar, Ç., P. G. de Groot, J. A. Marquart, and J. C. M. Meijers. 2011. Evolutionary conservation of the lipopolysaccharide binding site of β 2-glycoprotein I. *Thromb. Haemost.* 106: 1069–1075.

113. Lozier, J., N. Takahashi, and F. W. Putnam. 1984. Complete amino acid sequence of human plasma β2-glycoprotein I. *Proc. Natl. Acad. Sci. U. S. A.* 81: 3640–3644.

114. Bouma, B., P. G. de Groot, J. M. van den Elsen, R. B. Ravelli, A. Schouten, M. J. Simmelink, R. H. Derksen, J. Kroon, and P. Gros. 1999. Adhesion mechanism of human beta(2)-glycoprotein I to phospholipids based on its crystal structure. *EMBO J.* 18: 5166–5174.

115. Ojha, H., P. Ghosh, H. Singh Panwar, R. Shende, A. Gondane, S. C. Mande, and A. Sahu. 2019. Spatially conserved motifs in complement control protein domains determine functionality in regulators of complement activation-family proteins. *Commun. Biol.* 2: Online.

116. Ağar, Ç., G. M. A. Van Os, M. Mörgelin, R. R. Sprenger, J. A. Marquart, R. T. Urbanus, R. H. W. M. Derksen, J. C. M. Meijers, and P. G. De Groot. 2010. β2-Glycoprotein I can exist in 2 conformations: Implications for our understanding of the antiphospholipid syndrome. *Blood* 116: 1336–1343.

117. Iverson, G. M., E. J. Victoria, and D. M. Marquis. 1998. Anti-β2 glycoprotein I (β2GPI) autoantibodies recognize an epitope on the first domain of β2GPI. *Proc. Natl. Acad. Sci. U. S. A.* 95: 15542–15546.

118. Ioannou, Y., C. Pericleous, I. Giles, D. S. Latchman, D. A. Isenberg, and A. Rahman. 2007. Binding of antiphospholipid antibodies to discontinuous epitopes on domain I of human β2-glycoprotein I: Mutation studies including residues R39 to R43. *Arthritis Rheum.* 56: 280–290.

119. Norman, D. G., P. N. Barlow, M. Baron, A. J. Day, R. B. Sim, and I. D. Campbell. 1991. Three-dimensional structure of a complement control protein module in solution. *J. Mol. Biol.* 219: 717–725.

120. De Laat, B., R. H. W. M. Derksen, M. Van Lummel, M. T. T. Pennings, and P. G. De Groot. 2006. Pathogenic anti-β2-glycoprotein I antibodies recognize domain I of β2-glycoprotein I only after a conformational change. *Blood* 107: 1916–1924.

121. Wang, M. X., D. A. Kandiah, K. Ichikawa, M. Khamashta, G. Hughes, T. Koike, R. Roubey, and S. A. Krilis. 1995. Epitope specificity of monoclonal anti-beta 2-glycoprotein I antibodies derived from patients with the antiphospholipid syndrome. *J. Immunol.* 155: 1629–1636.

122. Steinkasser, A., P. N. Barlow, A. C. Willis, Z. Kertesz, I. D. Campbell, R. B. Sim, and D. G. Norman. 1992. Activity, disulphate mapping and structural modelling of the fifth domain of human β2-glycoprotein I. *FEBS Lett.* 313: 193–197.

123. Hunt, J., and S. Krilis. 1994. The fifth domain of beta 2-glycoprotein I contains a phospholipid binding site (Cys281-Cys288) and a region recognized by anticardiolipin antibodies. *J. Immunol.* 152: 653–659.

124. Slone, E. A., M. R. Pope, and S. D. Fleming. 2015. Phospholipid scramblase 1 is required for β2-glycoprotein I binding in hypoxia and reoxygenation-induced endothelial inflammation. *J. Leukoc. Biol.* 98: 791–804.

125. Ohkura, N., Y. Hagihara, T. Yoshimura, Y. Goto, and H. Kato. 1998. Plasmin can reduce the function of human β2 glycoprotein I by cleaving domain V into a nicked form. *Blood* 91: 4173–4179.

126. Schousboe, I. 1985. beta 2-Glycoprotein I: a plasma inhibitor of the contact activation of the intrinsic blood coagulation pathway. *Blood* 66: 1086–1091.

127. Horbach, D. A., E. van Oort, T. Lisman, J. C. Meijers, R. H. Derksen, and P. G. de Groot. 1999. Beta2-glycoprotein I is proteolytically cleaved in vivo upon activation of fibrinolysis. *Thromb. Haemost.* 81: 87–95.

128. Ieko, M., K. I. Sawada, T. Koike, A. Notoya, M. Mukai, M. Kohno, N. Wada, T. Itoh, and N. Yoshioka. 1999. The putative mechanism of thrombosis in antiphospholipid syndrome: Impairment of the protein C and the fibrinolytic systems by monoclonal anticardiolipin antibodies. *Semin. Thromb. Hemost.* 25: 503–507.

129. Nimpf, J., E. M. Bevers, P. H. H. Bomans, U. Till, H. Wurm, G. M. Kostner, and R. F. A. Zwaal. 1986. Prothrombinase activity of human platelets is inhibited by β2-glycoprotein-I. *BBA - Gen. Subj.* 884: 142–149.

130. Shi, T., G. M. Iverson, J. C. Qi, K. A. Cockerill, M. D. Linnik, P. Konecny, and S. A. Krilis. 2004. β2-Glycoprotein I binds factor XI and inhibits its activation by thrombin and factor XIIa: Loss of inhibition by clipped β2-glycoprotein I. *Proc. Natl. Acad. Sci. U. S. A.* 101: 3939–3944.

131. Miyakis, S., S. A. Robertson, and S. A. Krilis. 2004. Beta-2 glycoprotein I and its role in antiphospholipid syndrome - Lessons from knockout mice. *Clin. Immunol.* 112: 136–143.

132. Mori, T., H. Takeya, J. Nishioka, E. C. Gabazza, and K. Suzuki. 1996. β2-glycoprotein I modulates the anticoagulant activity of activated protein C on the phospholipid surface. *Thromb. Haemost.* 75: 49–55.

133. Sheng, Y., S. W. Reddel, H. Herzog, Y. X. Wang, T. Brighton, M. P. France, S. A. Robertson, and S. A. Krilis. 2001. Impaired Thrombin Generation in β2-Glycoprotein I Null Mice. *J. Biol. Chem.* 276: 13817–13821.

134. Keeling, D. M., A. J. G. Wilson, I. J. Mackie, D. A. Isenberg, and S. J. Machin. 1993. Role of β2-glycoprotein I and anti-phospholipid antibodies in activation of protein C in vitro. *J. Clin. Pathol.* 46: 908–911.

135. Miyakis, S., M. D. Lockshin, T. Atsumi, D. W. Branch, R. L. Brey, R. Cervera, R. H. W. M. Derksen, P. G. De Groot, T. Koike, P. L. Meroni, G. Reber, Y. Shoenfeld, A. Tincani, P. G. Vlachoyiannopoulos, and S. A. Krilis. 2006. International consensus statement on an update of the classification criteria for definite antiphospholipid syndrome (APS). *J. Thromb. Haemost.* 4: 295–306.

136. McDonnell, T., C. Wincup, I. Buchholz, C. Pericleous, I. Giles, V. Ripoll, H. Cohen, M. Delcea, and A. Rahman. 2020. The role of beta-2-glycoprotein I in health and disease associating structure with function: More than just APS. *Blood Rev.* 39: 100610. Online.

137. Arnout, J. 2000. The role of beta 2-glycoprotein I-dependent lupus anticoagulants in the pathogenesis of the antiphospholipid syndrome. *Verh. K. Acad. Geneeskd. Belg.* 62: 353–372.

138. Galli, M., G. Finazzi, E. M. Bevers, and T. Barbui. 1995. Kaolin clotting time and dilute Russell's viper venom time distinguish between prothrombin-dependent and beta 2-glycoprotein I-dependent antiphospholipid antibodies. *Blood* 86: 617–623.

139. Gropp, K., N. Weber, M. Reuter, S. Micklisch, I. Kopka, T. Hallström, and C. Skerka. 2011. β2-glycoprotein I, the major target in antiphospholipid syndrome, is a special human complement regulator. *Blood* 118: 2774–2783.

140. Agostinis, C., S. Biffi, C. Garrovo, P. Durigutto, A. Lorenzon, A. Bek, R. Bulla, C. Grossi, M. O. Borghi, P. L. Meroni, and F. Tedesco. 2011. In vivo distribution of β2 glycoprotein I under various pathophysiologic conditions. *Blood* 118: 4231–4238.

141. Fischetti, F., P. Durigutto, V. Pellis, A. Debeus, P. Macor, R. Bulla, F. Bossi, F. Ziller, D. Sblattero, P. Meroni, and F. Tedesco. 2005. Thrombus formation induced by antibodies to β2-glycoprotein I is complement dependent and requires a priming factor. *Blood* 106: 2340–2346.

142. Hart, M. L., K. A. Ceonzo, L. A. Shaffer, K. Takahashi, R. P. Rother, W. R. Reenstra, J. A. Buras, and G. L. Stahl. 2005. Gastrointestinal Ischemia-Reperfusion Injury Is Lectin Complement Pathway Dependent without Involving C1q. *J. Immunol.* 174: 6373–6380.

143. Williams, J. P., T. T. V. Pechet, M. R. Weiser, R. Reid, L. Kobzik, F. D. Moore, M. C. Carroll, and H. B. Hechtman. 1999. Intestinal reperfusion injury is mediated by IgM and complement. *J. Appl. Physiol.* 86: 938–942.

144. Zhang, P., J. C. Weaver, G. Chen, J. Beretov, T. Atsumi, M. Qi, R. Bhindi, J. C. Qi, M. C. Madigan, B. Giannakopoulos, and S. A. Krilis. 2016. The fifth domain of beta 2 glycoprotein I protects from natural IgM mediated cardiac ischaemia reperfusion injury. *PLoS One* 11: Online.

145. Fleming, S. D., M. R. Pope, S. M. Hoffman, T. Moses, U. Bukovnik, J. M. Tomich, L. M. Wagner, and K. M. Woods. 2010. Domain V Peptides Inhibit β2-Glycoprotein I-Mediated Mesenteric Ischemia/Reperfusion-Induced Tissue Damage and Inflammation. *J. Immunol.* 185: 6168–6178.

146. Nakagawa, H., S. Yasuda, E. Matsuura, K. Kobayashi, M. Ieko, H. Kataoka, T. Horita, T. Atsumi, and T. Koike. 2009. Nicked β2-glycoprotein I binds angiostatin 4.5 (plasminogen kringle 1-5) and attenuates its antiangiogenic property. *Blood* 114: 2553–2559.

147. Sakai, T., K. Balasubramanian, S. Maiti, J. B. Halder, and A. J. Schroit. 2007. Plasmin-cleaved β-2-glycoprotein 1 is an inhibitor of angiogenesis. *Am. J. Pathol.* 171: 1659–1669.

148. Beecken, W.-D. C., E. M. Ringel, J. Babica, E. Oppermann, D. Jonas, and R. A. Blaheta. 2010. Plasmin-clipped β2-glycoprotein-I inhibits endothelial cell growth by down-regulating cyclin A, B and D1 and up-regulating p21 and p27. *Cancer Lett.* 296: 160–167.

149. Beecken, W. D. C., T. Engl, E. M. Ringel, K. Camphausen, M. Michaelis, D. Jonas, J. Folkman, Y. Shing, and R. A. Blaheta. 2006. An endogenous inhibitor of angiogenesis derived from a transitional cell carcinoma: Clipped β2-glycoprotein-I. *Ann. Surg. Oncol.* 13: 1241–1251.

150. Yu, P., F. H. Passam, D. M. Yu, G. Denyer, and S. A. Krilis. 2008. Beta2-glycoprotein I inhibits vascular endothelial growth factor and basic fibroblast growth factor induced angiogenesis through its amino terminal domain. *J. Thromb. Haemost.* 6: 1215–1223.

151. Pope, M. R., U. Bukovnik, J. M. Tomich, and S. D. Fleming. 2012. Small β2-Glycoprotein I Peptides Protect from Intestinal Ischemia Reperfusion Injury. *J. Immunol.* 189: 5047–5056.

152. Reynolds, C. R., S. A. Islam, and M. J. E. Sternberg. 2018. EzMol: A Web Server Wizard for the Rapid Visualization and Image Production of Protein and Nucleic Acid Structures. *J. Mol. Biol.* 430: 2244–2248.

153. Ralph, P., M. A. S. Moore, and K. Nilsson. 1976. Lysozyme synthesis by established human and murine histiocytic lymphoma cell lines*. *J. Exp. Med.* 143: 1528–1533.

154. Ralph, P., and I. Nakoinz. 1975. Phagocytosis and cytolysis by a macrophage tumour and its cloned cell line. *Nature* 257: 393–394.

155. Sears, D. W., N. Osman, B. Tate, I. F. McKenzie, and P. M. Hogarth. 1990. Molecular cloning and expression of the mouse high affinity Fc receptor for IgG. *J. Immunol.* 144.

156. Stanley, E. R., L. J. Guilbert, R. J. Tushinski, and S. H. Bartelmez. 1983. CSF-1—A mononuclear phagocyte lineage-specific hemopoietic growth factor. *J. Cell. Biochem.* 21: 151–159.

157. Modolell, M., I. M. Corraliza, F. Link, G. Soler, and K. Eichmann. 1995. Reciprocal regulation of the nitric oxide synthase/arginase balance in mouse bone marrow-derived macrophages by TH 1 and TH 2 cytokines. *Eur. J. Immunol.* 25: 1101–1104.

158. Alderton, W. K., C. E. Cooper, and R. G. Knowles. 2001. Nitric oxide synthases: structure, function and inhibition. *Biochem. J.* 357: 593–615.

159. Weigert, A., and B. Brüne. 2008. Nitric oxide, apoptosis and macrophage polarization during tumor progression. *Nitric Oxide - Biol. Chem.* 19: 95–102.

160. Harada, K., Supriatno, S.-I. Kawaguchi, O. Tomitaro, H. Yoshida, and M. Sato. 2004. Overexpression of iNOS Gene Suppresses the Tumorigenicity and Metastasis of Oral Cancer Cells. *In Vivo (Brooklyn).* 18: 449–455.

161. Shang, Z. J., J. R. Li, and Z. B. Li. 2002. Effects of exogenous nitric oxide on oral squamous cell carcinoma: An in vitro study. *J. Oral Maxillofac. Surg.* 60: 905–910.

162. Aranda, E., C. Lopez-Pedrera, J. R. De La Haba-Rodriguez, and A. Rodriguez-Ariza. 2011. Nitric Oxide and Cancer: The Emerging Role of S-Nitrosylation. *Curr. Mol. Med.* 12: 50–67.

163. Baritaki, S., S. Huerta-Yepez, A. Sahakyan, I. Karagiannides, K. Bakirtzi, A. R. Jazirehi, B. Bonavida, and J. F. Kugel. 2010. Mechanisms of nitric oxide-mediated inhibition of EMT in cancer: Inhibition of the metastasis-inducer snail and induction of the metastasis-suppressor RKIP. *Cell Cycle* 9: 4931–4940.

164. Zhao, S. F., X. Y. Tong, and F. D. Zhu. 2005. Nitric oxide induces oral squamous cell carcinoma cells apoptosis with p53 accumulation. *Oral Oncol.* 41: 785–790.

165. Thomsen, L. L., D. W. Miles, L. Happerfield, L. G. Bobrow, R. G. Knowles, and S. Moncada. 1995. Nitric oxide synthase activity in human breast cancer. *Br. J. Cancer* 72: 41–44.

166. Gallo, O., I. Fini-Stochi, W. A. Vergari, E. Masini, L. Morbidelli, M. Ziche, and A. Franchi. 1998. Role of Nitric Oxide in Angiogenesis and Tumor Progression in Head and Neck Cancer | JNCI: Journal of the National Cancer Institute | Oxford Academic. *J. Natl. Cancer Inst.* 90: 587–596.

167. Ziche, M., L. Morbidelli, E. Masini, S. Amerini, H. J. Granger, C. A. Maggi, P. Geppetti, and F. Ledda. 1994. Nitric oxide mediates angiogenesis in vivo and endothelial cell growth and migration in vitro promoted by substance P. *J. Clin. Invest.* 94: 2036–2044.

168. Peñarando, J., L. M. López-Sánchez, R. Mena, S. Guil-Luna, F. Conde, V. Hernández, M. Toledano, V. Gudiño, M. Raponi, C. Billard, C. Villar, C. Díaz, J. Gómez-Barbadillo, J. De la Haba-Rodríguez, K. Myant, E. Aranda, and A. Rodríguez-Ariza. 2018. A role for endothelial nitric oxide synthase in intestinal stem cell proliferation and mesenchymal colorectal cancer. *BMC Biol.* 16: Online.

169. Kashiwagi, S., Y. Izumi, T. Gohongi, Z. N. Demou, L. Xu, P. L. Huang, D. G. Buerk, L. L. Munn, R. K. Jain, and D. Fukumura. 2005. NO mediates mural cell recruitment and vessel morphogenesis in murine melanomas and tissue-engineered blood vessels. *J. Clin. Invest.* 115: 1816–1827.

170. Simon, A., and J. W. M. Van Der Meer. 2007. Pathogenesis of familial periodic fever syndromes or hereditary autoinflammatory syndromes. *Am. J. Physiol. - Regul. Integr. Comp. Physiol.* 292: 86–98.

171. Haabeth, O. A. W., K. B. Lorvik, H. Yagita, B. Bogen, and A. Corthay. 2016. Interleukin-1 is required for cancer eradication mediated by tumor-specific Th1 cells. *Oncoimmunology* 5: Online.

172. Ghiringhelli, F., L. Apetoh, A. Tesniere, L. Aymeric, Y. Ma, C. Ortiz, K. Vermaelen, T. Panaretakis, G. Mignot, E. Ullrich, J. L. Perfettini, F. Schlemmer, E. Tasdemir, M. Uhl, P. Génin, A. Civas, B. Ryffel, J. Kanellopoulos, J. Tschopp, F. André, R. Lidereau, N. M. McLaughlin, N. M. Haynes, M. J. Smyth, G. Kroemer, and L. Zitvogel. 2009. Activation of the NLRP3 inflammasome in dendritic cells induces IL-1B-dependent adaptive immunity against tumors. *Nat. Med.* 15: 1170–1178.

173. Allen, I. C., E. M. E. Tekippe, R. M. T. Woodford, J. M. Uronis, E. K. Holl, A. B. Rogers, H. H. Herfarth, C. Jobin, and J. P. Y. Ting. 2010. The NLRP3 inflammasome functions as a negative regulator of tumorigenesis during colitis-associated cancer. *J. Exp. Med.* 207: 1045–1056.

174. Veltri, S., and J. W. Smith. 1996. Interleukin 1 trials in cancer patients: A review of the toxicity, antitumor and hematopoietic effects. *Stem Cells* 14: 164–176.

175. Walsh, L. J., G. Trinchieri, H. A. Waldorf, D. Whitaker, and G. F. Murphy. 1991. Human dermal mast cells contain and release tumor necrosis factor α, which induces endothelial leukocyte adhesion molecule 1. *Proc. Natl. Acad. Sci. U. S. A.* 88: 4220–4224.

176. Tracey, K. J., Y. Fong, D. G. Hesse, K. R. Manogue, A. T. Lee, G. C. Kuo, S. F. Lowry, and A. Cerami. 1987. Anti-cachectin/TNF monoclonal antibodies prevent septic shock during lethal bacteraemia. *Nature* 330: 662–664.

177. Victor, F. C., and A. B. Gottlieb. 2002. TNF-alpha and apoptosis: implications for the pathogenesis and treatment of psoriasis. *J. Drugs Dermatol.* 1: 264–275.

178. Brynskov, J., P. Foegh, G. Pedersen, C. Ellervik, T. Kirkegaard, A. Bingham, and T. Saermark. 2002. Tumour necrosis factor α converting enzyme (TACE) activity in the colonic mucosa of patients with inflammatory bowel disease. *Gut* 51: 37–43.

179. Swardfager, W., K. Lanctt, L. Rothenburg, A. Wong, J. Cappell, and N. Herrmann. 2010. A meta-analysis of cytokines in Alzheimer's disease. *Biol. Psychiatry* 68: 930–941.

180. Carswell, E. A., L. J. Old, R. L. Kassel, S. Green, N. Fiore, and B. Williamson. 1975. An endotoxin induced serum factor that causes necrosis of tumors. *Proc. Natl. Acad. Sci. U. S. A.* 72: 3666–3670.

181. Damento, G., S. C. Kavoussi, M. A. Materin, D. R. Salomão, P. A. Quiram, S. Balasubramaniam, and J. S. Pulido. 2014. Clinical and histologic findings in patients with uveal melanomas after taking tumor necrosis factor-α inhibitors. *Mayo Clin. Proc.* 89: 1481–1486.

182. Nardone, B., J. A. Hammel, D. W. Raisch, L. L. Weaver, D. Schneider, and D. P. West. 2014. Melanoma associated with tumour necrosis factor-α inhibitors: A Research on Adverse Drug events and Reports (RADAR) project. *Br. J. Dermatol.* 170: 1170–1172.

183. Raaschou, P., J. F. Simard, M. Holmqvist, and J. Askling. 2013. Rheumatoid arthritis, anti-tumour necrosis factor therapy, and risk of malignant melanoma: Nationwide population based prospective cohort study from Sweden. *BMJ* 346: Online.

184. Chen, Y., M. Friedman, G. Liu, A. Deodhar, and C. Q. Chu. 2018. Do tumor necrosis factor inhibitors increase cancer risk in patients with chronic immune-mediated inflammatory disorders? *Cytokine* 101: 78–88.

185. Amari, W., A. L. Zeringue, J. R. McDonald, L. Caplan, S. A. Eisen, and P. Ranganathan. 2011. Risk of non-melanoma skin cancer in a national cohort of veterans with rheumatoid arthritis. *Rheumatology (Oxford).* 50: 1431–1439.

186. Kumari, N., B. S. Dwarakanath, A. Das, and A. N. Bhatt. 2016. Role of interleukin-6 in cancer progression and therapeutic resistance. *Tumor Biol.* 37: 11553–11572.

187. Berek, J. S., C. Chung, K. Kaldi, J. M. Watson, R. M. Knox, and O. Martínez-Maza. 1991. Serum interleukin-6 levels correlate with disease status in patients with epithelial ovarian cancer. *Am. J. Obstet. Gynecol.* 164: 1038–1043.

188. Alexandrakis, M. G., F. H. Passam, D. S. Kyriakou, A. V. Christophoridou, K. Perisinakis, A. Hatzivasili, A. Foudoulakis, and E. Castanas. 2004. Serum Level of Interleukin-16 in Multiple Myeloma Patients and Its Relationship to Disease Activity. *Am. J. Hematol.* 75: 101–106.

189. Santer, F. R., K. Malinowska, Z. Culig, and I. T. Cavarretta. 2010. Interleukin-6 trans-signalling differentially regulates proliferation, migration, adhesion and maspin expression in human prostate cancer cells. *Endocr. Relat. Cancer* 17: 241–253.

190. Guo, Y., F. Xu, T. Lu, Z. Duan, and Z. Zhang. 2012. Interleukin-6 signaling pathway in targeted therapy for cancer. *Cancer Treat. Rev.* 38: 904–910.

191. Bellone, S., K. Watts, S. Cane', M. Palmieri, M. J. Cannon, A. Burnett, J. J. Roman, S. Pecorelli, and A. D. Santin. 2005. High serum levels of interleukin-6 in endometrial carcinoma are associated with uterine serous papillary histology, a highly aggressive and chemotherapy-resistant variant of endometrial cancer. *Gynecol. Oncol.* 98: 92–98.

192. Conze, D., L. Weiss, P. S. Regen, M. Rincón, D. Weaver, A. Bhushan, and P. Johnson. 2001. Autocrine production of interleukin 6 causes multidrug resistance in breast cancer cells. *Cancer Res.* 61: 8851–8858.

193. Braune, J., U. Weyer, C. Hobusch, J. Mauer, J. C. Brüning, I. Bechmann, and M. Gericke. 2017. IL-6 Regulates M2 Polarization and Local Proliferation of Adipose Tissue Macrophages in Obesity. *J. Immunol.* 198: 2927 LP – 2934.

194. Mauer, J., B. Chaurasia, J. Goldau, M. C. Vogt, J. Ruud, K. D. Nguyen, S. Theurich, A. C. Hausen, J. Schmitz, H. S. Brönneke, E. Estevez, T. L. Allen, A. Mesaros, L. Partridge, M. A. Febbraio, A. Chawla, F. T. Wunderlich, and J. C. Brüning. 2014. Signaling by IL-6 promotes alternative activation of macrophages to limit endotoxemia and obesity-associated resistance to insulin. *Nat. Immunol.* 15: 423–430.

195. Fu, X.-L., W. Duan, C.-Y. Su, F.-Y. Mao, Y.-P. Lv, Y.-S. Teng, P.-W. Yu, Y. Zhuang, and Y.-L. Zhao. 2017. Interleukin 6 induces M2 macrophage differentiation by STAT3 activation that correlates with gastric cancer progression. *Cancer Immunol. Immunother.* 66: 1597–1608.

196. Sutterwala, F. S., G. J. Noel, P. Salgame, and D. M. Mosser. 1998. Reversal of proinflammatory responses by ligating the macrophage Fcγ receptor type I. *J. Exp. Med.* 188: 217–222.

197. Anderson, C. F., and D. M. Mosser. 2002. A novel phenotype for an activated macrophage: the type 2 activated macrophage. *J. Leukoc. Biol.* 72: 101–106.

198. Shrivastava, R., and N. Shukla. 2019. Attributes of alternatively activated (M2) macrophages. *Life Sci.* 224: 222–231.

199. Zizzo, G., B. A. Hilliard, M. Monestier, and P. L. Cohen. 2012. Efficient clearance of early apoptotic cells by human macrophages requires "M2c" polarization and MertK induction. *J. Immunol.* 189: 3508–3520.

200. Ferrante, C. J., G. Pinhal-Enfield, G. Elson, B. N. Cronstein, G. Hasko, S. Outram, and S. J. Leibovich. 2013. The adenosine-dependent angiogenic switch of macrophages to an M2-like phenotype is independent of interleukin-4 receptor alpha (IL-4Rα) signaling. *Inflammation* 36: 921–931.

201. Chen, X. W., T. J. Yu, J. Zhang, Y. Li, H. L. Chen, G. F. Yang, W. Yu, Y. Z. Liu, X. X. Liu, C. F. Duan, H. L. Tang, M. Qiu, C. L. Wang, H. Zheng, J. Yue, A. M. Guo, and J.

Yang. 2017. CYP4A in tumor-associated macrophages promotes pre-metastatic niche formation and metastasis. *Oncogene* 36: 5045–5057.

202. Duluc, D. E., Y. Delneste, F. Tan, M.-P. Moles, L. Grimaud, J. Lenoir, L. Preisser, I. Anegon, L. Catala, N. Ifrah, P. Descamps, E. Gamelin, H. Gascan, M. Hebbar, and P. Jeannin. 2007. Tumor-associated leukemia inhibitory factor and IL-6 skew monocyte differentiation into tumor-associated macrophage-like cells. *Blood* 110: 4319–4330.

203. Aljabery, F., H. Olsson, O. Gimm, S. Jahnson, and I. Shabo. 2018. M2-macrophage infiltration and macrophage traits of tumor cells in urinary bladder cancer. *Urol. Oncol. Semin. Orig. Investig.* 36: 159.e19-159.e26.

204. Zhu, Y., J. M. Herndon, D. K. Sojka, K. W. Kim, B. L. Knolhoff, C. Zuo, D. R. Cullinan, J. Luo, A. R. Bearden, K. J. Lavine, W. M. Yokoyama, W. G. Hawkins, R. C. Fields, G. J. Randolph, and D. G. DeNardo. 2017. Tissue-Resident Macrophages in Pancreatic Ductal Adenocarcinoma Originate from Embryonic Hematopoiesis and Promote Tumor Progression. *Immunity* 47: 323–338.

205. Jetten, N., S. Verbruggen, M. J. Gijbels, M. J. Post, M. P. J. De Winther, and M. M. P. C. Donners. 2014. Anti-inflammatory M2, but not pro-inflammatory M1 macrophages promote angiogenesis in vivo. *Angiogenesis* 17: 109–118.

206. Qian, B. Z., and J. W. Pollard. 2010. Macrophage Diversity Enhances Tumor Progression and Metastasis. *Cell* 141: 39–51.

207. Massi, D., C. Marconi, A. Franchi, F. Bianchini, M. Paglierani, S. Ketabchi, C. Miracco, M. Santucci, and L. Calorini. 2007. Arginine metabolism in tumor-associated macrophages in cutaneous malignant melanoma: evidence from human and experimental tumors. *Hum. Pathol.* 38: 1516–1525.

208. Bowdish, D. M. E. 2016. Macrophage Activation and Polarization. In *Encyclopedia of Immunobiology* vol. 1. Elsevier Inc. 289–292.

209. Högger, P., U. Erpenstein, P. Rohdewald, and C. Sorg. 1998. Biochemical characterization of a glucocorticoid-induced membrane protein (RM3/1) in human monocytes and its application as model system for ranking glucocorticoid potency. *Pharm. Res.* 15: 296–302.

210. Van Den Heuvel, M. M., C. P. Tensen, J. H. Van As, T. K. Van Den Berg, D. M. Fluitsma, C. D. Dijkstra, E. A. Döpp, A. Droste, F. A. Van Gaalen, C. Sorg, P. Högger, and R. H. J. Beelen. 1999. Regulation of CD163 on human macrophages: Cross-linking of CD163 induces signaling and activation. *J. Leukoc. Biol.* 66: 858–866.

211. Shiraishi, D., Y. Fujiwara, H. Horlad, Y. Saito, T. Iriki, J. Tsuboki, P. Cheng, N. Nakagata, H. Mizuta, H. Bekki, Y. Nakashima, Y. Oda, M. Takeya, and Y. Komohara. 2018. CD163 is required for protumoral activation of macrophages in human and murine sarcoma. *Cancer Res.* 78: 3255–3266.

212. Troiano, G., V. C. A. Caponio, I. Adipietro, M. Tepedino, R. Santoro, L. Laino, L. Lo Russo, N. Cirillo, and L. Lo Muzio. 2019. Prognostic significance of CD68+ and CD163+ tumor associated macrophages in head and neck squamous cell carcinoma: A systematic review and meta-analysis. *Oral Oncol.* 93: 66–75.

213. Gomez-Brouchet, A., C. Illac, J. Gilhodes, C. Bouvier, S. Aubert, J. M. Guinebretiere, B. Marie, F. Larousserie, N. Entz-Werlé, G. de Pinieux, T. Filleron, V. Minard, V. Minville, E. Mascard, F. Gouin, M. Jimenez, M. C. Ledeley, S. Piperno-Neumann, L. Brugieres, and F. Rédini. 2017. CD163-positive tumor-associated macrophages and CD8-positive cytotoxic lymphocytes are powerful diagnostic markers for the therapeutic stratification of osteosarcoma patients: An immunohistochemical analysis of the biopsies fromthe French OS2006 phase 3 t. *Oncoimmunology* 6: Online.

214. Takeuchi, H., M. Tanaka, A. Tanaka, A. Tsunemi, and H. Yamamoto. 2016. Predominance of M2-polarized macrophages in bladder cancer affects angiogenesis, tumor grade and invasiveness. *Oncol. Lett.* 11: 3403–3408.

215. Zhao, X., J. Qu, Y. Sun, J. Wang, X. Liu, F. Wang, H. Zhang, W. Wang, X. Ma, X. Gao, and S. Zhang. 2017. Prognostic significance of tumor-associated macrophages in breast cancer: A meta-analysis of the literature. *Oncotarget* 8: 30576–30586.

216. Wu, S. Q., R. Xu, X. F. Li, X. K. Zhao, and B. Z. Qian. 2018. Prognostic roles of tumor associated macrophages in bladder cancer: A system review and meta-analysis. *Oncotarget* 9: 25294–25303.

217. Lee, W. J., M. H. Lee, H. T. Kim, C. H. Won, M. W. Lee, J. H. Choi, and S. E. Chang. 2019. Prognostic significance of CD163 expression and its correlation with cyclooxygenase-2 and vascular endothelial growth factor expression in cutaneous melanoma. *Melanoma Res.* 29: 501–509.

218. Wang, H., W. M. Hu, Z. J. Xia, Y. Liang, Y. Lu, S. X. Lin, and H. Tang. 2019. High numbers of CD163+ tumor-associated macrophages correlate with poor prognosis in multiple myeloma patients receiving bortezomib-based regimens. *J. Cancer* 10: 3239–3245.

219. Fiorentino, D. F., M. W. Bond, and T. R. Mosmann. 1989. Two types of mouse t helper cell: IV. Th2 clones secrete a factor that inhibits cytokine production by Thl clones. *J. Exp. Med.* 170: 2081–2095.

220. de Waal Malefyt, R., C. G. Figdor, and J. E. de Vries. 1995. Regulation of Human Monocyte Functions by Interleukin-10. In Springer, Berlin, Heidelberg. 37–52.

221. Das, A., C. S. Yang, S. Arifuzzaman, S. Kim, S. Y. Kim, K. H. Jung, Y. S. Lee, and Y. G. Chai. 2018. High-resolution mapping and dynamics of the transcriptome, transcription factors, and transcription co-factor networks in classically and alternatively activated macrophages. *Front. Immunol.* 9.

222. Fiorentino, D. F., A. Zlotnik, T. R. Mosmann, M. Howard, and A. O'Garra. 1991. IL-10 Inhibits Cytokine Production by Activated Macrophages - PubMed. *J. Immunol.* 147: 3815–3822.

223. Abrams, J., C. G. Figdor, R. De Waal Malefyt, B. Bennett, and J. E. De Vries. 1991. Interleukin 10(IL-10) inhibits cytokine synthesis by human monocytes: An autoregulatory role of IL-10 produced by monocytes. *J. Exp. Med.* 174: 1209–1220.

224. Zeni, E., L. Mazzetti, D. Miotto, N. Lo Cascio, P. Maestrelli, P. Querzoli, M. Pedriali, E. De Rosa, L. M. Fabbri, C. E. Mapp, and P. Boschetto. 2007. Macrophage expression of interleukin-10 is a prognostic factor in nonsmall cell lung cancer. *Eur. Respir. J.* 30: 627–632.

225. Wang, R., M. Lu, J. Zhang, S. Chen, X. Luo, Y. Qin, and H. Chen. 2011. Increased IL-10 mRNA expression in tumor-associated macrophage correlated with late stage of lung cancer. *J. Exp. Clin. Cancer Res.* 30: Online.

226. Zeng, L., C. O'Connor, J. Zhang, A. M. Kaplan, and D. A. Cohen. 2010. IL-10 promotes resistance to apoptosis and metastatic potential in lung tumor cell lines. *Cytokine* 49: 294–302.

227. Vahl, J. M., J. Friedrich, S. Mittler, S. Trump, L. Heim, K. Kachler, L. Balabko, N. Fuhrich, C. I. Geppert, D. I. Trufa, N. Sopel, R. Rieker, H. Sirbu, and S. Finotto. 2017. Interleukin-10-regulated tumour tolerance in non-small cell lung cancer. *Br. J. Cancer* 117: 1644–1655.

228. Li, Y., H. Yu, S. Jiao, and J. Yang. 2014. [Prognostic value of IL-10 expression in tumor tissues of breast cancer patients] - PubMed. *Chinese J. Cell. Mol. Immunol.* 30: 517–520.

229. Toiyama, Y., C. Miki, Y. Inoue, S. Minobe, H. Urano, and M. Kusunoki. 2010. Loss of tissue expression of interleukin-10 promotes the disease progression of colorectal carcinoma. *Surg. Today* 40: 46–53.

230. Ahmad, N., A. Ammar, S. J. Storr, A. R. Green, E. Rakha, I. O. Ellis, and S. G. Martin. 2018. IL-6 and IL-10 are associated with good prognosis in early stage invasive breast cancer patients. *Cancer Immunol. Immunother.* 67: 537–549.

231. Groux, H., F. Cottrez, M. Roleau, S. Mauze, S. Antonenko, T. McNeil, M. Bigler, M.-G. Rooncarlo, and R. L. Coffman. 1999. A Transgenic Model to Analyze the Immunoregulatory Role of IL-10 Secreted by Antigen-Presenting Cells | The Journal of Immunology. *J. Immunol.* 162: 1723–1729.

232. Berman, R. M., T. Suzuki, H. Tahara, P. D. Robbins, S. K. Narula, and M. T. Lotze. 1996. Systemic administration of cellular IL-10 induces an effective, specific, and long-lived immune response against established tumors in mice. *J. Immunol.* 157: 231–238.

233. Gérard, C. M., C. Bruyns, A. Delvaux, N. Baudson, J. L. Dargent, M. Goldman, and T. Velu. 1996. Loss of tumorigenicity and increased immunogenicity induced by interleukin-10 gene transfer in B16 melanoma cells. *Hum. Gene Ther.* 7: 23–31.

234. Seo, N., S. Hayakawa, M. Takigawa, and Y. Tokura. 2001. Interleukin-10 expressed at early tumour sites induces subsequent generation of CD4+ T-regulatory cells and systemic collapse of antitumour immunity. *Immunology* 103: 449–457.

235. Jansen, J. H., W. E. Fibbe, R. Willemze, and J. C. Kluin-Nelemans. 1990. Interleukin-4 - A regulatory protein. *Blut* 60: 269–274.

236. Tsunawaki, S., M. Sporn, A. Ding, and C. Nathan. 1988. Deactivation of macrophages by transforming growth factor-β. *Nature* 334: 260–262.

237. Kehrl, J. H., A. B. Roberts, L. M. Wakefield, S. Jakowlew, M. B. Sporn, and A. S. Fauci. 1986. Transforming growth factor beta is an important immunomodulatory protein for human B lymphocytes. *J. Immunol.* 137: 3855–60.

238. Wahl, S. M., D. A. Hunt, H. L. Wong, S. Dougherty, N. McCartney-Francis, L. M. Wahl, L. Ellingsworth, J. A. Schmidt, G. Hall, and A. B. Roberts. 1988. Transforming growth factor-beta is a potent immunosuppressive agent that inhibits IL-1-dependent lymphocyte proliferation. *J. Immunol.* 140: 3026–32.

239. Ranges, G. E., I. S. Figari, T. Espevik, and M. A. Palladino. 1987. Inhibition of cytotoxic T cell development by transforming growth factor β and reversal by recombinant tumor necrosis factor α. *J. Exp. Med.* 166: 991–998.

240. Bröcker, E. B., G. Zwadlo, B. Holzmann, E. Macher, and C. Sorg. 1988. Inflammatory cell infiltrates in human melanoma at different stages of tumor progression. *Int. J. Cancer* 41: 562–567.

241. Wang, H., L. Yang, D. Wang, Q. Zhang, and L. Zhang. 2017. Pro-tumor activities of macrophages in the progression of melanoma. *Hum. Vaccin. Immunother.* 13: 1556–1562.

242. Varney, M. L., S. L. Johansson, and R. K. Singh. 2005. Tumour-associated macrophage infiltration, neovascularization and aggressiveness in malignant melanoma: Role of monocyte chemotactic protein-1 and vascular endothelial growth factor-A. *Melanoma Res.* 15: 417–425.

243. Roubin, R., J. -P Césarini, W. H. Fridman, J. Pavie-Fischer, and H. H. Peter. 1975. Characterization of the mononuclear cell infiltrate in human malignant melanoma. *Int. J. Cancer* 16: 61–73.

244. Gartrell, R. D., D. K. Marks, T. D. Hart, G. Li, D. R. Davari, A. Wu, Z. Blake, Y. Lu, K. N. Askin, A. Monod, C. L. Esancy, E. C. Stack, D. T. Jia, P. M. Armenta, Y. Fu, D. Izaki, B. Taback, R. Rabadan, H. L. Kaufman, C. G. Drake, B. A. Horst, and Y. M. Saenger. 2018.

Quantitative analysis of immune infiltrates in primary Melanoma. *Cancer Immunol. Res.* 6: 481–493.

245. Jensen, T. O., H. Schmidt, H. J. Møller, M. Høyer, M. B. Maniecki, P. Sjoegren, I. J. Christensen, and T. Steiniche. 2009. Macrophage markers in serum and tumor have prognostic impact in American joint committee on cancer stage I/II melanoma. *J. Clin. Oncol.* 27: 3330–3337.

246. Hillen, F., C. I. M. Baeten, A. Van De Winkel, D. Creytens, D. W. J. Van Der Schaft, V. Winnepenninckx, and A. W. Griffioen. 2008. Leukocyte infiltration and tumor cell plasticity are parameters of aggressiveness in primary cutaneous melanoma. *Cancer Immunol. Immunother.* 57: 97–106.

247. Shapouri-Moghaddam, A., S. Mohammadian, H. Vazini, M. Taghadosi, S. A. Esmaeili, F. Mardani, B. Seifi, A. Mohammadi, J. T. Afshari, and A. Sahebkar. 2018. Macrophage plasticity, polarization, and function in health and disease. *J. Cell. Physiol.* 233: 6425–6440.

248. Mantovani, A., S. Sozzani, M. Locati, P. Allavena, and A. Sica. 2002. Macrophage polarization: tumor-associated macrophages as a paradigm for polarized M2 mononuclear phagocytes. *Trends Immunol.* 23: 549–55.

249. Chanmee, T., P. Ontong, K. Konno, and N. Itano. 2014. Tumor-associated macrophages as major players in the tumor microenvironment. *Cancers (Basel).* 6: 1670–1690.

250. Caras, I., C. Tucureanu, L. Lerescu, R. Pitica, L. Melinceanu, S. Neagu, and A. Salageanu. 2011. Influence of tumor cell culture supernatants on macrophage functional polarization: In vitro models of macrophage-tumor environment interaction. *Tumori* 97: 647–54.

251. Salageanu, A., I. Caras, C. Tucureanu, L. Lerescu, R. Pitica, L. Melinceanu, and S. Neagu. *Influence of tumor cell culture supernatants on macrophage functional polarization: in vitro models of macrophage-tumor environment interaction*,.

252. Mantovani, A., P. Allavena, S. Sozzani, A. Vecchi, M. Locati, and A. Sica. 2004. Chemokines in the recruitment and shaping of the leukocyte infiltrate of tumors. *Semin. Cancer Biol.* 14: 155–160.

253. Bottazzi, B., N. Polentarutti, R. Acero, A. Balsari, D. Boraschi, P. Ghezzi, M. Salmona, and A. Mantovani. 1983. Regulation of the macrophage content of neoplasms by chemoattractants. *Science (80-.).* 220: 210–212.

254. Nesbit, M., H. Schaider, T. H. Miller, and M. Herlyn. 2001. Low-Level Monocyte Chemoattractant Protein-1 Stimulation of Monocytes Leads to Tumor Formation in Nontumorigenic Melanoma Cells. *J. Immunol.* 166: 6483–6490.

255. Grimshaw, M. J., and F. R. Balkwill. 2001. Inhibition of monocyte and macrophage chemotaxis by hypoxia and inflammation - A potential mechanism. *Eur. J. Immunol.* 31: 480–489.

256. Turner, L., C. Scotton, R. Negus, and F. Balkwill. 1999. Hypoxia inhibits macrophage migration. *Eur. J. Immunol.* 29: 2280–2287.

257. Leek, R. D., and A. L. Harris. 2002. Tumor-associated macrophages in breast cancer. *J. Mammary Gland Biol. Neoplasia* 7: 177–189.

258. Leek, R. D., R. J. Landers, A. L. Harris, and C. E. Lewis. 1999. Necrosis correlates with high vascular density and focal macrophage infiltration in invasive carcinoma of the breast. *Br. J. Cancer* 79: 991–995.

259. Henze, A.-T., and M. Mazzone. 2016. The impact of hypoxia on tumor-associated macrophages. *J. Clin. Invest.* 126: 3672–3679.

260. Falleni, M., F. Savi, D. Tosi, E. Agape, A. Cerri, L. Moneghini, and G. P. Bulfamante. 2017. M1 and M2 macrophages' clinicopathological significance in cutaneous melanoma. *Melanoma Res.* 27: 200–210.

261. Wang, T., Y. Ge, M. Xiao, A. Lopez-Coral, R. Azuma, R. Somasundaram, G. Zhang, Z. Wei, X. Xu, F. J. Rauscher, M. Herlyn, and R. E. Kaufman. 2012. Melanoma-derived conditioned media efficiently induce the differentiation of monocytes to macrophages that display a highly invasive gene signature. *Pigment Cell Melanoma Res.* 25: 493–505.

262. Solinas, G., S. Schiarea, M. Liguori, M. Fabbri, S. Pesce, L. Zammataro, F. Pasqualini, M. Nebuloni, C. Chiabrando, A. Mantovani, and P. Allavena. 2010. Tumor-Conditioned Macrophages Secrete Migration-Stimulating Factor: A New Marker for M2-Polarization, Influencing Tumor Cell Motility. *J. Immunol.* 185: 642–652.

263. Leek, R. D., N. C. Hunt, R. J. Landers, C. E. Lewis, J. A. Royds, and A. L. Harris. 2000. Macrophage infiltration is associated with VEGF and EGFR expression in breast cancer. *J. Pathol.* 190: 430–6.

264. Torisu, H., M. Ono, H. Kiryu, M. Furue, Y. Ohmoto, J. Nakayama, Y. Nishioka, S. Sone, and M. Kuwano. 2000. Macrophage infiltration correlates with tumor stage and angiogenesis in human malignant melanoma: possible involvement of TNFalpha and IL-1alpha. *Int. J. cancer* 85: 182–188.

265. Gazzaniga, S., A. I. Bravo, A. Guglielmotti, N. Van Rooijen, F. Maschi, A. Vecchi, A. Mantovani, J. Mordoh, and R. Wainstok. 2007. Targeting tumor-associated macrophages and inhibition of MCP-1 reduce angiogenesis and tumor growth in a human melanoma xenograft. *J. Invest. Dermatol.* 127: 2031–2041.

266. Nishie, A., M. Ono, T. Shono, J. Fukushi, M. Otsubo, H. Onoue, Y. Ito, T. Inamura, K. Ikezaki, M. Fukui, T. Iwaki, and M. Kuwano. 1999. Macrophage infiltration and heme oxygenase-1 expression correlate with angiogenesis in human gliomas. *Clin. Cancer Res.* 5: 1107–1113.

267. DiPietro, L. A., and P. J. Polverini. 1993. Angiogenic macrophages produce the angiogenic inhibitor thrombospondin 1. *Am. J. Pathol.* 143: 678–684.

268. Ilkovitch, D., and D. M. Lopez. 2008. Immune modulation by melanoma-derived factors. *Exp. Dermatol.* 17: 977–985.

269. Mitchem, J. B., D. J. Brennan, B. L. Knolhoff, B. A. Belt, Y. Zhu, D. E. Sanford, L. Belaygorod, D. Carpenter, L. Collins, D. Piwnica-Worms, S. Hewitt, G. M. Udupi, W. M. Gallagher, C. Wegner, B. L. West, A. Wang-Gillam, P. Goedegebuure, D. C. Linehan, and D. G. DeNardo. 2013. Targeting tumor-infiltrating macrophages decreases tumor-initiating cells, relieves immunosuppression, and improves chemotherapeutic responses. *Cancer Res.* 73: 1128–1141.

270. Bohn, T., S. Rapp, N. Luther, M. Klein, T. J. Bruehl, N. Kojima, P. Aranda Lopez, J. Hahlbrock, S. Muth, S. Endo, S. Pektor, A. Brand, K. Renner, V. Popp, K. Gerlach, D. Vogel, C. Lueckel, D. Arnold-Schild, J. Pouyssegur, M. Kreutz, M. Huber, J. Koenig, B. Weigmann, H. C. Probst, E. von Stebut, C. Becker, H. Schild, E. Schmitt, and T. Bopp. 2018. Tumor immunoevasion via acidosis-dependent induction of regulatory tumor-associated macrophages. *Nat. Immunol.* 19: 1319–1329.

271. Affara, N. I., B. Ruffell, T. R. Medler, A. J. Gunderson, M. Johansson, S. Bornstein, E. Bergsland, M. Steinhoff, Y. Li, Q. Gong, Y. Ma, J. F. Wiesen, M. H. Wong, M. Kulesz-Martin, B. Irving, and L. M. Coussens. 2014. B cells regulate macrophage phenotype and response to chemotherapy in squamous carcinomas. *Cancer Cell* 25: 809–821.

272. Horikawa, M., V. Minard-Colin, T. Matsushita, and T. F. Tedder. 2011. Regulatory B cell production of IL-10 inhibits lymphoma depletion during CD20 immunotherapy in mice. *J. Clin. Invest.* 121: 4268–4280.

273. Shiao, S. L., B. Ruffell, D. G. De Nardo, B. A. Faddegon, C. C. Park, and L. M. Coussens. 2015. TH2-polarized CD4+ T Cells and macrophages limit efficacy of radiotherapy. *Cancer Immunol. Res.* 3: 518–525.

274. Arlauckas, S. P., C. S. Garris, R. H. Kohler, M. Kitaoka, M. F. Cuccarese, K. S. Yang, M. A. Miller, J. C. Carlson, G. J. Freeman, R. M. Anthony, R. Weissleder, and M. J. Pittet. 2017. In vivo imaging reveals a tumor-associated macrophage-mediated resistance pathway in anti-PD-1 therapy. *Sci. Transl. Med.* 9.

275. Jinushi, M., S. Chiba, H. Yoshiyama, K. Masutomi, I. Kinoshita, H. Dosaka-Akita, H. Yagita, A. Takaoka, and H. Tahara. 2011. Tumor-associated macrophages regulate tumorigenicity and anticancer drug responses of cancer stem/initiating cells. *Proc. Natl. Acad. Sci. U. S. A.* 108: 12425–12430.

276. Fidler, I. J. 1974. Inhibition of Pulmonary Metastasis by Intravenous Injection of Specifically Activated Macrophages. *Cancer Res.* 34.

277. Chakraborty, N. G., T. Okino, P. Stabach, S. J. Padula, H. Yamase, E. Morse, R. I. Sha'afi, D. R. Twardzik, L. J. Shultz, and B. Mukherji. 1991. Adoptive transfer of activated human autologous macrophages results in regression of transplanted human melanoma cells in SCID mice. *In Vivo* 5: 609–614.

278. Wang, H., L. Zhang, L. Yang, C. Liu, Q. Zhang, and L. Zhang. 2017. Targeting macrophage anti-tumor activity to suppress melanoma progression. *Oncotarget* 8: 18486–18496.

279. Georgoudaki, A. M., K. E. Prokopec, V. F. Boura, E. Hellqvist, S. Sohn, J. Östling, R. Dahan, R. A. Harris, M. Rantalainen, D. Klevebring, M. Sund, S. E. Brage, J. Fuxe, C. Rolny, F. Li, J. V. Ravetch, and M. C. I. Karlsson. 2016. Reprogramming Tumor-Associated Macrophages by Antibody Targeting Inhibits Cancer Progression and Metastasis. *Cell Rep.* 15: 2000–2011.

280. Wanderley, C. W., D. F. Colón, J. P. M. Luiz, F. F. Oliveira, P. R. Viacava, C. A. Leite, J. A. Pereira, C. M. Silva, C. R. Silva, R. L. Silva, C. A. Speck-Hernandez, J. M. Mota, J. C. Alves-Filho, R. C. Lima-Junior, T. M. Cunha, and F. Q. Cunha. 2018. Paclitaxel Reduces Tumor Growth by Reprogramming Tumor-Associated Macrophages to an M1 Profile in a TLR4-Dependent Manner. *Cancer Res.* 78: 5891–5900.

281. Pyonteck, S. M., L. Akkari, A. J. Schuhmacher, R. L. Bowman, L. Sevenich, D. F. Quail, O. C. Olson, M. L. Quick, J. T. Huse, V. Teijeiro, M. Setty, C. S. Leslie, Y. Oei, A. Pedraza, J. Zhang, C. W. Brennan, J. C. Sutton, E. C. Holland, D. Daniel, and J. A. Joyce. 2013. CSF-1R inhibition alters macrophage polarization and blocks glioma progression. *Nat. Med.* 19: 1264–1272.

282. Ries, C. H., M. A. Cannarile, S. Hoves, J. Benz, K. Wartha, V. Runza, F. Rey-Giraud, L. P. Pradel, F. Feuerhake, I. Klaman, T. Jones, U. Jucknischke, S. Scheiblich, K. Kaluza, I. H. Gorr, A. Walz, K. Abiraj, P. A. Cassier, A. Sica, C. Gomez-Roca, K. E. deVisser, A. Italiano, C. LeTourneau, J. P. Delord, H. Levitsky, J. Y. Blay, and D. Rüttinger. 2014. Targeting tumor-associated macrophages with anti-CSF-1R antibody reveals a strategy for cancer therapy. *Cancer Cell* 25: 846–859.

283. Chen, X. J., L. F. Han, X. G. Wu, W. F. Wei, L. F. Wu, H. Y. Yi, R. M. Yan, X. Y. Bai, M. Zhong, Y. H. Yu, L. Liang, and W. Wang. 2017. Clinical significance of CD163+ and CD68+ tumor-associated macrophages in high-risk HPV-related cervical cancer. *J. Cancer* 8: 3868–3875.

284. Gensel, J. C., T. J. Kopper, B. Zhang, M. B. Orr, and W. M. Bailey. 2017. Predictive screening of M1 and M2 macrophages reveals the immunomodulatory effectiveness of post spinal cord injury azithromycin treatment. *Sci. Rep.* 7.

285. Gries, A., J. Nimpf, H. Wurm, G. M. Kostner, and T. Kenner. 1989. Characterization of isoelectric subspecies of asialo-β2-glycoprotein I. *Biochem. J.* 260: 531–534.

286. Hamdan, R., S. N. Maiti, and A. J. Schroit. 2007. Interaction of β2-glycoprotein 1 with phosphatidylserine-containing membranes: Ligand-dependent conformational alterations initiate bivalent binding. *Biochemistry* 46: 10612–10620.

287. Mehdi, H., A. Naqvi, and M. I. Kamboh. 2000. A hydrophobic sequence at position 313-316 (Leu-Ala-Phe-Trp) in the fifth domain of apolipoprotein H (β2-glycoprotein I) is crucial for cardiolipin binding. *Eur. J. Biochem.* 267: 1770–1776.

288. Fleming, S. D. 2012. Naturally occurring autoantibodies mediate ischemia/reperfusion-induced tissue injury. *Adv. Exp. Med. Biol.* 750: 174–185.

289. Slone, E. A., and S. D. Fleming. 2014. Membrane lipid interactions in intestinal ischemia/reperfusion-induced Injury. *Clin. Immunol.* 153: 228–240.

290. Passam, F. H., J. C. Qi, K. Tanaka, K. I. Matthaei, and S. A. Krilis. 2010. In vivo modulation of angiogenesis by beta 2 glycoprotein I. *J. Autoimmun.* 35: 232–240.

291. Jonkman, J. E. N., J. A. Cathcart, F. Xu, M. E. Bartolini, J. E. Amon, K. M. Stevens, and P. Colarusso. 2014. An introduction to the wound healing assay using live-cell microscopy. *Cell Adhes. Migr.* 8: 440–451.

292. Rodriguez, L. G., X. Wu, and J. L. Guan. 2005. Wound-Healing Assay. In *Cell Migration: Developmental Methods and Protocols* Humana Press, Totowa, NJ. 23–29.

293. Kendall, R. L., and K. A. Thomas. 1993. Inhibition of vascular endothelial cell growth factor activity by an endogenously encoded soluble receptor. *Proc. Natl. Acad. Sci. U. S. A.* 90: 10705–10709.

294. Neiva, K. G., Z. Zhang, M. Miyazawa, K. A. Warner, E. Karl, and J. E. Nör. 2009. Cross talk initiated by endothelial cells enhances migration and inhibits anoikis of squamous cell carcinoma cells through STAT3/Akt/ERK signaling. *Neoplasia* 11: 583–593.

295. Chang, Q., I. Jurisica, T. Do, and D. W. Hedley. 2011. Hypoxia predicts aggressive growth and spontaneous metastasis formation from orthotopically grown primary xenografts of human pancreatic cancer. *Cancer Res.* 71: 3110–3120.

296. Yasuda, S., T. Atsumi, M. Ieko, and T. Koike. 2004. β2-glycoprotein I, anti-β2-glycoprotein I, and fibrinolysis. *Thromb. Res.* 114: 461–465.

297. DeNardo, D. G., and B. Ruffell. 2019. Macrophages as regulators of tumour immunity and immunotherapy. *Nat. Rev. Immunol.* 19: 369–382.

298. Da Silva, I. A., S. C. Stone, R. M. Rossetti, S. Jancar, and A. P. Lepique. 2017. Modulation of Tumor-Associated Macrophages (TAM) Phenotype by Platelet-Activating Factor (PAF) Receptor. *J. Immunol. Res.* 2017: Online.

299. Liu, C.-Y., J.-Y. Xu, X.-Y. Shi, W. Huang, T.-Y. Ruan, P. Xie, and J.-L. Ding. 2013. M2-polarized tumor-associated macrophages promoted epithelial-mesenchymal transition in pancreatic cancer cells, partially through TLR4/IL-10 signaling pathway. *Lab. Investig.* | 93: 844–854.

300. Ambarus, C. A., S. Krausz, M. van Eijk, J. Hamann, T. R. D. J. Radstake, K. A. Reedquist, P. P. Tak, and D. L. P. Baeten. 2012. Systematic validation of specific phenotypic markers for in vitro polarized human macrophages. *J. Immunol. Methods* 375: 196–206.

301. Chevrier, S., J. H. Levine, V. R. T. Zanotelli, K. Silina, D. Schulz, M. Bacac, C. H. Ries, L. Ailles, M. A. S. Jewett, H. Moch, M. van den Broek, C. Beisel, M. B. Stadler, C. Gedye, B. Reis, D. Pe'er, and B. Bodenmiller. 2017. An Immune Atlas of Clear Cell Renal Cell Carcinoma. *Cell* 169: 736–749.

302. Almatroodi, S. A., C. F. McDonald, I. A. Darby, and D. S. Pouniotis. 2016. Characterization of M1/M2 Tumour-Associated Macrophages (TAMs) and Th1/Th2 Cytokine Profiles in Patients with NSCLC. *Cancer Microenviron.* 9.

303. Vodovotz, Y., C. Bogdan, J. Paik, Q. W. Xie, and C. Nathan. 1993. Mechanisms of suppression of macrophage nitric oxide release by transforming growth factor γ. *J. Exp. Med.* 178: 605–613.

304. Müller, E., M. Speth, P. F. Christopoulos, A. Lunde, A. Avdagic, I. Øynebråten, A. Corthay, and R. A. Harris. 2018. Both Type I and Type II Interferons Can Activate Antitumor M1 Macrophages When Combined With TLR Stimulation. 9: 1–16.

305. Bates, R. C., and A. M. Mercurio. 2003. Tumor necrosis factor-α stimulates the epithelial-tomesenchymal transition of human colonic organoids. *Mol. Biol. Cell* 14: 1790–1800.

306. Scott, D. J., M. A. Hull, E. J. Cartwright, W. K. Lam, A. Tisbury, R. Poulsom, A. F. Markham, C. Bonifer, and P. L. Coletta. 2001. Lack of inducible nitric oxide synthase promotes intestinal tumorigenesis in the ApcMin/+ mouse. *Gastroenterology* 121: 889–899.

307. Matsushita, T., and K. Takehara. 2019. Soluble CD163 is a potential biomarker in systemic sclerosis. *Expert Rev. Mol. Diagn.* 19: 197–199.

308. Helm, O., J. Held-Feindt, E. Grage-Griebenow, N. Reiling, H. Ungefroren, I. Vogel, U. Krüger, T. Becker, M. Ebsen, C. Röcken, D. Kabelitz, H. Schäfer, and S. Sebens. 2014. Tumor-associated macrophages exhibit pro- and anti-inflammatory properties by which they impact on pancreatic tumorigenesis. *Int. J. Cancer* .

309. Leek, R. D., C. E. Lewis, R. Whitehouse, M. Greenall, J. Clarke, and A. L. Harris. 1996. Association of macrophage infiltration with angiogenesis and prognosis in invasive breast carcinoma. *Cancer Res.* 56: 4625–4629.

310. Pardali, E., M. J. Goumans, and P. ten Dijke. 2010. Signaling by members of the TGF-β family in vascular morphogenesis and disease. *Trends Cell Biol.* 20: 556–567.

311. Tiemessen, M. M., S. Kunzmann, C. B. Schmid-Weber, J. Garssen, C. A. F. M. Bruijnzeel-Koomen, E. F. Knol, and E. Van Hoffen. 2003. Transforming growth factor-β inhibits human antigen-specific CD4+ T cell proliferation without modulating the cytokine response | International Immunology | Oxford Academic. *Int. Immunol.* 15: 1495–1504.

312. Gilbert, K. M., M. Thoman, K. Bauche, T. Pham, and W. O. Weigle. 1997. Transforming growth factor-β1 induces antigen-specific unresponsiveness in naive T cells. *Immunol. Invest.* 26: 459–472.

313. George, M. L., M. G. Tutton, F. Janssen, A. Arnaout, A. M. Abulafi, S. A. Eccles, and R. I. Swift. *VEGF-A, VEGF-C, and VEGF-D in Colorectal Cancer Progression*,.

314. Fukumura, D., R. Xavier, T. Sugiura, Y. Chen, E. C. Park, N. Lu, M. Selig, G. Nielsen, T. Taksir, R. K. Jain, and B. Seed. 1998. Tumor induction of VEGF promoter activity in stromal cells. *Cell* 94: 715–725.

315. Haque, A. S. M. R., M. Moriyama, K. Kubota, N. Ishiguro, M. Sakamoto, A. Chinju, K. Mochizuki, T. Sakamoto, N. Kaneko, R. Munemura, T. Maehara, A. Tanaka, J. N. Hayashida, S. Kawano, T. Kiyoshima, and S. Nakamura. 2019. CD206+ tumor-associated macrophages promote proliferation and invasion in oral squamous cell carcinoma via EGF production. *Sci. Rep.* 9.

316. Azad, A. K., M. V. S. Rajaram, and L. S. Schlesinger. 2014. Exploitation of the Macrophage Mannose Receptor (CD206) in Infectious Disease Diagnostics and Therapeutics. *J. Cytol. Mol. Biol.* 1.

317. Hu, W., Y. Qian, F. Yu, W. Liu, Y. Wu, X. Fang, and W. Hao. 2015. Alternatively activated macrophages are associated with metastasis and poor prognosis in prostate adenocarcinoma. *Oncol. Lett.* 10: 1390–1396.

318. Tanaka, T., M. Narazaki, and T. Kishimoto. 2014. Il-6 in inflammation, Immunity, And disease. *Cold Spring Harb. Perspect. Biol.* 6: Online.

319. Smalley, H., J. M. Rowe, F. Nieto, J. Zeledon, K. Pollard, J. M. Tomich, and S. D. Fleming. 2020. Beta2 glycoprotein I-derived therapeutic peptides induce sFlt-1 secretion to reduce melanoma vascularity and growth. *Cancer Lett.* 495: 66–75.

320. Smalley, H., J. M. Rowe, F. Nieto, J. Zeledon, K. Pollard, J. M. Tomich, and S. D. Fleming. Beta2 glycoprotein I-derived therapeutic peptides induce sFlt-1 secretion to reduce melanoma vascularity and growth. *Cancer Lett.* .

321. DiNapoli, M. R., C. L. Calderon, and D. M. Lopez. 1996. The altered tumoricidal capacity of macrophages isolated from tumor-bearing mice is related to reduced expression of the inducible nitric oxide synthase gene. *J. Exp. Med.* 183: 1323–1329.

322. Edwards, P., J. C. Cendan, D. B. Topping, L. L. Moldawer, S. Mackay, E. M. Copeland, and D. S. Lind. 1996. Tumor cell nitric oxide inhibits cell growth in vitro, but stimulates tumorigenesis and experimental lung metastasis in vivo. In *Journal of Surgical Research* vol. 63. Academic Press Inc. 49–52.

323. Zhang, X. M., and Q. Xu. 2001. Metastatic melanoma cells escape from immunosurveillance through the novel mechanism of releasing nitric oxide to induce dysfunction of immunocytes. *Melanoma Res.* 11: 559–567.

324. Chin, K., Y. Kurashima, T. Ogura, H. Tajiri, S. Yoshida, and H. Esumi. 1997. Induction of vascular endothelial growth factor by nitric oxide in human glioblastoma and hepatocellular carcinoma cells. *Oncogene* 15: 437–442.

325. Jenkins, D. C., I. G. Charles, L. L. Thomsen, D. W. Moss, L. S. Holmes, S. A. Baylis, P. Rhodes, K. Westmore, P. C. Emson, and S. Moncada. 1995. Roles of nitric oxide in tumor growth. *Proc. Natl. Acad. Sci. U. S. A.* 92: 4392–4396.

326. Smita, M., K. Naidu, A. N. Suryakar, S. C. Swami, R. V Katkam, and K. M. Kumbar. 2007. Oxidative Stress and Antioxidant Status in Cervical Cancer Patients. *Indian J. Clin. Biochem.* 22: 140–144.

327. Chen, G. G., W. L. Tak, H. Xu, J. H. Y. Yip, M. Li, T. S. K. Mok, and A. P. C. Yim. 2008. Increased inducible nitric oxide synthase in lung carcinoma of smokers. *Cancer* 112: 372–381.

328. Mitchell, J. B., D. A. Wink, W. DeGraff, J. Gamson, L. K. Keefer, and M. Krishna. 1993. Hypoxic mammalian cell radiosensitization by nitric oxide - PubMed. *Cancer Res.* 53: 5845–5848.

329. Soler, M. N., P. Bobé, K. Benihoud, G. Lemaire, B. A. Roos, and S. Lausson. 2000. Gene therapy of rat medullary thyroid cancer by naked nitric oxide synthase II DNA injection. *J. Gene Med.* 2: 344–352.

330. Xu, W., L. Liu, and I. G. Charles. 2002. Microencapsulated iNOS-expressing cells cause tumor suppression in mice. *FASEB J.* 16: 1–18.

331. García-Tuñón, I., M. Ricote, A. Ruiz, B. Fraile, R. Paniagua, and M. Royuela. 2006. Role of tumor necrosis factor-alpha and its receptors in human benign breast lesions and tumors (in situ and infiltrative). *Cancer Sci.* 97: 1044–1049.

332. Nabors, L. B., E. Suswam, Y. Huang, X. Yang, M. J. Johnson, and P. H. King. 2003. Tumor necrosis factor alpha induces angiogenic factor up-regulation in malignant glioma cells: a role for RNA stabilization and HuR. *Cancer Res.* 63: 4181–4187.

333. Ferrajoli, A., M. J. Keating, T. Manshouri, F. J. Giles, A. Dey, Z. Estrov, C. A. Koller, R. Kurzrock, D. A. Thomas, S. Faderl, S. Lerner, S. O'Brien, and M. Albitar. 2002. The clinical significance of tumor necrosis factor-alpha plasma level in patients having chronic lymphocytic leukemia. *Blood* 100: 1215–1219.

334. Hoving, S., A. L. B. Seynhaeve, S. T. Van Tiel, G. Aan De Wiel-Ambagtsheer, E. A. De Bruijn, A. M. M. Eggermont, and T. L. M. Ten Hagen. 2006. Early destruction of tumor vasculature in tumor necrosis factor-α-based isolated limb perfusion is responsible for tumor response. *Anticancer. Drugs* 17: 949–959.

335. Mackay, F., H. Loetscher, D. Stueber, G. Gehr, and W. Lesslauer. 1993. Tumor Necrosis Factor ± (TNF-±)-induced Cell Adhesion to Human Endothelial Cells Is under Dominant Control of One TNT Receptor Type, TNF-R55. *J. Exp. Med.* 177: 1277–1286.

336. Lejeune, F. J., D. Liénard, M. Matter, and C. Rüegg. 2006. Efficiency of recombinant human TNF in human cancer therapy. *Cancer Immun.* 6: Online.

337. Wang, L., J. Q. Liu, F. Talebian, Z. Liu, L. Yu, and X. F. Bai. 2015. IL-10 enhances CTL-mediated tumor rejection by inhibiting highly suppressive CD4+ T cells and promoting CTL persistence in a murine model of plasmacytoma. *Oncoimmunology* 4: 1–9.

338. Carmi, Y., S. Dotan, P. Rider, I. Kaplanov, M. R. White, R. Baron, S. Abutbul, M. Huszar, C. A. Dinarello, R. N. Apte, and E. Voronov. 2013. The Role of IL-1β in the Early Tumor Cell–Induced Angiogenic Response. *J. Immunol.* 190: 3500–3509.

339. Cassetta, L., S. Fragkogianni, A. H. Sims, A. Swierczak, L. M. Forrester, H. Zhang, D. Y. H. Soong, T. Cotechini, P. Anur, E. Y. Lin, A. Fidanza, M. Lopez-Yrigoyen, M. R. Millar, A. Urman, Z. Ai, P. T. Spellman, E. S. Hwang, J. M. Dixon, L. Wiechmann, L. M. Coussens, H. O. Smith, and J. W. Pollard. 2019. Human Tumor-Associated Macrophage and Monocyte Transcriptional Landscapes Reveal Cancer-Specific Reprogramming, Biomarkers, and Therapeutic Targets. *Cancer Cell* 35: 588-602.e10.

340. Mantovani, A., F. Marchesi, A. Malesci, L. Laghi, and P. Allavena. 2017. Tumour-associated macrophages as treatment targets in oncology. *Nat. Rev. Clin. Oncol.* 14: 399–416.

341. Etzerodt, A., K. Tsalkitzi, M. Maniecki, W. Damsky, M. Delfini, E. Baudoin, M. Moulin, M. Bosenberg, J. H. Graversen, N. Auphan-Anezin, S. K. Moestrup, and T. Lawrence. 2019. Specific targeting of CD163+ TAMs mobilizes inflammatory monocytes and promotes T cell-mediated tumor regression. *J. Exp. Med.* 216: 2394–2411.

342. Clark, N. M., and P. D. Bos. 2019. Tumor-Associated Macrophage Isolation and In Vivo Analysis of Their Tumor-Promoting Activity. *Methods Mol. Biol.* 1884: 151–160.

343. Rose, S., A. Misharin, and H. Perlman. 2012. A novel Ly6C/Ly6G-based strategy to analyze the mouse splenic myeloid compartment. *Cytom. Part A* 81 A: 343–350.

344. Cassetta, L., R. Noy, A. Swierczak, G. Sugano, H. Smith, L. Wiechmann, and J. W. Pollard. 2016. Isolation of mouse and human tumor-associated macrophages. *Adv. Exp. Med. Biol.* 899: 211–229.

Appendix A - Supplementary Figures and Tables

Supplementary Table 4.1 The melting temperatures and sequences for primers used in RT-PCR.

RT-PCR Primer Sequences			
Protein	Primers	Melting Temperature	Sequence
18S	18S FWD[a]	56 °C	GGTTGATCCTGCCAGTAGC
	18S REV	56 °C	GCGACCAAAGGAACCATAAC
Endoglin	Endoglin FWD	55 °C	CTTCCAAGGACAGCCAAGAG
	Endoglin REV	55 °C	GTGGTTGCCATTCAAGTGTG
VEGFa variant 1	VEGF-A FWD	55.6 °C	AGAGCAACATCACCATGCAG
	VEGF-A REV	55.6 °C	TTTCTTGCGCTTTCGTTTTT
Endosialin	Endosialin FWD	56.7 °C	CCCCTCTTCCTACCAACTCC
	Endosialin REV	56.7 °C	CCTTCCCTTGGGACTAGAGG
KDR (VEGFR2)	KDR FWD	57.1 °C	GGCGGTGGTGACAGTATCTT
	KDR REV	57.1 °C	GTCACTGACAGAGGCGATGA
Flt-1 (VEGFR1)	Flt-1 FWD	56.3 °C	TATAAGGCAGCGGATTGACC
	Flt-1 REV	56.3 °C	TCATACACATGCACGGAGGT
CD31 (PECAM-1)	CD31 FWD	56 °C	TGCTCTCGAAGCCCAGTATT
	CD31 REV	56 °C	TGTGAATGTTGCTGGGTCAT

[a]FWD is forward primer, REV is reverse primer

Supplementary Table 4.2 The melting temperatures and sequences for primers used in RT-PCR.

RT-PCR Primer Sequences			
Protein	Primers	Melting Temperature	Sequence
18S	18S FWD[a]	56 °C	GGTTGATCCTGCCAGTAGC
	18S REV	56 °C	GCGACCAAAGGAACCATAAC
Arg-1	Arg-1 FWD	52.7	CGATTCACCTGAGTTGAT
	Arg-1 REV	54.8	AAGCCAAGGTTAAAGCCACT
iNOS	iNOS Fwd	57.1	CAC CTT GGA GTT CAC CCA GT
	iNOS Rev	57.1	ACC ACT CGT ACT TGG GAT GC
IL-10	IL-10 Fwd	52.5	CCA AGC CTT ATC GGA AAT GA
	IL-10 Rev	52.7	TTT TCA CAG GGG AGA AAT CG
IL-1beta	IL-1b FWD	51.1	TCTATACCTGTCCTGTGTAATG
	IL-1b REV	54.6	GCTTGTGCTCTGCTTGTG
IL-6	IL-6 Fwd	56.3	AGT TGC CTT GGG ACT GA
	IL-6 Rev	54.4	TCC ACG ATT TCC CAG AGA AC
TNFa	TNFalpha Fwd	56.4	TAT GGC TCA GGG TCC AAC TC
	TNFalpha Rev	55.6	CTC CCT TTG CAG AAC TCA GG
VEGF a variant 1	VEGFa FWD	55.6	AGAGCAACATCACCATGCAG
	VEGFa REV	51.8	TTTCTTGCGCTTTCGTTTTT

Appendix B - Copyright Permissions and Outside Software

Figures in Chapter 1 (excluding Figures 1-4 and 1-5), were created with BioRender.com.

Figure 1-5 was created using EzMol. EzMol is a software wizard on top of 3Dmol.js, incorporating jQuery UI and Spectrum. EzMol is funded by Imperial College London and the BBSRC.

Reynolds CR, Islam SA, Sternberg MJE (2018). "EzMol: A web server wizard for the rapid visualization and image production of protein and nucleic acid structures." J Mol Biol